POLARIZATION OF THE BLACKBODY RADIATION AT 3.2 CM

****

George Peter Nanos, Jr.

Library
Naval Postgraduate School
Monterey, California 93940

POLARIZATION OF THE BLACKBODY RADIATION AT 3.2 CM

GEORGE PETER NANOS, JR.

A DISSERTATION

PRESENTED TO THE

FACULTY OF PRINCETON UNIVERSITY

IN CANDIDACY FOR THE DEGREE

OF DOCTOR OF PHILOSOPHY

RECOMMENDED FOR ACCEPTANCE BY THE

DEPARTMENT

OF

PHYSICS

OCTOBER, 1973

T156816

Library
Naval Postgraduate School
Monterey, California 93940

TABLE OF CONTENTS

TABLES

FIGURES

ACKNOWLEDGEMENTS

It's difficult to remember all the help one receives in an undertaking of this sort, both because the long span of time makes recollection of every aid difficult and because many times the help is too subtle to be noticed. Who can tell at which point in a long discussion an idea is born? For this reason, I would first like to thank all the members of the Gravitation Research Group at Princeton University with whom I have worked for the past four years. I don't think there is a member who has not increased my knowledge of physics in some way and thus, at least indirectly, aided this work.

In particular, I would like to thank my advisor, David T. Wilkinson, who provided the inspiration and impetus for this investigation. Even while on sabbatical during the first year, he managed to keep track of my progress and help me over the rough spots. During this time I was also fortunate to have the help of Mike Hauser as a substitute advisor when Dave was in Hawaii for long periods.

Much preliminary work on this problem was done by three Princeton undergraduates, William F. Baron, William N. Cunningham, and Donald McCarthy, as their senior theses. Their methods and difficulties saved many hours of frustration and wasted effort. During the first summer, Brian Corey worked with me in preparing and testing parts of the apparatus. In addition to providing help and advice on computer programming, data analysis and statistics, Ed Groth also went to the additional trouble of designing his pulsar

timing clock so that it would provide time information for my experiment.

In addition to Ed and Brian, Larry Rudnick and Claude Swanson engaged in sometimes endless discussions of various aspects of the experiment and analysis, much to my benefit. Anyone in the Physics Department who has extensively used the facilities of the Princeton University Computer Center cannot have failed to receive a great deal of help from Victor Bearg. In actual construction of the apparatus, Mr. Clark Smeltzer lent me a wealth of machine tool experience.

The complete results of the Cambridge 1407 MHz polarization survey were kindly sent to me by Dr. John R. Shakeshaft of the Mullard Radio Astronomy Observatory.

Much of the funds for support of this work came from the National Science Foundation. I would also like to thank the United States Navy for supporting my studies through the Junior Line Officer Advanced Educational (Burke) Program and for releasing me from my other duties as a naval officer to pursue them.

For help in preparing this manuscript and for love and support through the long hours of work, I wish to thank my wife, Joanne. For inspiring me to study physics, I am grateful to my undergraduate advisor Dr. Ralph A. Goodwin and the Physics Faculty at the Naval Academy. Finally, for encouraging me to make the most of my talents and to follow my dreams wherever they lead, I thank my parents.

ABSTRACT

POLARIZATION OF THE COSMIC BLACKBODY RADIATION AT 3.2 CM.

GEORGE PETER NANOS, JR.

A 3.2 Dicke Radiometer configured as a polarimeter was used to make measurements of the linear polarization of the Primeval Fireball along a declination of 40.35° N. The resolution of the instrument was 15° in declination and 1 hour in right ascension. Harmonic analysis of the Stokes parameters of the radiation, Q and U, sets limits on sidereal variations, which in turn limit the possible contributions of cosmological origin. Results are related to the isotropy of the cosmic background radiation and the symmetry of the universe.

I. INTRODUCTION

1.1 HISTORY OF THE FIREBALL

In 1929 it became clear from the work of Edwin Hubble that the universe is expanding, and that the recession velocity of a galaxy is nearly a linear function of its distance.[1] This result gave impetus to the development of expanding universe cosmologies based on solutions to Einstein's equations. Of the many ensuing models, among the most successful and well established is the homogeneous and isotropic universe with cosmological constant equal to zero, based on the work of Friedman and Lemaitre.[2,3]

One important feature of this model is the existence of a singularity at t=0; i.e., at some finite time in the past the scale factor in the universe was small and the density of matter and radiation was very high. This feature is known as the "fireball" hypothesis and the subsequent expansion and evolution of the universe is called the "Big Bang".

During the early stages of the fireball expansion, the matter in the universe was extremely hot, much greater than 10^{10} ^{o}K, and was in thermal equilibrium with the radiation. Being thermal, this radiation had a Planckian spectrum given by

$$dE_1 = \frac{8\pi h\nu_1^3}{c^3} \frac{1}{e^{h\nu_1/kT_1}} \, d\nu_1. \qquad (1.1)$$

The first description of this type of blackbody-radiation filled model was given by Tolman in 1931.[4] Later he showed that under adiabatic expansion the radiation spectrum is still given by (1.1),

where the temperature T is now given by

$$T'(t) = T_o \frac{a_o}{a(t)} = T_o \frac{1}{1+z} , \qquad (1.2)$$

where a(t) is the scale factor of the universe at time t, and 1+z is the redshift due to the first order Doppler effect from the expansion, viewed by a comoving observer.

Alpher and Gamow in 1948 needed the fireball in their attempt to explain element formation in the early universe and in their theory derived a temperature of 5 ^{o}K for the remnants observed today, a figure quite close to the 2.7 ^{o}K obtained experimentally.[5] Interest in this result waned as other explanations of element formation proved more attractive until, working independently, R. H. Dicke and his colleagues at Princeton were drawn to the idea to explain the reprocessing of heavy elements into hydrogen in a closed oscillating universe.[6]

At the same time that two of these co-workers, P. G. Roll and D. T. Wilkinson, were building a radiometer to search for this radiation, Penzias and Wilson at Bell Laboratories realized that what they previously had considered to be excess receiver noise at 7.35 cm. and had tried to eliminate, was in fact the remnant of the primeval fireball that the Princeton group was searching for.[7] Soon afterward the 3.2 cm. measurement of Roll and Wilkinson confirmed the result and showed that the spectrum over this range was consistent with that of a 2.7 ^{o}K blackbody.[8] Following this, a host of other measurements have been performed,[9-28] all of which tend to support the hypothesis to a greater or lesser degree, at least in the Rayleigh-Jeans part of the spectrum. At wavelengths greater than

a few tens of centimeters or shorter than a millimeter, the situation is not as clear. At longer wavelengths contributions due to sources within the galaxy make separating out the blackbody difficult while short wavelength observations suffer greatly from absorption and emission in the atmosphere. If one excludes the rocket data at very short wavelengths, the reliability of which seems open to question at the present time, Peebles has shown that the available data supports the fireball reasonably well.[29]

ANISOTROPY

Accepting the idea that one is looking at fossil radiation from early in the history of the universe, it is natural to ask what information it carried from this early epoch. As the early universe expanded and cooled, at one point the primeval plasma recombined and the mean free path for photon scattering became very large, so large in fact that most of the fireball photons we observe were probably last scattered during the recombination at z=1000. Only a subsequent reionization of the matter could bring the scattering epoch closer. Therefore, the spatial distribution reflects the distribution and temperature of matter at this early time.

Tests for isotropy in the distribution of the radiation have been conducted by several investigators including the Princeton group.[36-38] At the present time no significant departure from spherical symmetry has been found for angular resolutions on the order of 1° of arc. In addition to early symmetry of the fireball, the data can be used to deduce our peculiar velocity relative to the local comoving frame. This effect appears as a 24 hr. asymmetry with a hot spot in the direction of motion due to the added Doppler shift.[39-41]

1.2 COSMOLOGICAL CAUSES OF POLARIZATION

As was pointed out by Martin Rees in 1968,[42] the type of expansion asymmetries which would give rise to anisotropies in the microwave background would also give rise to linear polarization of the radiation through the mechanism of Thomson scattering. Following his lead and using much the same notation, I will briefly demonstrate the existence of a linearly polarized component of the background, given an asymmetric expansion.

In this I will consider only one particular class of asymmetric universes, those with axially symmetric Euclidean metrics of the form $ds^2 = dt^2 - A(t)^2 (dx^2 + dy^2) - W(t)^2 dz^2$ and containing no magnetic field. Models of this type have been investigated extensively by Thorne (1967),[43] Jacobs (1968),[44] and others and are particularly attractive because of their simplicity, their close relation to the standard Einstein-de Sitter universe, and the straightforward way in which they lead to a polarization. In the case of three inequivalent directions, the situation would be much more complex (there being azimuthal dependence to the equations) and the calculations correspondingly more difficult.

Taking our given metric we can first define Hubble's constants in each direction, $a = dA/Adt$ and $w = dW/Wdt$. From these we can compute an average expansion constant $h = (2a+w)/3$ and a differential constant $\Delta h = (w-a)$ and using them, can discuss the existence of a temperature asymmetry in this type of universe. As was mentioned in the preceding section, Tolman showed that in the Einstein-de Sitter case the temperature of radiation is inversely proportional to the scale

factor, which in turn is proportional to $V^{1/3}$. In our case V the volume is proportional to A^2W and in a similar way we can write

$$T \propto (A^2W)^{-1/3}, \tag{1.3}$$

where T is an average temperature over all directions of observation. At any time t, one can define an approximate isotropy parameter equal to $\Delta T/T = \epsilon$. ΔT is the temperature difference between the A and W directions and can be written

$$\begin{aligned} \Delta T &= t_s \, d/dt \, (T_w - T_a) \\ &\propto t_s \, d/dt \, (1/W - 1/A) \\ &\simeq t_s \, \Delta h/(A^2W)^{1/3} \quad . \end{aligned} \tag{1.4}$$

Here t_s is the time since the last scattering, and is given by λ, the mean free path of the photons, divided by the velocity of light; i.e.

$$\begin{aligned} t_s &= \frac{\lambda}{c} \\ &= \frac{1}{nI(t)\sigma_T c} \quad , \end{aligned} \tag{1.5}$$

where n = the number density of electrons

I(t) = the percentage of them which are ionized

σ_T = the Thomson scattering cross section.

Putting this form into the previous equation, we have finally,

$$\begin{aligned} \epsilon &= (A^2W)^{1/3} \, \Delta T \\ &= \frac{\Delta h}{nI(t)\sigma_T c} \quad . \end{aligned} \tag{1.6}$$

To obtain a more precise result requires consideration of the cosmological redshift in an asymmetrically expanding universe as is done in Appendix A2. In particular for the axial model being considered, the temperature of the radiation as a function of the

direction of observation with respect to the axis of the universe is shown to be

$$T = T_o \left[\frac{A_o^2}{A^2} \sin^2\theta + \frac{W_o^2}{W^2} \cos^2\theta\right]^{-\frac{1}{2}} , \qquad (1.7)$$

in the absence of scattering.

Throughout this discussion the zero subscript will refer to the value of a quantity at the present time. In the event that the expansion asymmetry is small, as it is in the case we are considering, this equation can be cast in a little more convenient form as

$$T = T_{AV}(1 + \epsilon \sin^2\theta). \qquad (1.8)$$

Taking this type of temperature distribution as a starting point, the polarization of the microwave background through the mechanism of Thomson scattering can now be demonstrated. As shown in Figure 1.1, we will define the polarization of an electromagnetic wave from the microwave background as seen by an observer in terms of the plane containing the line of sight to the observer and the direction of asymmetric expansion. The direction perpendicular to this plane is called the 'a' direction while the direction which lies in this plane and is, of course, perpendicular to the direction of propagation is called the coplanar or 'w' direction. Following Rees, I will write the temperature of the radiation polarized in each direction in the following way:

$$T_a = T\,(1 + \epsilon_a \sin^2\theta)$$
$$T_w = T\,(1 + \epsilon_w \sin^2\theta) , \qquad (1.9)$$

where T now refers to T_{av}.

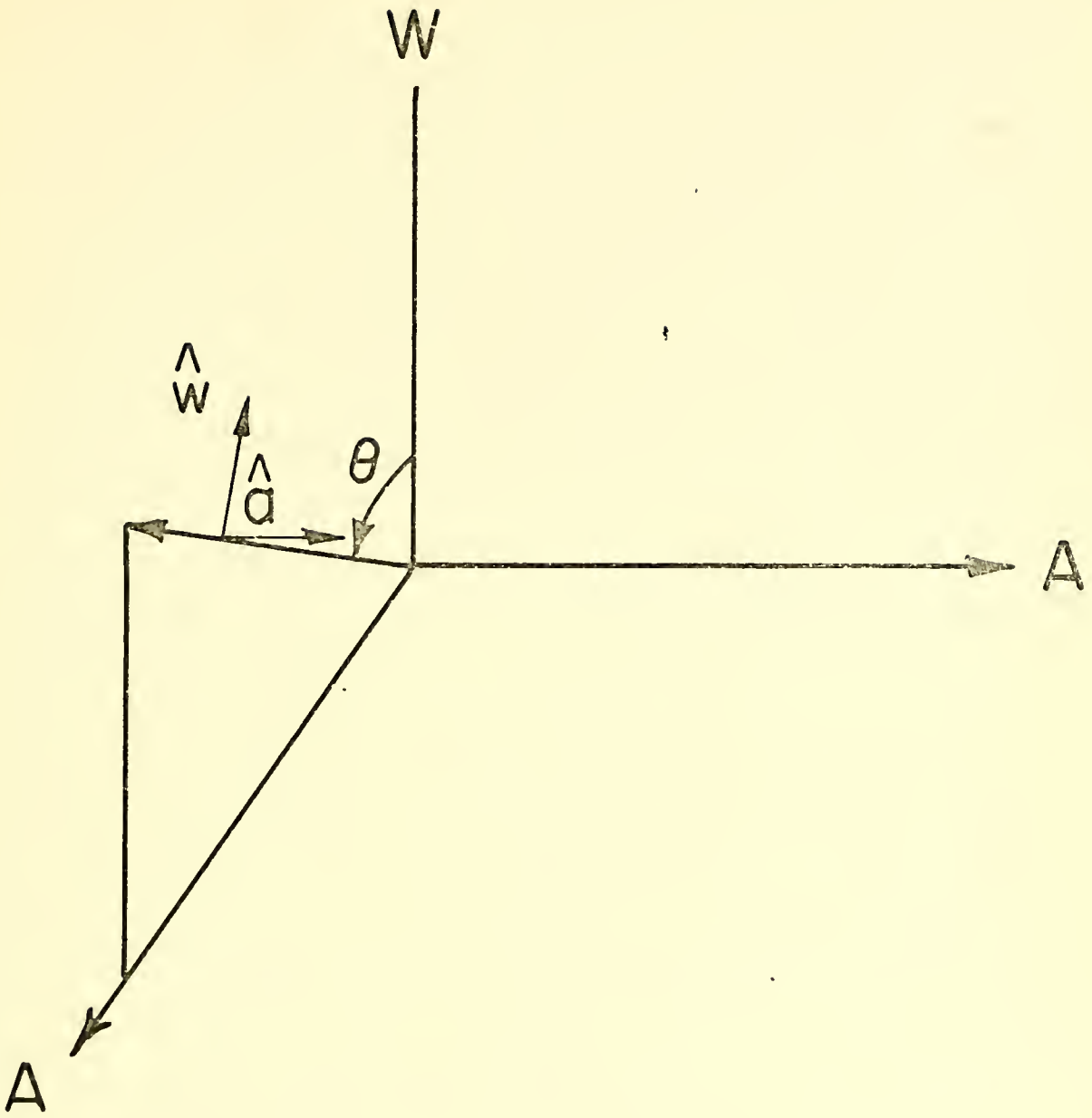

FIG. 1.1

DEFINITION OF THE POLARIZATION REFERENCE PLANE

By doing so,I can characterize the polarization completely by means of the parameters ϵ_a and ϵ_w. In fact, the evolution of the polarization with time may be ascertained by constructing and solving the differential equation, describing the change of these parameters with expansion and scattering of radiation. It must be understood that this type of approach is only valid when the temperature is low enough, say 10^9 °K, for elastic Thomson scattering to be the primary mode of interaction with the photons and when the asymmetry in the expansion is small enough that the above expansions of the temperature distribution are valid. In light of the small observed temperature asymmetry this latter condition doesn't seem too unreasonable. At this time there doesn't seem to be any evidence for a very hot plasma greater than $T = 10^9$ °K at a recent epoch.

If we express the temperature of the radiation in the two polarizations of the microwave background in the way described above, we can compute the effect on the asymmetry parameters ϵ_a and ϵ_w of a single Thompson scattering. In Appendix A3 the result in matrix form after integration over all angles of incidence is shown to be

$$\begin{pmatrix} \epsilon_a' \\ \epsilon_w' \end{pmatrix} = \begin{pmatrix} 0 & 0 \\ -1/2 & 7/30 \end{pmatrix} \begin{pmatrix} \epsilon_a \\ \epsilon_w \end{pmatrix} , \qquad (1.10)$$

where the primed quantities refer to the values after scattering. The most notable effect in this calculation is that the asymmetry in the orthogonal 'a' component is destroyed by the scattering process while the asymmetry parameter in the coplanar polarization is preserved. If to begin with, both parameters had been equal to ϵ, the effect of the scattering would have been to increase the maximum polarization

from zero to 1/30 ϵ, which demonstrates the effect of scattering in producing a polarization.

Because we know the time scale over which this change occurs, we can write an expression for the rate of change of the asymmetry parameters with time as follows:

$$\frac{d}{dt}\begin{pmatrix}\epsilon_a\\ \epsilon_w\end{pmatrix} = \frac{\Delta\begin{pmatrix}\epsilon_a\\ \epsilon_w\end{pmatrix}}{\Delta t}$$

$$= \frac{1}{t_s}\left[\begin{pmatrix}\epsilon_a'\\ \epsilon_w'\end{pmatrix} - \begin{pmatrix}\epsilon_a\\ \epsilon_w\end{pmatrix}\right]$$

$$= nI(t)\,\sigma_T c \begin{pmatrix}-1 & 0\\ -1/2 & -23/30\end{pmatrix}\begin{pmatrix}\epsilon_a\\ \epsilon_w\end{pmatrix}. \qquad (1.11)$$

In addition to the effect of scattering on ϵ_a and ϵ_w, one must consider the effect of expansion even though this is not what leads to the existence of a polarization. From equations 1.5 and 1.6 we find that the growth of a temperature asymmetry with time due solely to expansion is $t_s\,\Delta h$. This implies

$$\frac{d}{dt}\begin{pmatrix}\epsilon_a\\ \epsilon_w\end{pmatrix}_{Exp} = \frac{\Delta\begin{pmatrix}\epsilon_a\\ \epsilon_w\end{pmatrix}}{\Delta t}$$

$$= \frac{t_s \Delta h \begin{pmatrix}1\\ 1\end{pmatrix}}{t_s} = \Delta h \begin{pmatrix}1\\ 1\end{pmatrix}. \qquad (1.12)$$

Combining this with the previous result we obtain a final differential equation for ϵ_a and ϵ_w:

$$\frac{d}{dt}\begin{pmatrix}\epsilon_a\\ \epsilon_w\end{pmatrix} = \Delta h \begin{pmatrix}1\\ 1\end{pmatrix} + \frac{nI(t)\sigma_T c}{1}\begin{pmatrix}-1 & 0\\ -1/2 & -23/30\end{pmatrix}\begin{pmatrix}\epsilon_a\\ \epsilon_w\end{pmatrix}. \qquad (1.13)$$

Using the result from Appendix A1 that $\Delta h = \Delta h_0 / A^2 W$ and noting that

$n = n_o/A^2W$ simplifies the expression to

$$\frac{d}{dt}\begin{pmatrix}\epsilon_a\\ \epsilon_w\end{pmatrix} = \frac{\Delta h_o}{A^2W}\begin{pmatrix}1\\ 1\end{pmatrix} + \frac{n_o I(t)\sigma_T c}{A^2W}\begin{pmatrix}-1 & 0\\ -1/2 & -23/30\end{pmatrix}\begin{pmatrix}\epsilon_a\\ \epsilon_w\end{pmatrix}. \quad (1.14)$$

It is also shown in Appendix A1 that A and W can be expressed in the following way:

$$A = A_o\,(t/t_o)^{2/3}$$
$$W = A + qA^{-1/2}, \quad ; \quad (1.15)$$

which demonstrates their time dependence explicitly, leaving only one unknown function of time in the equation I(t). The use of q here should not be confused with the deceleration parameter. I only use it for consistency with Thorne's notation. Since we have no theoretical or experimental handle on the functional dependence of I(z), I will follow Rees and set it equal to one in order to obtain a useful approximate solution. Adding this to the above, we obtain the following two differential equations for the asymmetry parameters:

$$\frac{d\epsilon_a}{dt} + \frac{n_o\sigma_T c}{A^3{}_o(t/t_o)^2 + qA_o{}^{3/2}(t/t_o)}\,\epsilon_a = \frac{\Delta h_o}{A^3{}_o(t/t_o)^2 + qA_o{}^{3/2}(t/t_o)}$$

$$\frac{d\epsilon_w}{dt} + \frac{n_o\sigma_T c}{A^3{}_o(t/t_o)^2 + qA_o{}^{3/2}(t/t_o)}\left(\frac{1}{2}\,\epsilon_a + \frac{23}{30}\,\epsilon_w\right) = \frac{\Delta h_o}{A^3{}_o(t/t_o)^2 + qA_o{}^{3/2}(t/t_o)}. \quad (1.16)$$

Solutions to these are easy to obtain and are given by

$$\epsilon_a = \frac{\Delta h_o}{n_o \sigma_T c}\left(1 + \frac{qt_o}{A_o^{3/2} t}\right)^{n_o \sigma_T c t_o / q A_o^{3/2}}$$

$$\epsilon_w = \frac{15\Delta h_o}{7 n_o \sigma_T c}\left(1 + \frac{qt_o}{A_o^{3/2} t}\right)^{n_o \sigma_T c t_o / q A_o^{3/2}}, \qquad (1.17)$$

which asymptotically approach

$$\epsilon_a = \frac{\Delta h_o}{n_o \sigma_T c}$$

$$\epsilon_w = \frac{15\Delta h_o}{7 n_o \sigma_T c} . \qquad (1.18)$$

In the event that q is a small number, as long as $t > qt_o/A_o^{3/2}$, these values are reached and, in fact, it is shown in Appendix A2 that ϵ being small is equivalent to requiring that q be small.

From the asymptotic solutions we can now compute $\epsilon = \frac{1}{2}(\epsilon_a + \epsilon_w)$ and the degree of polarization $(T_a - T_w)/T$.

$$\epsilon = \frac{11}{7}\frac{\Delta h_o}{n_o \sigma_T c}$$

$$= \epsilon_o \qquad (1.19)$$

$$(T_w - T_a)/T = \frac{8}{7}\frac{\Delta h_o}{n_o \sigma_T c} \sin^2\theta$$

$$= \frac{8}{11}|\epsilon| \sin^2\theta$$

This is the scattering induced polarization which we wished to demonstrate. Although the assumption that $I(t)$ is identically equal to one is unrealistic, the solution so obtained may now be applied to more tenable pictures of the evolution of the universe to test for an anisotropic expansion.

II. APPARATUS

2.1 THE MEASUREMENT OF LINEARLY POLARIZED RADIATION

In order to measure and understand the effect of a cosmological linear polarization, we must first understand how polarized radiation is measured. The simplest kind of polarimeter is shown in Figure 2.1a. It consists of a polarization sensitive antenna, of which the simplest is the center fed, linear dipole shown, followed by a radio receiver. To measure polarization, you aim the polarimeter at a source and rotate it until you obtain the maximum signal. The angle between the axis of the dipole and some suitable reference position is the angle of the polarized signal; and the difference between this signal and lowest signal received, as the device is rotated through 360 degrees, is proportional to the magnitude of the polarization. This method is fine and,because of its simplicity,is probably the best as long as the signal is strong enough to give a clear difference between maximum and minimum.

In many practical applications the signal is quite small and has to compete with a large amount of system noise from the receiving equipment itself. In this case the apparatus in Figure 2.1b is better. It consists of two antennas of the dipole type with their polarization sensitive directions oriented at right angles to each other and each connected to its own receiver. When this is aimed at a source, a signal S_i will appear at the output of each receiver:

$$\begin{aligned} S_1 &= c(T_u + T_p \cos^2\theta + T_{REC_1}) \\ S_2 &= c(T_u + T_p \sin^2\theta + T_{REC_2}), \end{aligned} \tag{2.1}$$

where T_u is the temperature of the unpolarized radiation from the source,

T_p is the temperature of the polarized component,

θ is the angle of the polarization with respect to antenna one,

C is a proportionality constant depending on the gain of the receivers, the method of detection, and the receiver bandwidths.

T_{REC} is the equivalent noise temperature of each receiver.

Subtracting the two signals gives an expression for T_p and θ,

$$S_1 - S_2 = c[T_p \cos 2\theta + (T_{REC_1} - T_{REC_2})]. \tag{2.2.}$$

If the noise figures of the two receivers are the same, the second expression in the brackets has mean zero and, for sampling times long compared to the reciprocal of the receiver bandwidth, a Gaussian distribution. Thus the time average of this term is zero and we can define

$$Q = \frac{< S_1 - S_2 >_{Time}}{c} = T_p \cos 2\theta. \tag{2.3}$$

Rotating the antenna system by forty-five degrees gives another pair of signals,

$$\begin{aligned} S_1' &= c[T_u + T_p \cos^2(\theta + \pi/4) + T_{REC_1}] \\ S_2' &= c[T_u + T_p \sin^2(\theta + \pi/4) + T_{REC_2}], \end{aligned} \tag{2.4}$$

from which a second parameter can be defined in a similar way

$$U = \frac{< S_1' - S_2' >}{c} = T_p \sin 2\theta. \tag{2.5}$$

In terms of these parameters the polarization temperature and angle are given as

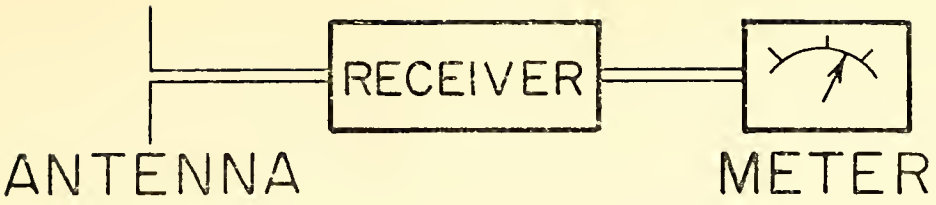

(a)

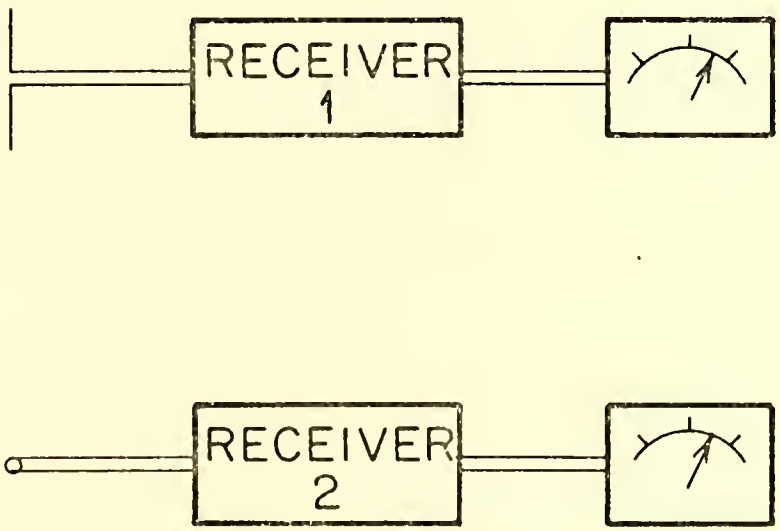

(b)

FIG. 2.1

TWO TYPES OF POLARIMETER

$$T_p = \sqrt{Q^2 + U^2}$$
$$\theta = \frac{1}{2} \text{ ARCTAN } \left(\frac{U}{Q}\right) . \tag{2.6}$$

It is clear that these two parameters, known as the Stokes parameters, uniquely determine the polarization of a source and thus together form a complete set of orthogonal measurements to determine this quantity.

For many applications this type of polarimeter works quite well, but it too has limitations. Even when one finds two receivers with well matched noise figures, drifts in the gain of the devices, which are not necessarily random in nature, can cause problems. If the signal one is seeking to measure is of the same order as the product of the receiver noise and the size of the average fluctuations in gain between the two receivers, serious errors in the measurement result. These errors cannot be averaged out. A solution to this problem, diagrammed in Figure 2.2, is the replacement of the two receivers with a single Dicke receiver which is set to switch synchronously between the two antennas.[45] The power entering each antenna is written as

$$T_1 = T_u + T_p \cos^2\theta$$
$$T_2 = T_u + T_p \sin^2\theta. \tag{2.7}$$

The signal after the switch and before the receiver is given by

$$Q = T_1 - T_2 = T_p \cos 2\theta \, f(\omega t), \tag{2.8}$$

where $f(\omega t)$ is a periodic function at the switching frequency, with amplitude one, which is dependent upon the switching characteristics of the receiver and the modulating signal. After passing through the

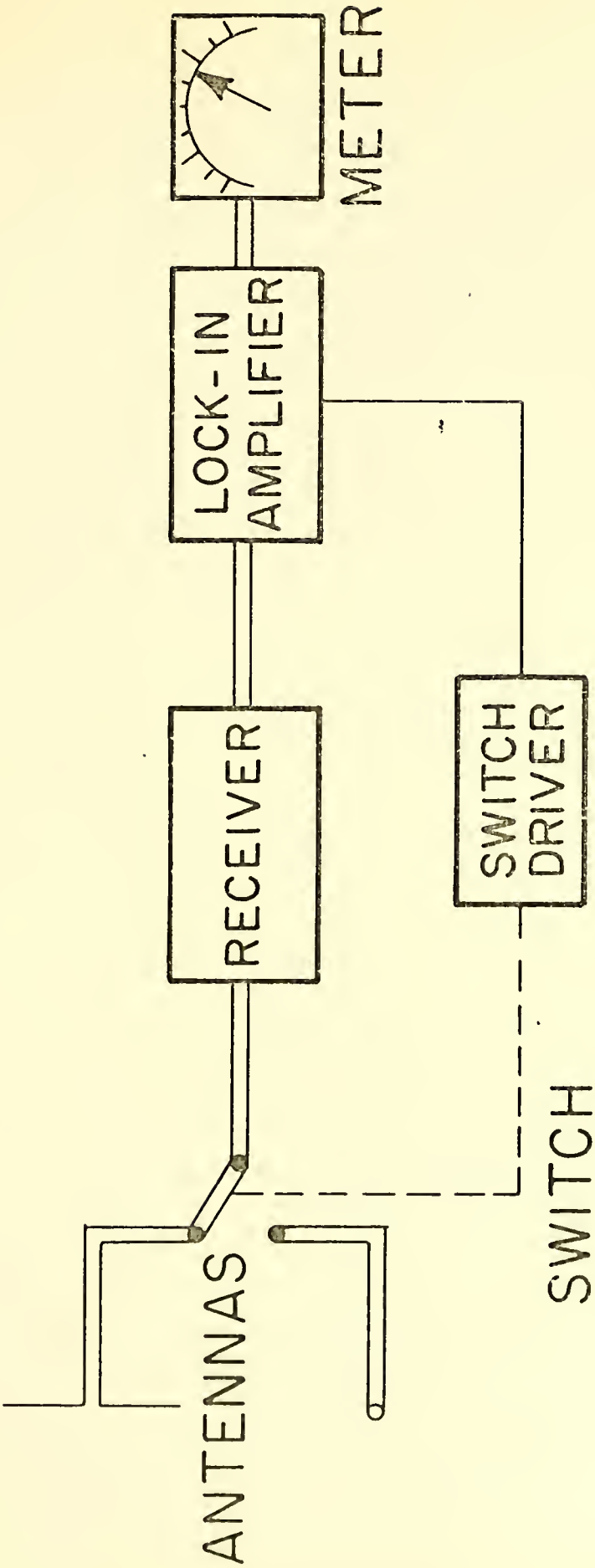

FIG. 2.2

DICKE POLARIMETER

receiver, the signal picks up a contribution due to receiver noise, which is a sum of contributions at all frequencies up to the cutoff of the IF and video amplifiers. In particular, the contributions due to gain fluctuations are at low frequencies, which means that by choosing the switching frequency high enough, we can isolate the wanted signal from the gain fluctuations. Now if the signal is processed through a phase sensitive detector like a lock-in amplifier, only the wanted signal and those noise contributions with frequencies in a limited bandwidth around the switching frequency are recovered and the contributions from gain fluctuations are excluded:

$$S = c[Q + T_{REC}\ (\Delta\nu)]. \tag{2.9}$$

Again taking a time average we can recover the parameter Q,

$$Q = \frac{\langle S \rangle_{Time}}{c}\ . \tag{2.10}$$

If the antennas are rotated by 45 degrees, U can be measured in a similar way.

The above progress is not gained without cost. By switching between the two antennas we are only looking at each one half of the time and effectively throwing away half the available signal. The minimum detectable signal in a radio receiver as a function of system noise temperature, integration time, and bandwidth is given by[46]

$$\Delta T_{min} = \frac{T_{REC}}{\sqrt{\Delta\nu\Delta t}}\ . \tag{2.11}$$

This tells us that if we have a receiver with bandwidth $\Delta\nu$ and we wish to measure Q or U to an accuracy ΔT then we must carry out the above time average for a period Δt in order to eliminate the effects of T_{Rec}. For the Dicke receiver, since we are throwing away half the

signal, things become worse by a factor of two:

$$\Delta T_{min} = 2 \frac{T_{REC}}{\sqrt{\Delta\nu\Delta t}} . \qquad (2.12)$$

If, instead of a wide band pre-multiplication amplifier, a narrow band tuned amplifier is used, then the first harmonic at the switching frequency alone is extracted and the corresponding loss in sensitivity is $4/\pi\sqrt{2}$. This loss is more than made up for by the freedom from overloading and simpler amplifiers made possible by this approach. Finally, if the switching is also done sinusoidally (something which is often done as a matter of convenience), the sensitivity is further reduced by the factor $4/\pi$. Putting these together gives the expression for a sinusoidally switched Dicke radiometer with narrow tuned video amplifier

$$\Delta T_{min} = 2\sqrt{2} \frac{T_{REC}}{\sqrt{\Delta\nu\Delta t}} . \qquad (2.13)$$

2.2 TERRESTRIAL OBSERVATION OF A COSMOLOGICAL LINEAR POLARIZATION

Next we ask, what kind of signal does polarized background radiation produce in an earthbound radiometer, given the orientation of the axis of the asymmetric expansion with respect to the rotation axis of the earth, the latitude of the observer, and the direction in which the observer is looking. In order to simplify the question and the subsequent analysis, I will assume that the earthbound observer will make all his observations by pointing his polarimeter at the zenith. It will turn out later that there are sound experimental reasons for this procedure in addition to the computational ones.

If we were to step away from the earth for a moment and aim our polarimeter in a direction at an angle θ with respect to the axis of the universe, and if we aligned our polarimeter with the sensitive axis of the antenna aligned with the coplanar direction, then from equations 1.9 we find that we would measure a Stokes parameter Q given by

$$\begin{aligned} Q &= T_w - T_a \\ &= T(\epsilon_w - \epsilon_a) \sin^2\theta, \end{aligned} \tag{2.14}$$

or in an equivalent, and for my purposes more convenient, form as

$$T_w - T_a = (T_w - T_a)_{max} \sin^2\theta. \tag{2.15}$$

Now, stepping back on the earth which is rotating about an axis, which forms an angle Φ with respect to the symmetry axis of the universe, I observe the zenith which is a direction whose declination is given by the latitude of the point of observation and whose right ascension is just the local sidereal time at the observation site. Figure 2.3 is a schematic representation of the situation, showing the experimental geometry.

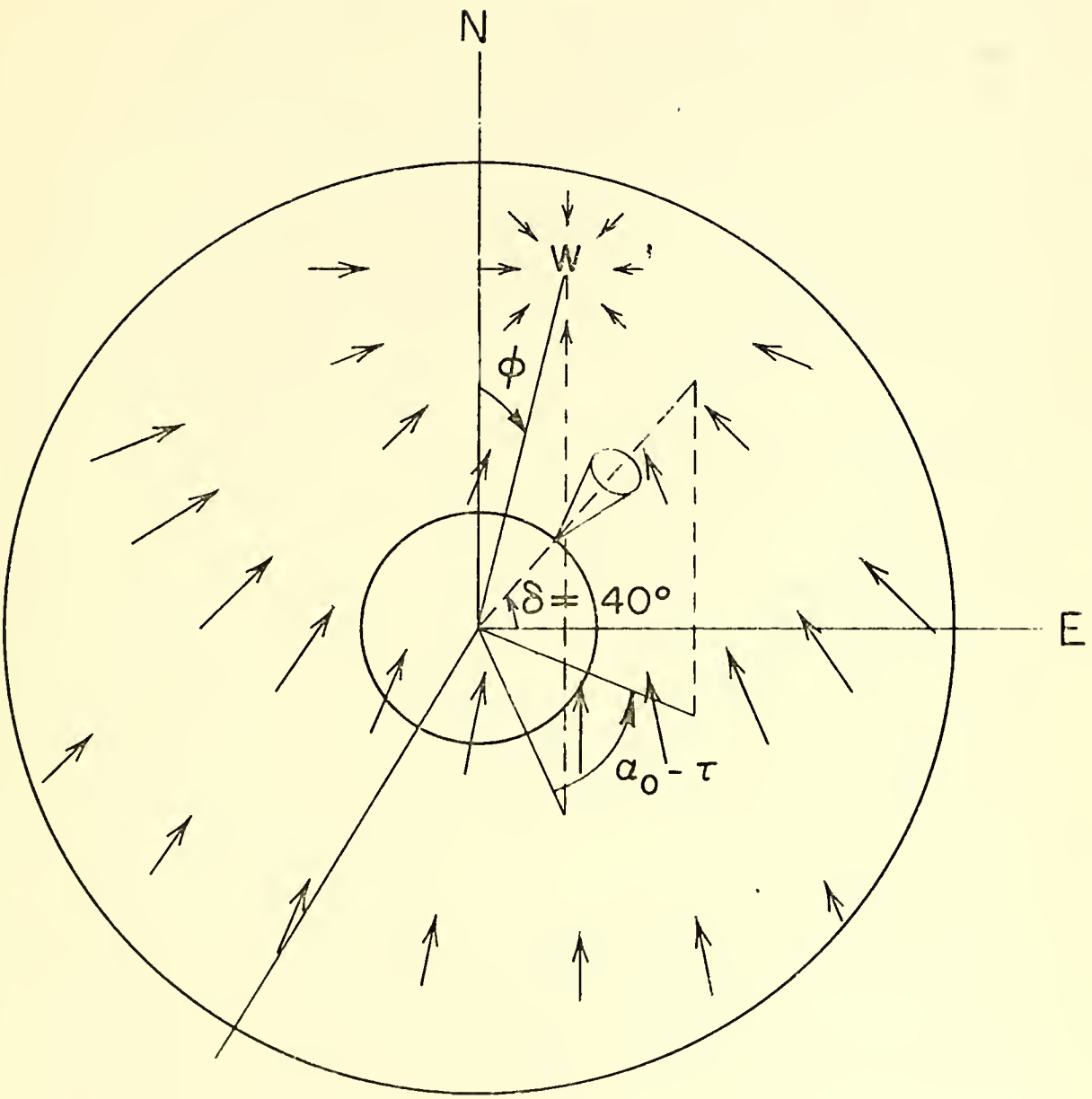

FIG. 2 3

RELATIONSHIP BETWEEN AN AXIALLY SYMMETRIC COSMOLOGICAL POLARIZATION AND THE ROTATION AXIS OF THE EARTH

Given this situation, I show in Appendix A4 that the polarimeter will measure a quantity

$$T_1 - T_2 = (T_w - T_a)_{max} \left\{ [\cos^2\delta(1 - \frac{3}{2}\sin^2\Phi) + \sin^2\Phi(1 - \frac{1}{2}\cos^2\delta)\cos 2(\alpha_o - t) - 1/2 \sin 2\Phi \sin 2\delta \cos(\alpha_o - t)] \cos^2\beta - [\sin^2\Phi \sin\delta \sin 2(\alpha_o - t) - \sin 2\Phi \cos\delta \sin(\alpha_o - t)] \sin^2\beta \right\}, \quad (2.16)$$

where t is the local mean sidereal time at the observation site,

β is the angle between the sensitive direction of the antenna and the direction of the North Celestial pole,

δ is the declination of the zenith, and

α_o is the right ascension of the symmetry axis of the universe.

As the polarimeter sweeps out a circle of constant declination night after night, we can add the output records synchronously at the sidereal rate and, in this way, perform the time average needed to overcome the noise temperature of the receiver. If we alternate the orientation of the radiometer between two positions 45 degrees apart, we can make the two orthogonal measurements, necessary to uniquely specify the polarization, simultaneously.

From equation 2.16 we can see that by grouping all the constants together, the result can be expressed more simply as

$$T_1 - T_2 = (T_w - T_a)_{max} \left\{ A + B\cos 2(\alpha_o - t + \delta_1) + C\cos(\alpha_o - t + \delta_2) \right\}, \quad (2.17)$$

with relationships between the coefficients easily derivable from the parent equation. This form displays the harmonic dependence upon local sidereal time and thus the dependence upon right ascension. In general then, each measured parameter will have a 12 hour and a 24 hour harmonic component. It is the object of this experiment to measure the polariza-

tion parameters as well as possible and look for the harmonic dependence which would indicate the existence of a large scale polarization of cosmological origin, obeying this simple model.

2.3 THE FARADAY SWITCHED POLARIMETER

The device used to perform this experiment is an offspring of the Dicke type receiver called a Faraday switched polarimeter. As is shown in Figure 2.4, instead of two polarization sensitive antennas connected to the receiver through a single pole double-throw switch, one conical type polarization insensitive antenna is used. This horn feeds into an axially symmetric chamber containing a thin ferrite rod. Application of a sinusoidal magnetic field to the ferrite causes the incoming radiation to be rotated back and forth synchronously. The chamber is followed by a dual mode transducer which resolves incoming radiation into two orthogonal components and thus acts as an analyzer. One port of the dual mode transducer is connected to the receiver while the other is dumped into a suitable matched load. The net effect of this arrangement is the same as was obtained using two antennas, only now some of the matching problems have been eliminated. With the field on the ferrite in one direction, radiation from one polarization is rotated by the Faraday effect and passes through the dual mode transducer into the receiver. If the field is then reversed and the magnitude has been adjusted so that the radiation is rotated 90 degrees in going from one state to the other, the orthogonal polarization will now be presented to the receiver. In this way a switched signal, proportional to the temperature difference between the two directions, is produced.

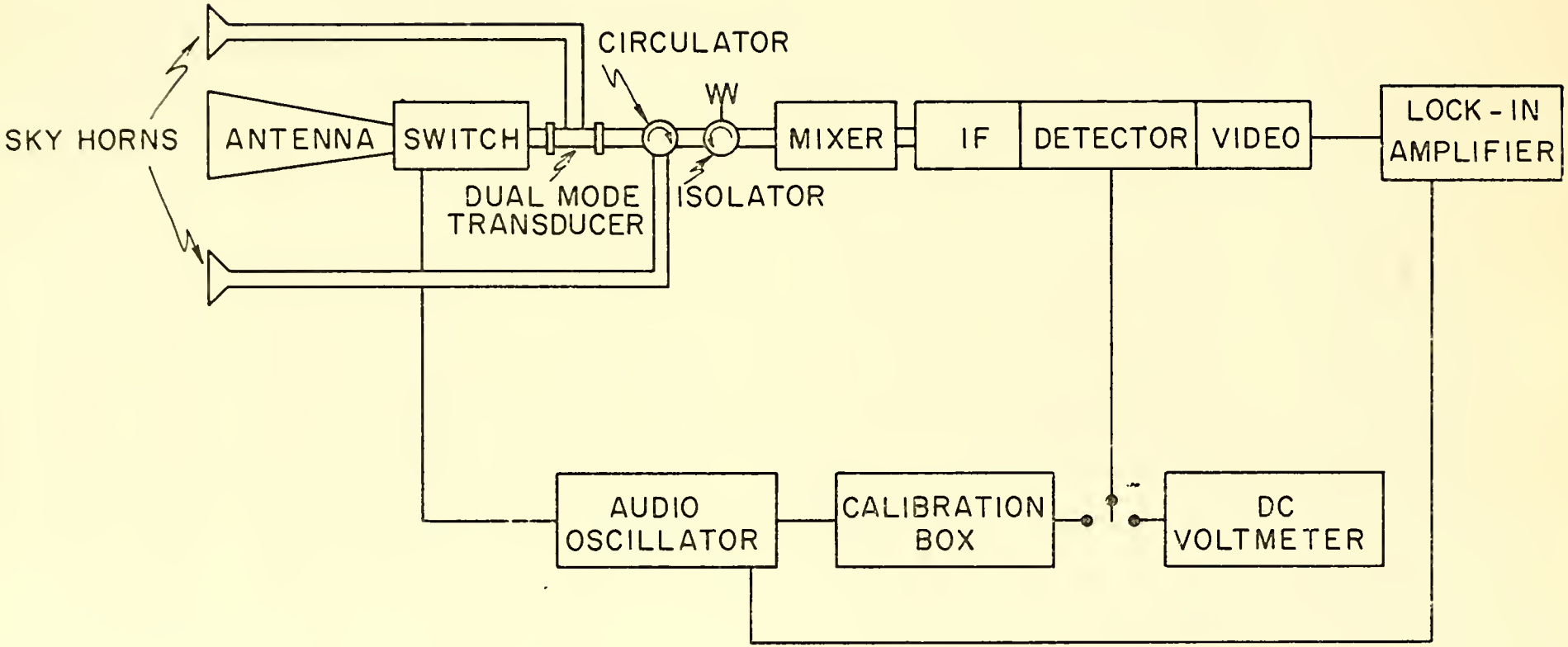

FARADAY SWITCHED POLARIMETER

FIG. 2.4

The rest of this chapter will be devoted to this device and its calibration. Frequent reference will be made to Appendix B where the detailed specifications and measured parameters are given.

2.4 THE ANTENNA

A conical optimum gain horn with an aperture choke for suppression of the backlobes was used in this experiment. Provision was made for insertion of a calibration probe in the side of the horn and this feature was used for part of the time. Later analysis showed that the probe increased the sensitivity of the polarimeter to ground radiation, an effect which is described quantitatively in Appendix B1.

The full width of the main lobe between half power points was about 15 degrees, giving the polarimeter a resolution of one hour in right ascension.

2.5 THE SWITCH

The heart of the polarimeter is the Faraday switch used to rotate between orthogonal polarizations. Because it was used to produce the signal, any departure from ideal operation will intimately affect the results of the experiment. In this section I will present those principles of operation necessary to an understanding of the polarimeter. A more detailed analysis of the operating principles and parameters of the switch and how they are affected by outside influences is given in Appendix B2.

The basic principles can be most easily understood by considering the switch as an ideal Faraday rotator. As shown in Figure 2.5, the active element is a thin cylindrical piece of ferrite mounted coaxially

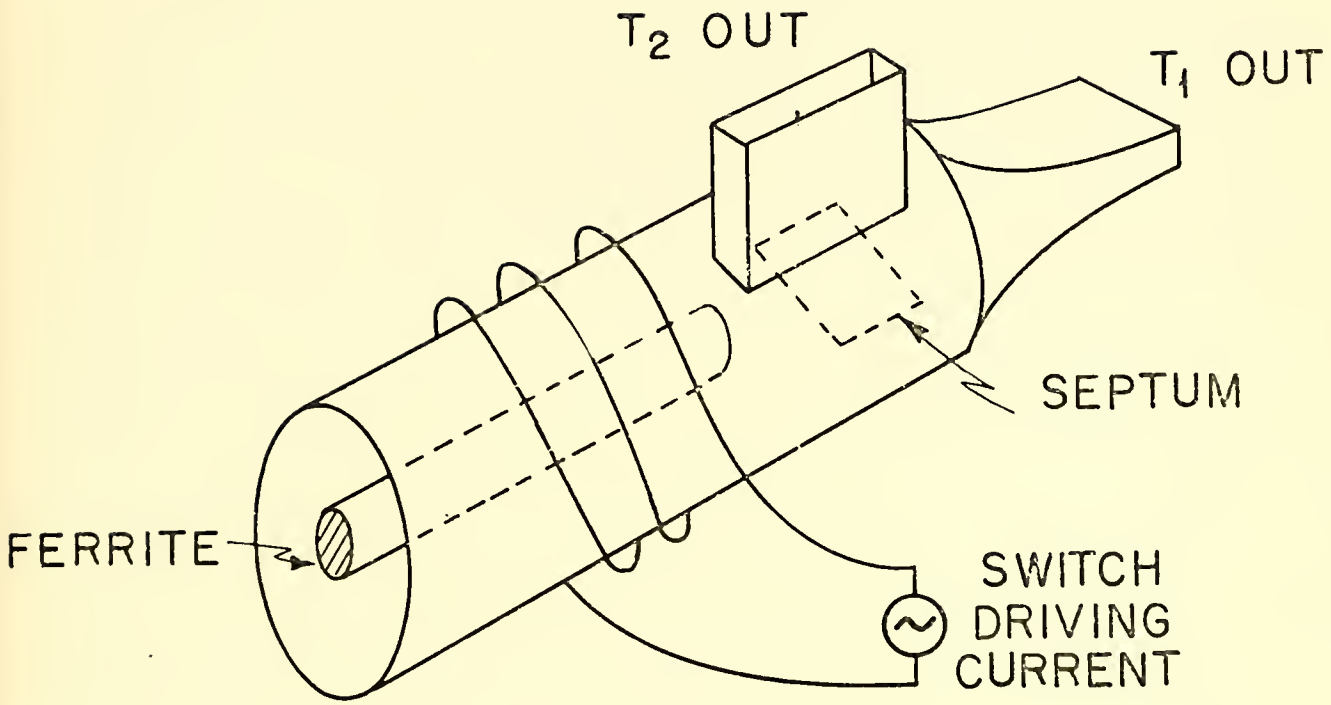

THE SWITCH

FIG. 2.5

in a section of circular waveguide around which is wrapped a coil of wire. Putting a current through the coil produces a longitudinal magnetic field in the ferrite which in turn produces the Faraday effect, by causing the magnetic moments of the ferromagnetic ions to align with the field. If then, a circularly polarized wave propagates along the axis, its velocity is either decreased or increased depending on whether its helicity has the same or opposite sense, relative to the precession of the ferromagnetic moments. Since a plane polarized wave is composed of equal left and right circularly polarized components, one component is retarded relative to the other and the plane of polarization is rotated. By placing an oscillating current of sufficient magnitude on the driving coil, the propagating wave can be rotated first in one direction by 45 degrees over the length of the ferrite, and when the current is reversed, 45 degrees in the opposite direction. Now if the rotator is followed by a dual mode transducer which acts as an analyzer, separating the radiation into two orthogonal components, one obtains, in either arm of the transducer, radiation which is modulated at the switching frequency. The amplitude of the modulated signal is proportional to the difference between two polarization components of the incoming radiation, referenced to a coordinate system, which has one of its axes bisecting the angle between the sensitive directions of the dual mode transducer. The graphs in Figure 2.6 depict the result for incident polarized radiation in two situations. In one case, the direction of polarization is parallel to one of the axes of the reference coordinate system, giving the maximum signal. In the other case, the incident radiation is at an angle of 45 degrees to this direction or, in other words, parallel

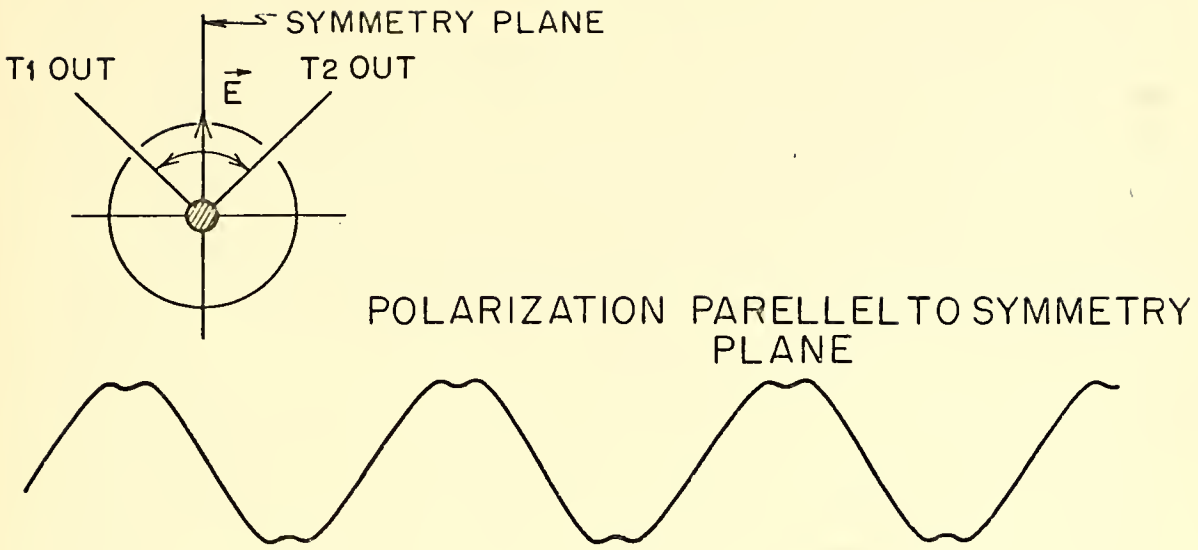

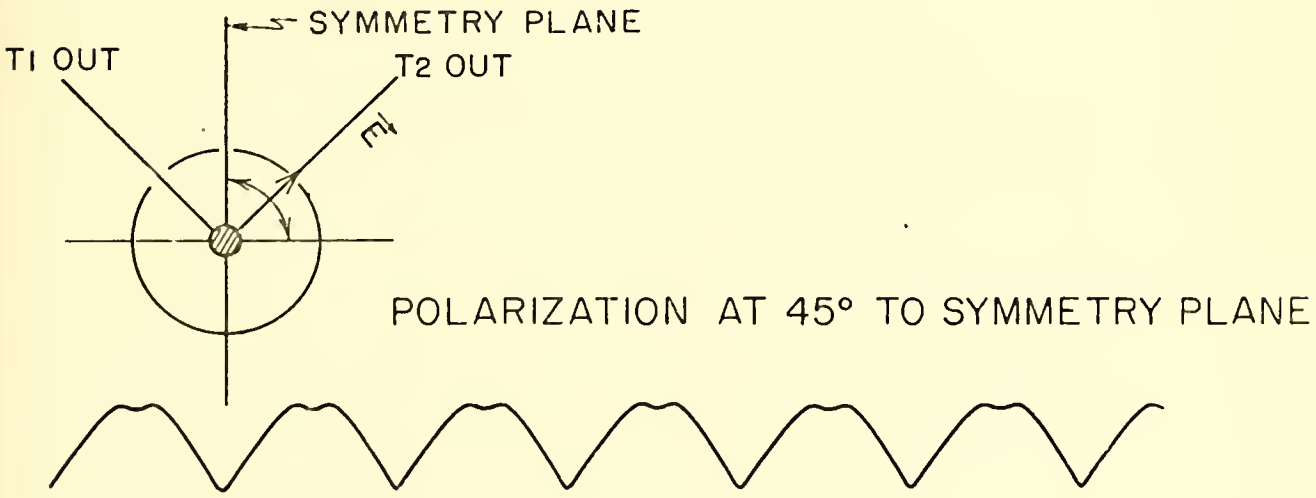

FIG. 2.6

SIGNAL PRODUCED BY THE SWITCH FOR TWO ORIENTATIONS OF INCOMING RADIATION

to the direction of one of the sensitive directions of the dual mode transducer, giving zero signal. That this second case in fact gives zero signal comes about because the output has a periodicity at twice the switching frequency. Since the lock-in extracts only the first harmonic of the switching frequency, this contribution is zero.

It should be noted that I am looking at temperature, a quantity which for an extended blackbody source is related to the incident power by

$$P = kT\Delta\nu, \tag{2.18}$$

in the Rayleigh-Jeans portion of the spectrum. Therefore, I am sensitive to a quantity which is proportional to the square of the incident field. Because of the lack of dependence on the sign of the incident field, positions of the polarimeter which differ by a rotation of 180 degrees about the ferrite axis are equivalent, while positions 90 degrees apart are opposite in sign.

In practice this symmetry is not perfect, being broken by an offset due to absorption and emission of radiation by the switch itself. To make matters worse,this offset is a function of three major perturbing influences; the temperature of the ferrite, changes in ferrite magnitization due to DC fields like the earth's magnetic field, and mechanical strains transmitted to the ferrite through its mountings. In order to reduce the effects of temperature, the polarimeter was mounted in a temperature controlled environment, where, except under extreme conditions of heating or cooling, the temperature was maintained to about one degree centigrade. Effects from magnetic fields were removed by encasing the entire microwave front end of the device in a shield constructed of extremely high

permeability material. Finally, mechanical strains were kept to a minimum by mounting the axis of the polarimeter vertically, and thus parallel to the gravitational force.

One can choose to take the signal out of either arm of the dual mode transducer, since these outputs give the same signal, differing only by 180 degrees in phase at the switching frequency. In fact, it would be possible to use both outputs to advantage as will be discussed later. In this experiment I used only one arm, attaching a small standard gain horn, aimed at the sky, to the other. In this way the unwanted signal was discarded and the unused port of the switch was terminated in a cold load.

Returning to the subject of the switch offset, though I have described how perturbing influences were kept from altering it, I haven't yet explained how to eliminate it as an instrumental effect. The easiest way to accomplish this is to take alternate readings of the polarization, separated by a rotation of 90 degrees about the ferrite axis. This would result in two signals

$$S_1 = T_1 + T_{offset}$$
$$S_2 = - T_1 + T_{offset}, \qquad (2.19)$$

and by subtracting them we would obtain

$$S_1 - S_2 = 2T_1, \qquad (2.20)$$

a quantity in which the offset has been subtracted out. Of course, this procedure depends on being able to shield out the effects of the earth's magnetic field and the perturbing influence of gravitational strains. Having the polarimeter axis vertical keeps the gravitational forces constant with rotation.

2.6 THE CIRCULATOR AND ISOLATOR

These components are designed to provide isolation between the microwave mixer and the back of the switch. Because the local oscillator is not perfectly monochromatic and still has a power contribution at the sideband frequencies, isolation is made necessary to prevent power leakage back up the waveguide. For the Gunn oscillator used, the power in the sidebands was on the order of -140 db below the center frequency power. As this is a factory claim and wasn't directly measured, adding a factor of ten might be appropriate; so -130 db might be more comfortable. For input powers of between one and two millawatts this means that there may be as much as 2×10^{-16} watts left in the sidebands. It might not seem like much but being in the Rayleigh-Jeans portion of the spectrum and with a bandwidth of 96 MHZ, we find that a millidegree corresponds to 1.4×10^{-18} watts. In short, we may find as much as 100 millidegrees worth of power leaking out of the mixer in the sidebands we are sensitive to.

Ordinarily this would probably be no problem, but the reflection coefficient of the back of the switch is a strong function of magnetization. For that reason one doesn't want to provide it with a nice source of power at the sideband frequencies, which it could modulate through reflection and send back, masquerading as real signal.

To provide isolation, a circulator and isolator were inserted between the switch and mixer. Figure 2.7 diagrams the operating characteristics of the circulator. Power leaving the switch is passed to the mixer. Power from the mixer is passed to the third port which is terminated in a standard gain horn aimed at the sky, and a cold

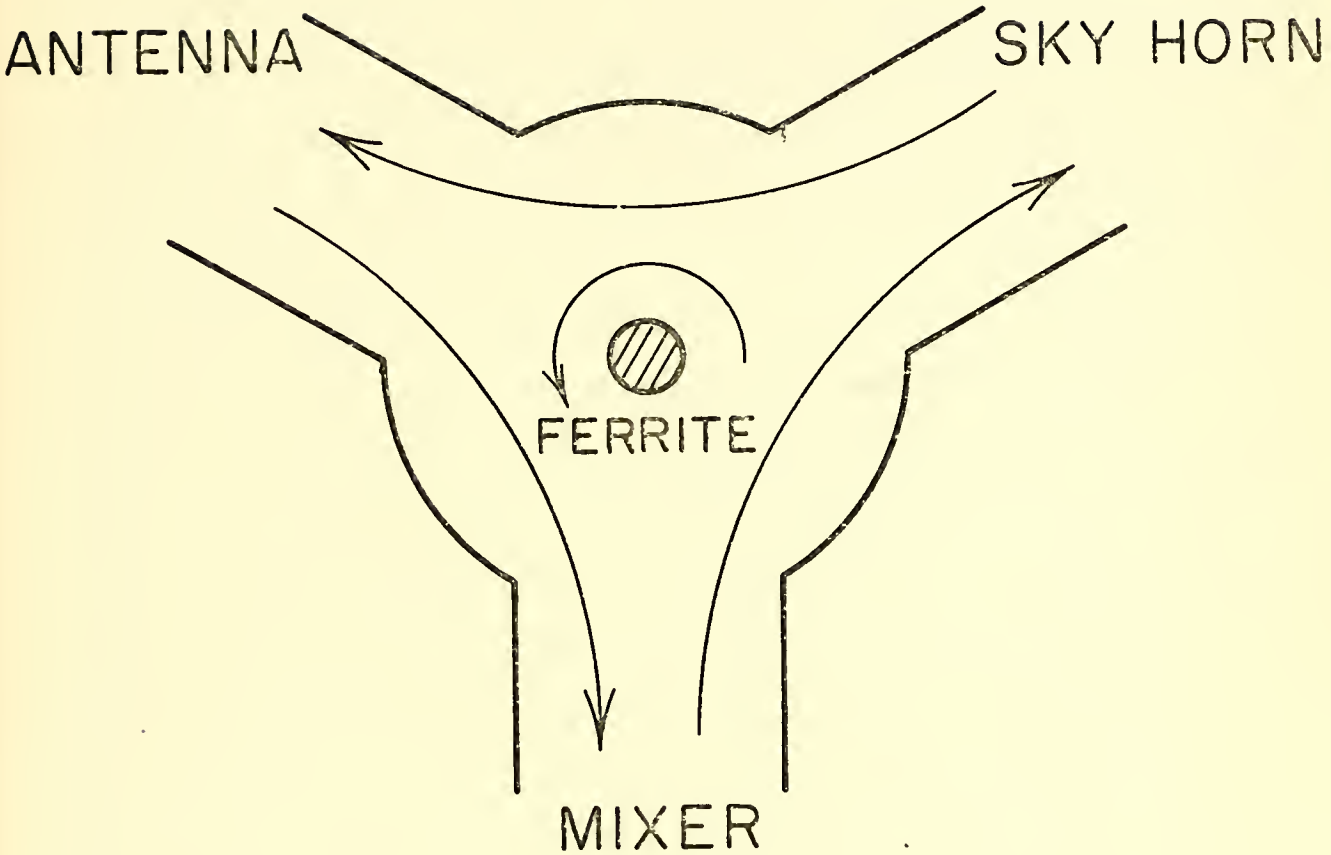

CIRCULATOR

FIG. 2.7

5 ^{o}K from the sky illuminates the back of the switch, giving it little signal to modulate by reflection. About 30 db worth of isolation is provided in this way.

Another 40 db is provided by the isolator, which is inserted between the circulator and the mixer. It, in fact, is also a circulator but with its third port terminated internally in a matched load. The addition of these two devices reduces the residual local oscillator power reaching the switch to about 10^{-23} watts or 10^{-5} mdeg. K, a much more acceptable level.

Because these two devices depend on ferrites for their operation, it was thought that perhaps, like the switch, they would be subject to variations in their operation due to stray magnetic fields. It might not have been as severe in this case, as neither of these devices uses an oscillating field to produce a signal. None the less, they pass the offset produced by the switch and if their absorption is changed by a large enough amount, they could produce an orientation dependent signal. For this reason they were tested by an application of field along the axes of their ferrite devices. This should be their most sensitive directions. No measurable effect was observed for fields up to 11 Gauss.

2.7 THE RECEIVER

A standard off the shelf model heterodyne receiver, having a separate double balance mixer and IF amplifier was used at 9.37 GHz. The width of each sideband was 48 MHz, giving a total receiver bandwidth of 96 MHz. Local oscillator power was provided by a Gunn oscillator coupled through a frequency meter and attenuation pad.

The only unusual operating characteristic of this receiver was a bad impedance match between the mixer preamplifier and IF amplifier. If a resonant length of cable were used and the system perturbed by some electrical interference, oscillatory breakdown could occur. By judicious choice of cable lengths and careful shielding against interference, the problem was eliminated. Because a chart record of the lock-in output was kept and because this problem gave a striking signature, those times that it did occur (as the result of extreme electrical interference in thunderstorms, for example) were easily seen and the affected data eliminated.

One modification was made to the standard IF amplifier and that was the addition of a BNC terminal to allow measuring the DC voltage at the second detector before it was capacitively coupled to the video stage. As will be explained in the next section, this was needed for the calibration procedure used.

2.8 CALIBRATION

Because there were no standard polarized blackbody sources available for calibration at 3.2 cm, another method had to be employed. The procedure used involves two steps. First, the change in voltage at the second detector as a function of antenna temperature is determined, followed by a measurement of the gain through the rest of the system.

The calibration was begun by measuring the DC voltage at the second detector with the polarimeter looking at the sky. The size of this voltage is proportional to the power entering the horn from the sky plus some offset due to receiver noise and biasing of the electronics. Next, a piece of eccosorb microwave absorber, a good unpolarized blackbody source at ambient temperatures, was placed over the antenna and the voltage again read. This time the voltage is proportional to the power from the eccosorb plus the same offsets that were present before. In this way we have measured the following two quantities:

$$V_{sky} = C_1 (T_{sky} + T_{offset})$$

$$V_{eccosorb} = C_1 (T_{eccosorb} + T_{offset}), \qquad (2.21)$$

where C_1 is a constant dependent on the gain of the receiver. Combination of these two allows one to determine C_1 and thus the response in Volts/^{o}K of the receiver to this point. Now imagine that the polarimeter is looking at an extended blackbody source which is 100% polarized, such that the temperature in the direction of polarization is equal to the temperature of the eccosorb and such that the temperature in the orthogonal direction is equal to the temperature

of the sky. If this source were aligned with the symmetry axis of the switch, it would generate a signal at the second detector at the switching frequency, like that in Figure 2.8. In this way one can say that a polarized source of magnitude $T_{eccosorb}-T_{sky}$ will produce a signal at the second detector whose effective first harmonic peak-to-peak value is $1.164\ (V_{eccosorb}-V_{sky})$, where the calibration value derived in Appendix B2 has been used. Redefining C_1 to accommodate the calibration factor, it can be written

$$C_1 = \frac{1.164\ (V_{sky}-V_{eccosorb})}{(T_{sky}-T_{eccosorb})} \quad , \tag{2.22}$$

where a typical value for $V_{sky}-V_{eccosorb}$ was 7.0 mv measured to an accuracy of .1 mv and for $T_{sky}-T_{eccosorb}$ was $-290.0^{\circ}K$ measured to an accuracy of $.25^{\circ}K$.

Next, I insert a calibration signal at the second detector. This is a sinewave of known peak-to-peak amplitude, which is derived from the audio oscillator through a special circuit. With the lock-in phase adjusted for maximum signal, the output voltage is read and a second parameter C_2, which gives the gain of the rest of the receiver, is computed:

$$C_2 = \frac{V_{lock\text{-}in}}{V_{calibration\ signal}} \quad . \tag{2.23}$$

The product of C_2 and C_1 then gives the gain of the entire polarimeter.

In practice, the measurement was done utilizing the output of the entire data collection system rather than just that of the lock-in. In this way the overall gain of the entire system could be measured and individual intermediate steps, where human reading errors could multiply, were minimized.

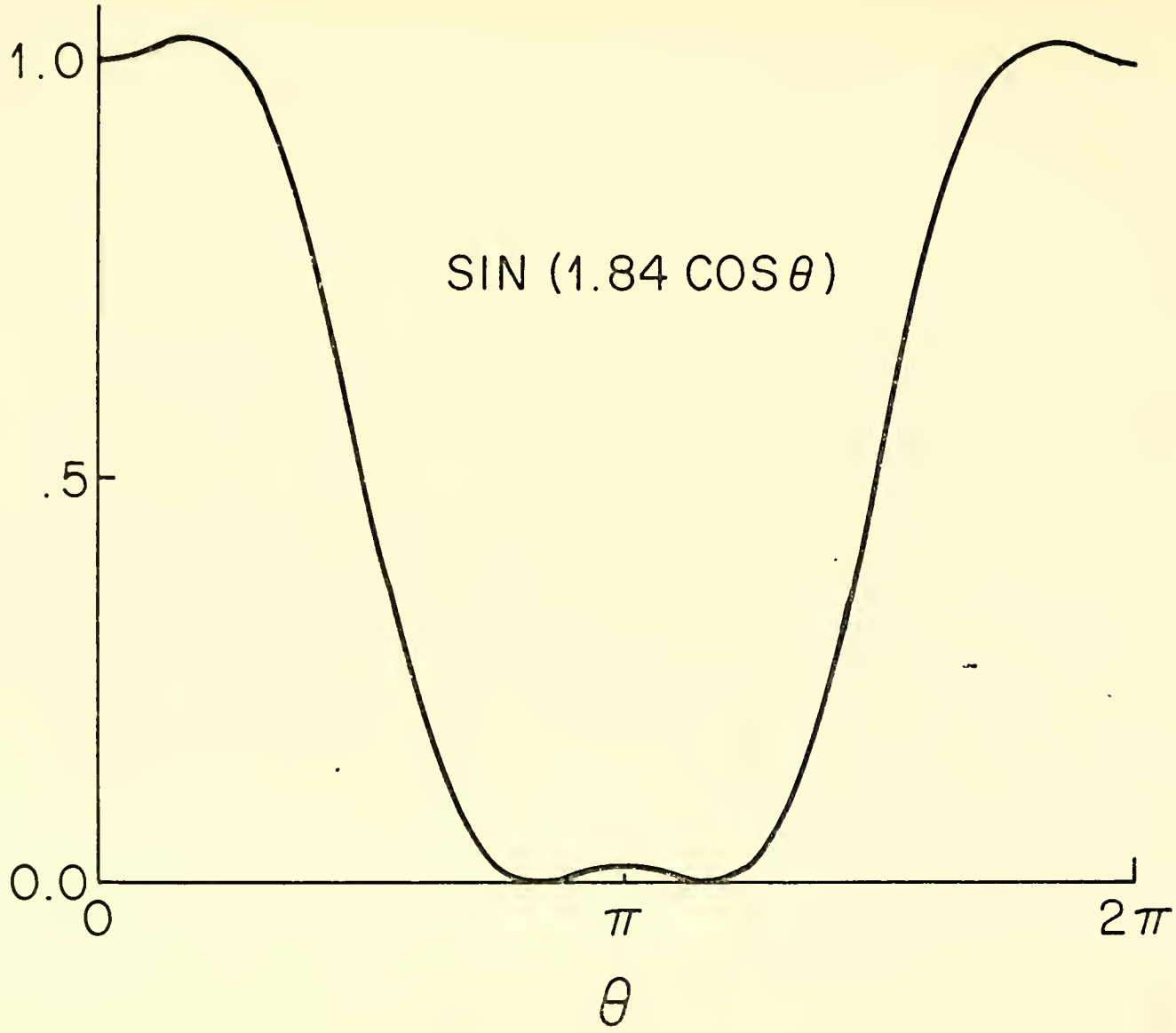

FIG. 2.8
OUTPUT WAVEFORM FROM SWITCH
FOR MAXIMUM SIGNAL

Although the temperature of the eccosorb was always known, that of the sky couldn't be with great certainty. For this reason, I picked a standard temperature of $5^{\circ}K$ for the sky for purposes of calibration, even though, typically, the actual temperature will fluctuate from $5\text{-}10^{\circ}K$. It was felt that the error introduced by this assumption was only on the order of 5/300 or about 2%, which, compared to the uncertainty due to receiver noise alone, is negligible.

After a few calibrations it became clear that the overall gain stability of the system was good enough that a calibration on the order of once a week was enough to ensure good accuracy. Table 2.1 is a list of calibrations taken during the data collection period. The units in which C_1 C_2 is expressed are counts per second at the output of the voltage-to-frequency converter per millidegree Kelvin at the polarimeter input. The output of this device is directly proportional to the lock-in output and was used to make integration of the signal and digitization of the result much easier. The entries are segregated into two groups because work on the receiver changed the overall gain midway through the data taking period. Figure 2.9 plots the distributions of C_1 C_2 for the two groups, which appear approximately normally distributed. It is interesting to note that if the data had been interpreted using the mean of each group of calibrations, the expected error in the calibration, equal to the standard deviation of the measurements divided by the mean, would be about 2.8%.

As a final comment, I would like to discuss the overall effectiveness of this method considering that there was no true polarized

TABLE 2.1

POLARIMETER CALIBRATIONS

First Group

Date	C_1C_2 (CNTS/mdeg K)	Date	C_1C_2 (CNTS/mdeg K)
8/11/72	40.50	11/20/72	40.31
8/24/72	39.91	11/29/72	40.91
9/7/72	42.28	12/7/72	39.81
9/18/72	40.75	12/14/72	39.84
9/26/72	40.57	12/29/72	39.08
10/2/72	41.79	1/4/73	40.43
10/10/72	42.85	1/7/73	39.11
10/23/72	41.96	1/11/73	41.64
10/30/72	39.82	1/18/73	42.61
11/9/72	41.55	1/26/73	41.75

$\overline{C_1C_2} = 40.83$ $\quad \sigma_{C_1C_2} = 1.14$ $\quad \sigma_{C_1C_2}/\overline{C_1C_2} = .028$

Second Group

Date	C_1C_2 (CNTS/mdeg K)	Date	C_1C_2 (CNTS/mdeg K)
2/4/73	43.93	4/24/73	45.00
2/13/73	44.42	5/6/73	44.49
2/20/73	42.40	5/29/73	43.32
2/28/73	42.72	6/11/73	44.81
3/9/73	44.12	7/4/73	45.63
3/20/73	44.21	7/20/73	44.07
3/28/73	44.16	8/1/73	45.24
4/6/73	44.48	8/10/73	47.47
4/16/73	43.00		

$\overline{C_1C_2} = 44.32$ $\quad \sigma_{C_1C_2} = 1.19$ $\quad \sigma_{C_1C_2}/\overline{C_1C_2} = 0.27$

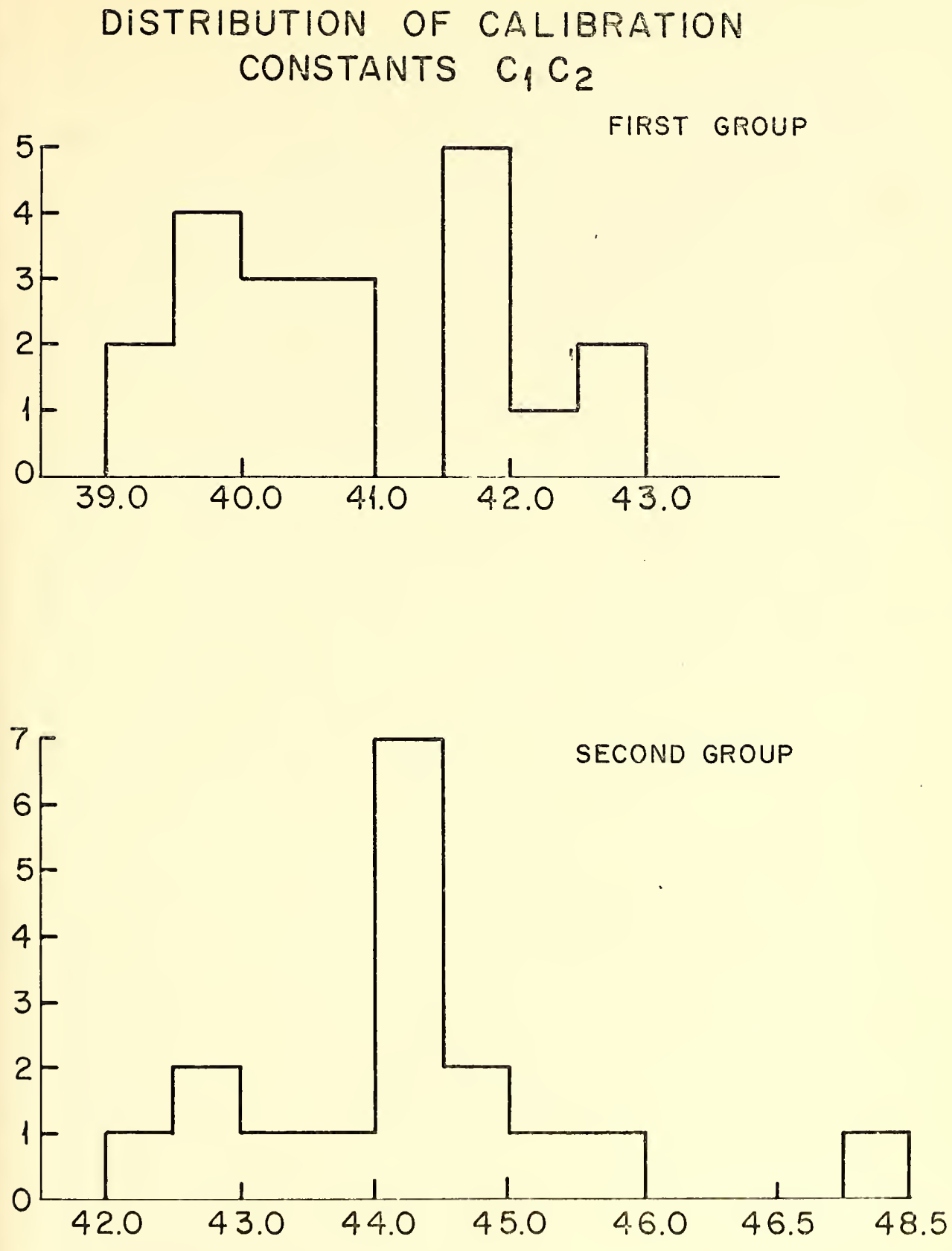
DISTRIBUTION OF CALIBRATION CONSTANTS C_1 C_2
FIRST GROUP
5
4
3
2
1
0
39.0
40.0
41.0
42.0
43.0
SECOND GROUP
7
6
5
4
3
2
1
0
42.0
43.0
44.0
45.0
46.0
46.5
48.5

FIG. 2.9

standard against which to calibrate. As a means to justify the method, I made a comparison between the results given by my polarimeter and the results given by a polarization sensitive power radiometer, both measuring the same polarized source. Used as a source was a klystron radiating through a rectangular standard gain horn suspended four stories above the measuring devices and giving an almost fully polarized signal. A reading with the polarimeter was sandwiched in between two readings taken with the power radiometer. Agreement between the two radiometer readings was 2%, while agreement between their mean and the polarimeter reading was 4%. Because the power radiometer and the polarimeter used most of the same components (the only difference being the addition of a second dual mode transducer and comparison load between the antenna and the mouth of the switch), changing configuration meant partial dismantling of the apparatus. During this time great care was taken to maintain alignment with the source, but not all the microwave plumbing was uniform. For this reason it was felt that the errors involved were ones of alignment and not ones of calibration. The error in each measurement due to receiver noise was only about 15 mdeg.K, while the signal was about 280^{o}K. Given this, the discrepancy between the two power radiometer measurements must also have been due to alignment, as the calibration constant only varied about .1% between the two runs.

III. PROCEDURE

3.1 EXPERIMENTAL PROCEDURE

For the reasons explained in previous sections, data were taken by the polarimeter with its axis mounted vertically and observing the zenith. Rotation of the earth sweeps out a circle of constant declination in the sky. By rotating the polarimeter by 45 degrees between observations, measurement of the Q and U Stokes parameters can be made.

There is one additional source of systematic error inherent in this method. This source can be eliminated by data taking procedures. In Chapter 2 and Appendix B2, I discuss at length the problems of external parameters influencing the offset of the Faraday rotation switch. Aside from these problems, it is easy to show that any offset at all is harmful. For example, for a switch offset of 50 millidegrees entering the receiver, any gain fluctuations on the order of 2% will produce systematic effects of around a millidegree in the data, an unacceptable level. To remove this we must find some way of eliminating the offset from the data in such a way that the effects of nonrandom gain fluctuations will be eliminated.

A possible solution utilizes the symmetry properties of the switch itself. With the polarimeter aligned with one polarization axis north-south, it produces a signal proportional to $T_{NS}-T_{EW}+T_{offset}$. Rotating the axis of the polarimeter by ninety degrees produces a signal $T_{EW}- T_{NS}+ T_{offset}$ where the contribution due to T_{offset} doesn't change. It is a systematic effect in the polarimeter itself, and is independent of external orientation if the switch is

properly shielded. The readings taken in the two positions are subtracted to give

$$\frac{S_1 - S_2}{2} = T_{NS} - T_{EW} ,$$

from which the offset has been eliminated. Of course, how well this subtraction works depends on how constant the offset is over the rotation timescale. Keeping the integration times short reduces sensitivity to longer term drifts in the offset.

Combining the idea of rotating the polarimeter by ninety degrees between equivalent readings with the need to take readings separated by forty-five degrees, one arrives at a natural solution to both problems; that is, by rotating by forty-five degree steps around the compass. In this way one measures both Stokes parameters and for each measurement there are two others separated from it by ninety degrees, to subtract out switch offset.

The polarimeter was mounted on a rotating platform with magnetically actuated reed switches located at forty-five degree intervals around the periphery, and labeled one through eight. Data taking was conducted by rotating the table in a clockwise direction until it actuated a switch, stopping and integrating for five minutes at that position, and then recording the result and moving on to the next position. When the recording at position eight was completed, the table would reverse direction and return to position one.

To obtain the most useful results, it was felt that the following experimental quantities had to be measured:

1. The output of the integrator, which sums the polarimeter output for five minutes.
2. The time of the observation. This quantity can be easily converted to local mean sidereal time which is identical to the right ascension of the observation.
3. The angular position of the polarimeter, which determines which Stokes parameter one is measuring and with which sign.
4. The temperatures of the switch, the inside of the observation shed, and the outside environment. The first of these was needed to correlate the switch offset with temperature. I also kept track of the inside shed temperature to insure that my temperature controller was working properly. In the event that ground radiation became a large problem, measuring the temperature of the surrounding buildings would help in removing the effect.

The apparatus involved in taking and recording these observations is the subject of the next few sections. Figure 3.1 is a diagram of the entire system. It was felt that by automating as much as possible, the chances for human error could be reduced, especially in an undertaking of this type where the observations extend over many months.

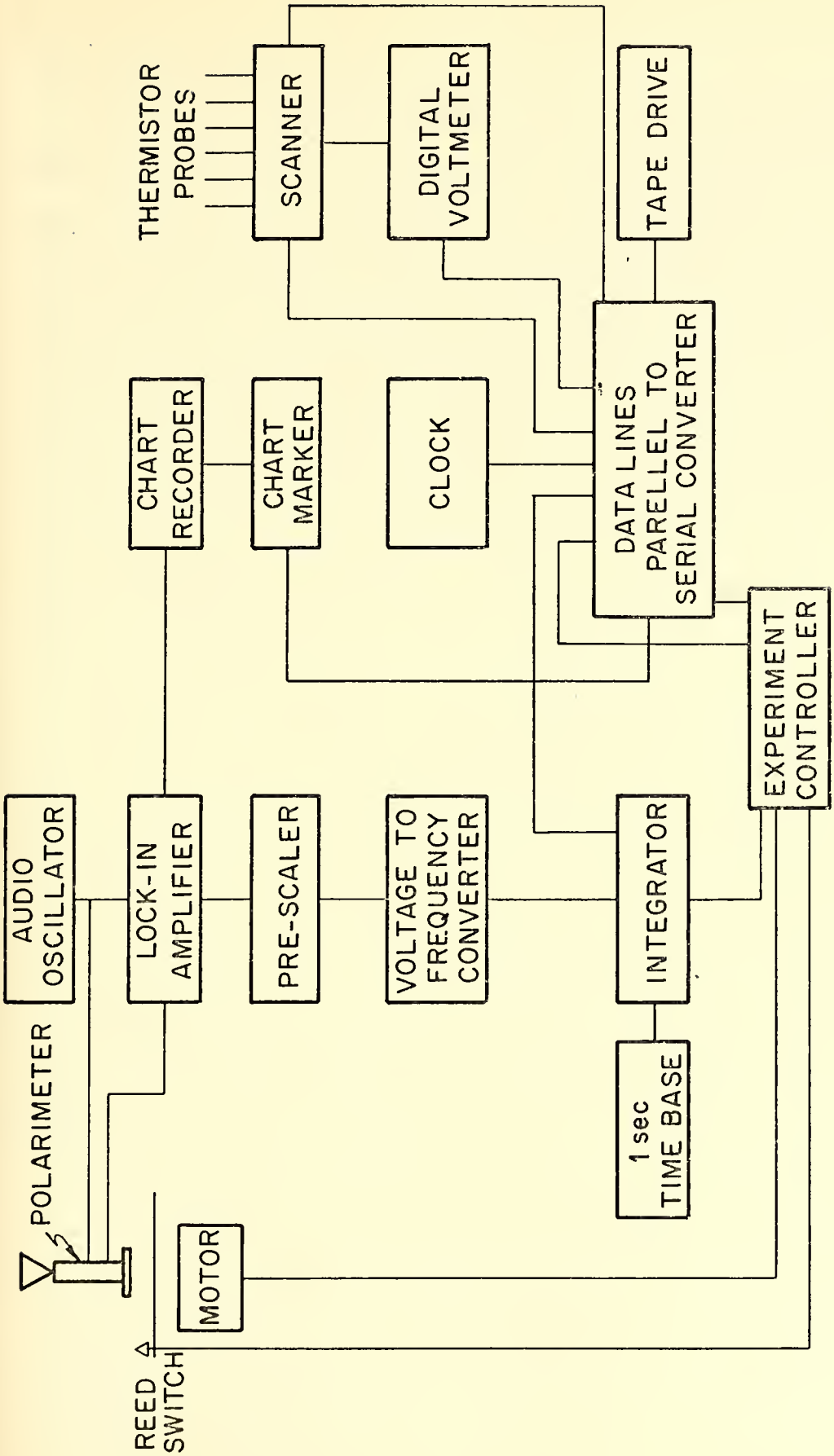

DATA COLLECTION SYSTEM

FIG. 3.1

3.2 PREPARATION OF SIGNAL

The output of the lock-in amplifier was recorded in two ways. First the output itself was recorded directly so that any abnormalities in function or signal received could be detected and evaluated. Two examples which were easiest to detect in this way were rain and local thunderstorm activity. The most dependable way found for recording was a hand wound, galvanometer movement, Esterline Angus chart recorder which could be left unattended for two to three days at a time. Combined with a marking device which delineated the integration periods in each position and the hours of the day, I was able to relate a disturbance in the apparatus to a recorded data point.

To integrate the output of the lock-in, I used a prescaler and voltage-to-frequency converter which changed a -10 to +10 volt output to a 0 to 100,000 Hz signal. Integration was performed by a remotely controlled scaler, which was capable of integrating the signal for periods from zero to 9999 seconds, could divide the input by powers of ten, and could display six digits of output information in binary coded decimal form. This result was presented in parallel form to a parallel to serial converter which prepared it for recording.

3.3 TIMING

Time information was provided by a clock built by E. Groth and used primarily for pulsar timing. Needless to say its micro-second accuracy was not needed, but it did provide time in days, hours, minutes and seconds of Eastern Standard Time relative to epoch 1970.0. Upon completion of each integration period, the output of the clock was stored and the result presented to the parallel-to-serial converter for recording. This provided a convenient and reproducable point from which to calculate the time of the middle of each integration run.

3.4 TEMPERATURE MEASUREMENT

The temperature at key locations was measured using four linearized thermistor composites connected to a measuring circuit and digital voltmeter through a multiplexing scanner. During each run one of the thermistor probes was measured and recorded. The output of the digital voltmeter and the position of the scanner were presented to the parallel-to-serial converter for recording. It was thought that this information might be used to correlate out the temperature dependent effects.

3.5 RECORDING OF DATA

The data outputs are ultimately recorded in IBM compatible form on digital tape. The intermediary in the process is the parallel-to-serial converter. When strobed, it takes all the data presented to it in parallel form and feeds it serially one byte at a time to an incremental nine track 800 byte per inch tape unit. In addition, it controls the blocking of the data into files and records to facilitate analysis. This device plus the scaler and dvm scanner were constructed by Karl C. Davis.

3.6 EXPERIMENT CONTROL

Overall control and sequencing of the experiment was performed by an experiment control box, the function of which was to command the polarimeter, the integrator and parallel-to-serial converter and sequence their functions properly. The order of operations while the experiment was being conducted was:

1. Rotate to a new position. If at position eight, rewind until reaching position eight again and then step forward to position one.
2. Start integration.
3. Stop integration and record data.
4. Recording finished, rotate to a new position.

Cycle time for the apparatus with a three hundred second integration time was three hundred and three seconds except when rewinding, in which case it was three hundred and twenty seconds. The device would maintain this timing without losing a second for a week or more, making it very easy to spot malfunctions and timing errors.

All switching in the system is either low voltage or solid state to avoid radio frequency interference with the sensitive receiver. For this reason, AC switching for the polarimeter rotation motors is tied to the zero crossing of the line voltage, using a semiconductor triac.

IV. ANALYSIS AND INTERPRETATION

4.1 DATA EDITING

Data was taken for this experiment from 1 February 1972 until 10 August 1973. The data before 9 August 1972 was mainly for test and evaluation of the device and has been discarded out of hand. The data since that time is considered suitable for analysis and has been searched for the effects of cosmological polarization. The twelve month data set contains approximately 94,000 individual polarization measurements, of which about half were devoted to each Stokes parameter. As in any experiment of this length, bad weather, equipment malfunctions, and human errors took their toll, resulting in discarded readings.

My guiding principle in throwing away data was not to, if at all possible. When necessary it would have been best to completely automate the procedure in order to avoid human intervention with its attendant bias. But at certain points, in particular the screening of chart recordings of the lock-in output, there was no other way. In general there were four sources of abnormality in the lock-in output:

1. The most common and troublesome was rain. The polarimeter was insensitive to clouds and other forms of bad weather, but precipitation would collect on the mylar window covering the apparatus and appear as a strongly polarized signal. This would many times drive the lock-in off scale. Data showing this type of behavior was rejected along with enough data on either side to insure that all

contamination was removed.

2. The next most frequent source of interference was thunderstorm activity, especially in the summer months. This was characterized by strong and repeated noise spikes in the output signal, which caused the data to be discarded. Isolated noise spikes were not thrown away by manual means. Later stages of automated editing evaluated their effect and provided more impartial criteria for their elimination.
3. During the summer months when the sun reaches altitudes close to the zenith, its presence as a hot source produces a lock-in signal when acting on the non-symmetric antenna gain pattern. Again this data was not deleted manually but was handled later when all data with the sun above the ground shield and geometrically illuminating the antenna were discarded
4. Finally, there would be an occasional malfunction in the receiver and its associated equipment, which would usually be indicated by a lack of receiver noise in the output trace. This was easily noticed, the receiver repaired and the data removed.

A miscellaneous problem that does not fit into any of the above categories, but which at one point had me convinced that the apparatus was broken, was that of a small very inconspicuous spider. By slowly crawling around in the antenna throat he did a great imitation of serious receiver gain drifts. Naturally his virtuoso performance was eliminated.

Removal of bad data constituted the first stage of editing. Next I searched for timing errors to make sure that the automated data collection apparatus was functioning properly and that the integration periods were uniform. These events fell into two categories, clock errors and actual erratic operation. In the former case the equipment would be operating normally, but the clock would indicate the wrong time. Resetting of the clock for pulsar timing was the most common cause of this and would appear as a step function in the cycle, which would be followed by a step with the opposite sign when the correction was completed. The cycle time of the apparatus was consistent enough to enable one to reconstruct the correct time even when the step remained for several hours.

Harder to correct was difficulty due to erratic behavior of the apparatus, which was usually associated with thunderstorm activity or other forms of electrical interference. In most of these cases, where the orderly sequence of readings could not be restored, the errors were left for a later stage where they would automatically be eliminated.

On the average of every one or two weeks, the cycle would lose a second or two in phase for no apparent reason. No attempt was made to correct for this. In later processing, isolated errors in timing of up to five seconds were allowed to pass. A change in the integration period of up to five seconds means an error in the measurement of under two percent or far less than the uncertainty due to receiver noise alone.

As a final editing procedure, the problem of isolated interference spikes in the data was considered. Preliminary examination showed that after removal of switch offset, the averaged signal would be within 10 millidegrees of zero. The minimum detectable signal or standard deviation of the noise for a single processed reading was about 15 millidegrees based on measurements of scatter in the data. The clipping level for rejection of spikes was set three full standard deviations above the 10 millidegree level, at 56 millidegrees Kelvin. Only 387 points had to be eliminated in this way.

In all, out of about 94,000 points collected, only 38,029 points or about 40.4% of the data were actually used. Unfortunately they were not uniformly distributed throughout the year for two reasons. First, more data get thrown out in summer when the sun is higher in the sky. Worsening the effect was a very wet spring and early summer in the Princeton area, combined with unstable air and much electrical storm activity.

4.2 PRELIMINARY PROCESSING

The final stage of data preparation is carrying out the subtraction (described under experimental procedure) for removal of the switch offset. At this point we have two roughly equal sets of measurements of the two Stokes parameters describing the polarization. Each of these sets contains measurements at four of the polarimeter positions. One set comprises all the odd numbered switch positions and the other has the even, as in Figure 4.1. For the Q parameters, that position closest to North or position two, was called positive in accordance with normal convention. It was found by checking with a polarized source placed due North of the apparatus that this position actually pointed 11.75 degrees to the Northeast of North. I will still call this the Q' parameter (primed to distinguish it) and correct the discrepancy at a later stage. For the U' parameters, the positive direction is that closest to the Northeast or position three. Positions 180 degrees relative to two and three have the same sign by symmetry, while those 90 degrees away have the opposite sign.

To perform the subtraction, each reading was assigned its characteristic sign and then adjacent pairs of measurements within each set were averaged as in Figure 4.2. The time of observation assigned to each averaged pair is the average of the midpoints of each integration period.

If we look at this operation from another point of view, we see that what we are doing is multiplying the data by a periodic signal of frequency twice that of the polarimeter rotation frequency. This is exactly what is done in the mixer stage of a lock-in amplifier.

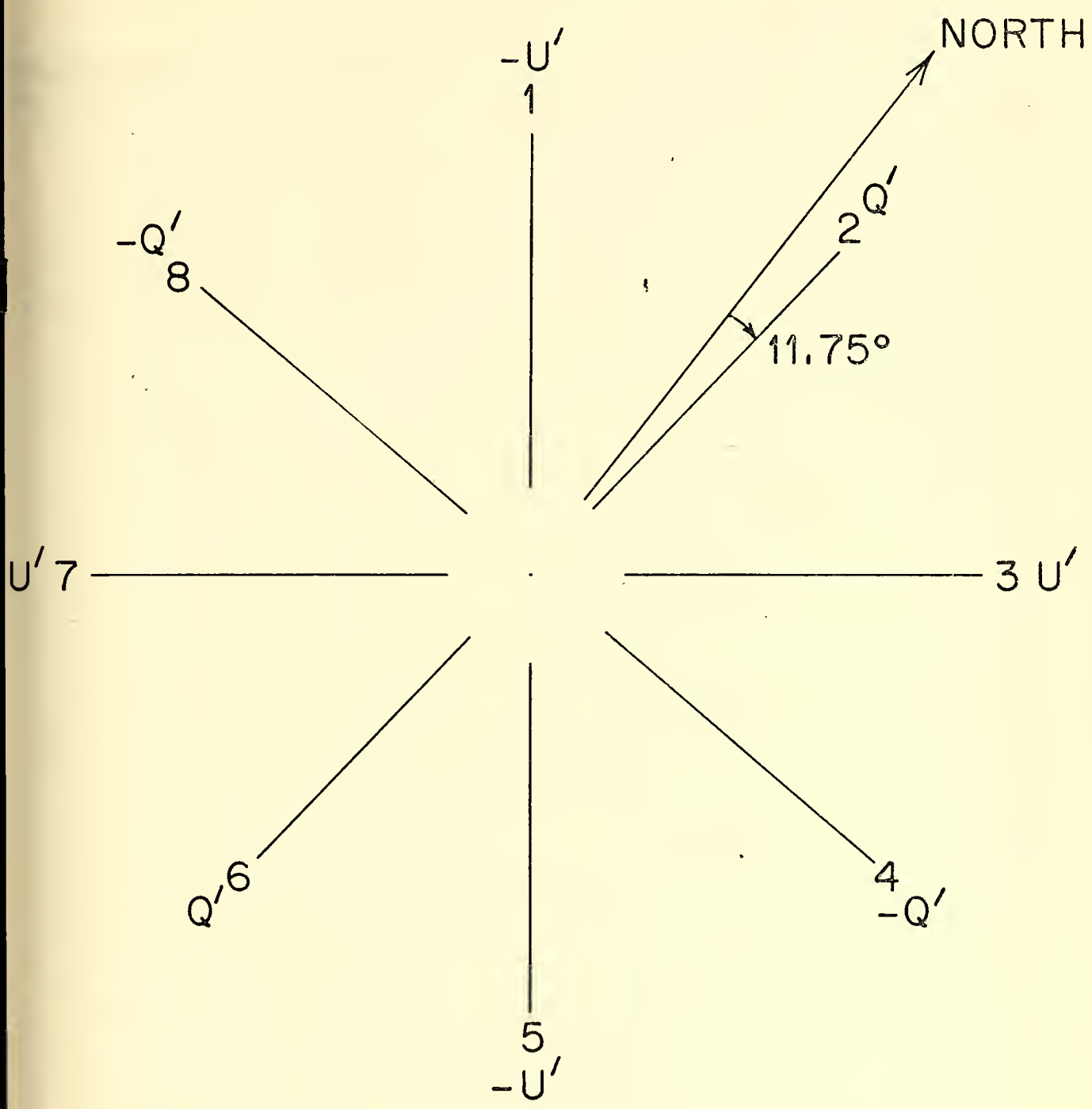

POLARIMETER POSITIONS

FIG. 4.1

POLARIMETER POSITION	TIME	INTEGRATOR OUTPUT	Q'	U'	TIME OF AVERAGE
1	15:45:39	1628.97			
				-1.54	15:48:12
2	15:50:42	1663.33			
			0.33		15:53:15
3	15:55:45	1625.90			
				-23.67	15:58:18
4	16:00:48	1663.98			
			1.13		16:03:21
5	16:55:51	1673.23			
				11.31	16:08:24
6	16:10:54	1661.72			
			7.89		16:13:27
7	16:15:57	1695.85			
				-8.43	16:18:38
8	16:21:00	1677.49			
			12.33		16:23:41
1	16:26:20	1712.71			
				-25.89	16:28:53
2	16:31:23	1652.83			
			-6.06		16:33:56
3	16:36:26	1660.93			
				4.84	16:38:59
4	16:41:29	1640.70			
			-21.76		16:44:02
5	16:46:32	1651.24			
				1.69	16:49:05
6	16:51:35	1684.21			
			26.57		16:54:08
7	16:56:38	1654.63			
8	17:01:41	1737.35			

SUBTRACTION SCHEME

FIG. 4.2

Because we do the Q' and U' parameters separately, we extract both phases of the signal simultaneously just as in a two phase or vector lock-in. To visualize things a little more clearly, consider the effect on incident DC polarized radiation as the polarimeter is rotated. The rotation causes a sinusoidal variation in intensity. Because of the 180 degree symmetry of the switch, this signal has twice the rotation frequency of the polarimeter. Now by multiplying by a periodic signal the way we have done, we demodulate the signal and extract the fundamental Fourier component for each phase, exactly as is done in a lock-in. A double lock-in technique of this type gives good immunity against effects from gain fluctuations and drifts in the switch offset, which are on a time scale longer than half the polarimeter rotation period, or twenty minutes.

4.3 ANALYSIS

I now have two sets of independent measurements, the Q' and U' parameters, each with a time resolution of about ten minutes in sidereal time. One might think that this could be interpreted as a spatial resolution in terms of right ascension. This is not true because of the low resolution of the antenna, which is only about one hour in right ascension. To bin the data on any sidereal time scale shorter than this is to attempt to display resolution which does not exist. The next logical step is to bin the data at its true resolution limit, one hour in right ascension (local sidereal time).

In order to check for serious solar effects, the binning was also carried out in solar time. After binning, Q' and U' were transformed

to the true Q and U parameters before further analysis. The results of the binning are shown in Figure 4.3 for solar time and Figure 4.4 for sidereal time. The temporal or spatial center of each bin may be obtained by subtracting thirty minutes from the bin number. In other words, bin four contains all the data between three and four hours.

In each set of data there is a DC level, which when combined from both sets gives a resultant DC polarization vector with magnitude of 1.10 ± .14 millidegrees Kelvin and direction 116.34 ± 3.64 degrees from North. On the reciprocal of this bearing is the most prominent feature on the horizon, a tower containing elevator motors on the roof of Jadwin Physics Laboratory. When reviewing the data in smaller segments, it was found that this level wasn't constant throughout the year of observation. During the first two months, the DC vector was 6.6 ± .28 millidegrees with a direction of 150.46 ± 1.21 degrees. Other than this, no other abnormalities were found. Closer examination showed that the change took place sometime close to the tenth of October. Checking my notebook, I discovered that on the fifteenth of October I had decided that the calibration probe installed in the antenna wasn't being used and should be removed. It appeared that the presence of a stub in the horn had perturbed the gain pattern enough to significantly alter the response to ground radiation, in effect, making the polarimeter six times more sensitive to the elevator tower radiation. The discrepancy in angle of about +36 degrees can be traced to the fact that the calibration probe was located approximately -40 degrees from the positive symmetry plane of the switch. When the polarimeter was aligned at 150 degrees, the probe was aimed at the tower. A check was performed with a slotted

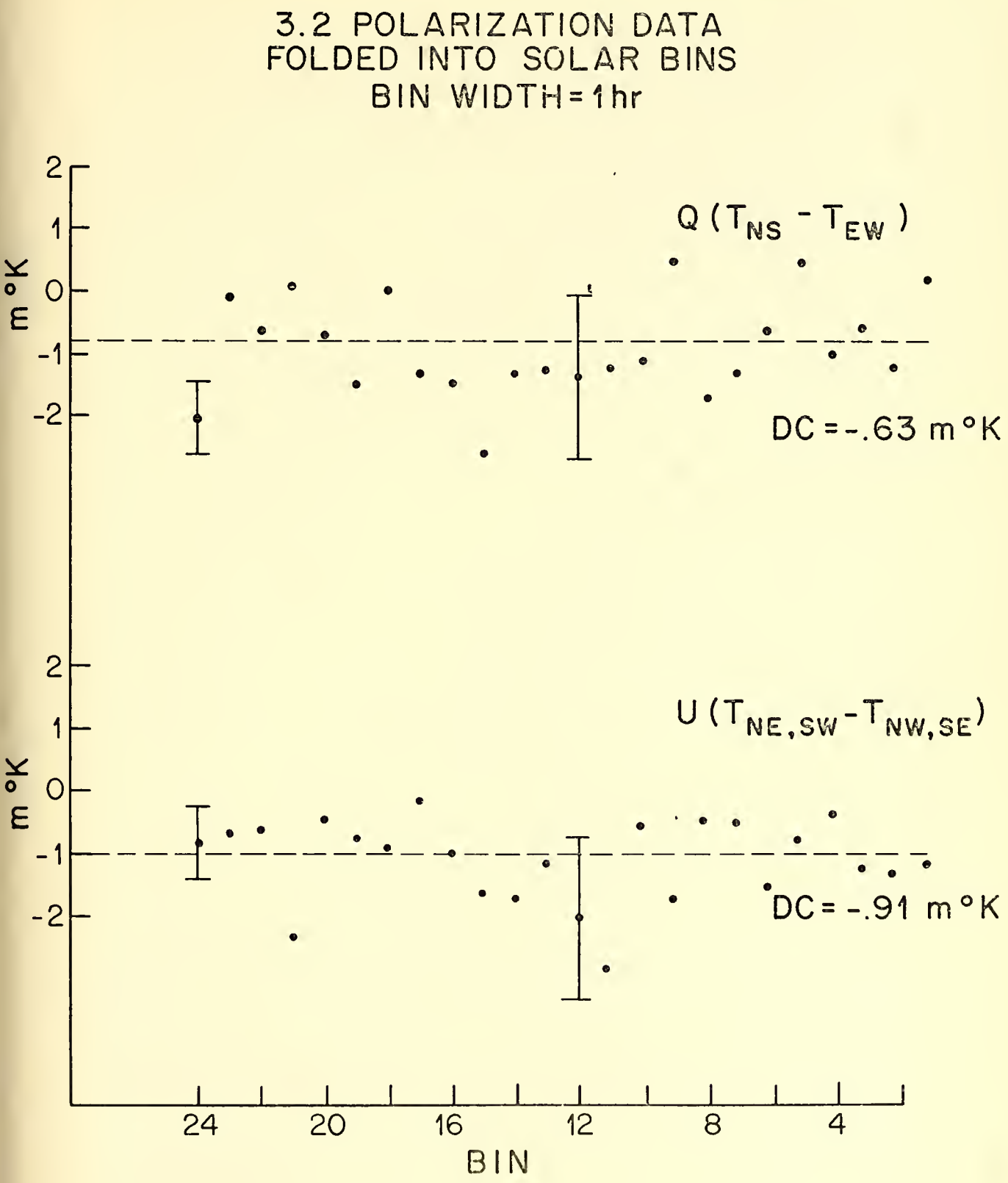
3.2 POLARIZATION DATA
FOLDED INTO SOLAR BINS
BIN WIDTH = 1 hr
Q ($T_{NS} - T_{EW}$)
DC = -.63 m°K
U ($T_{NE,SW} - T_{NW,SE}$)
DC = -.91 m°K
m°K
2
1
0
-1
-2
24
20
16
12
8
4
BIN

FIG. 4.3

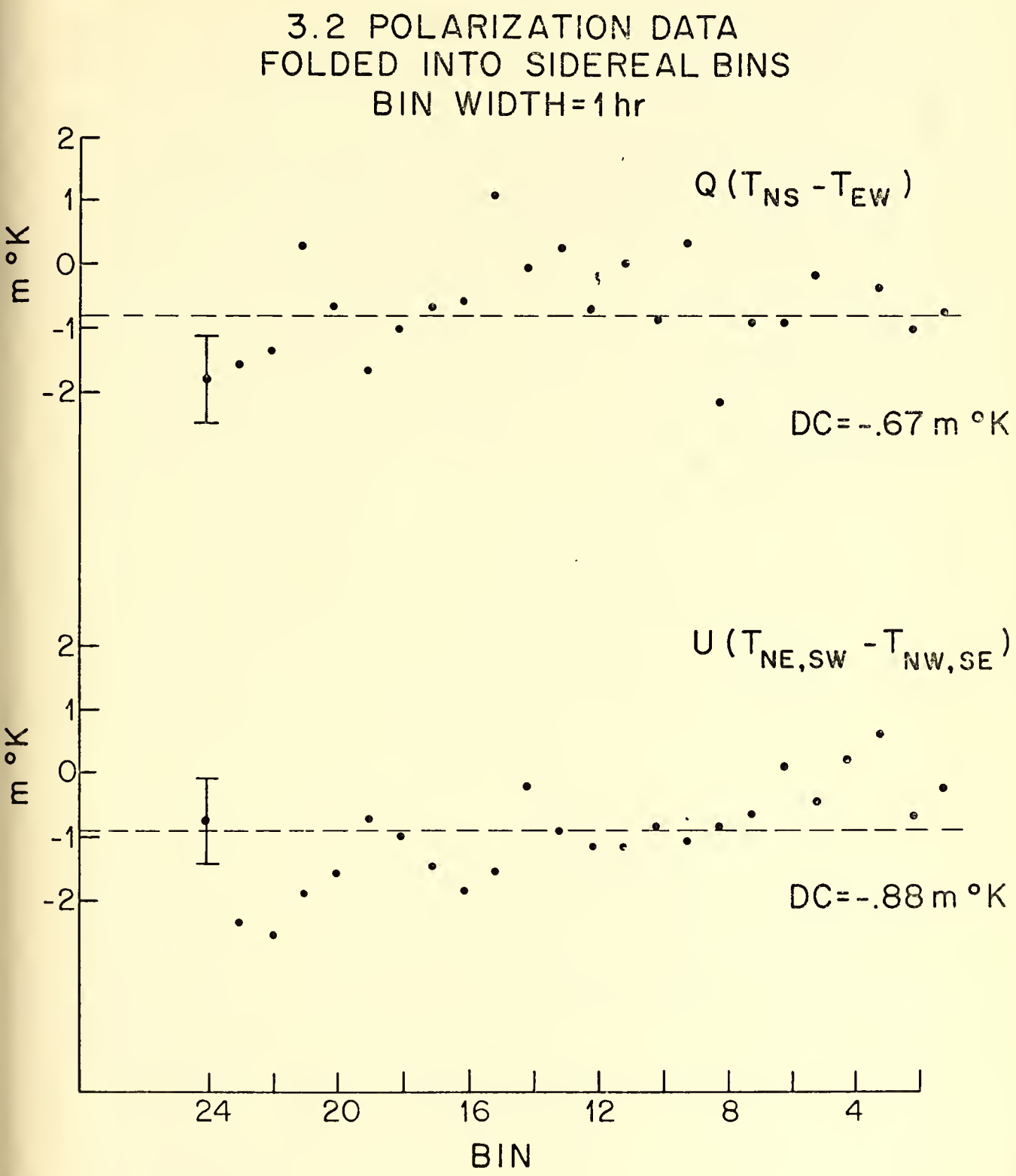
3.2 POLARIZATION DATA
FOLDED INTO SIDEREAL BINS
BIN WIDTH=1 hr
Q (T_NS - T_EW)
DC=-.67 m °K
U (T_NE,SW - T_NW,SE)
DC=-.88 m °K
m °K
2
1
0
-1
-2
24
20
16
12
8
4
BIN

FIG. 4.4

plate providing a polarized source to determine whether or not the probe changed the effective position angle of the switch's symmetry plane. No change could be detected between the position angle with or without the probe.

Because the only effect of the probe was to change the DC level of the first two months data, this effect was subtracted out by adjusting the level of these data to agree with the average level of the rest of the year. Failure to do this would have left a step function in the data and produced possible harmonic contamination from the spectrum of frequencies contained in a step. The only other alternative would have been to discard the data and no other reason to do this could be found.

It seems fairly certain that a good portion of the DC signal is due to ground radiation. From equation 2.16 with β equal to zero we obtain the expression for the Q Stokes parameter, given an axially symmetric universe. This parameter has a DC component given by

$$Q_{DC} = (T_w - T_a)_{max} \cos^2\delta \left(1 - \frac{3}{2} \sin^2\Phi\right) , \qquad (4.1)$$

where δ is the declination and Φ is the angle between the rotation axis of the earth and the symmetry axis of the universe. For β equal to 45 degrees we get the U Stokes parameter for which the predicted DC value is zero. The experimentally measured values for these two quantities are

$$\begin{aligned} Q_{DC} &= - .67 \pm .14 \text{ mdeg K}, \\ U_{DC} &= - .88 \pm .14 \text{ mdeg K}. \end{aligned} \qquad (4.2)$$

It's interesting to note that the U component which is supposed to be zero is larger than Q, the non-zero component predicted by the model. Taking this with the fact that the resulting vector points right at the elevator tower argues for this being a local effect due to ground radiation. Yet the possibility of a nonzero contribution from the galaxy or an asymmetrically expanding universe cannot be ruled out. The estimates of the ground radiation are nowhere near accurate enough to allow separating out the ground contribution in an effect this small. For this reason the result for Q in (4.2) must be taken as an upper limit on the DC polarization from an asymmetrically expanding universe:

$$Q_{DC} < .85 \text{ mdeg K, with } 90\% \text{ confidence.}$$

This ends the analysis of the DC part of the signal. Next I will subtract the respective DC component from each Q and U value and investigate the result for evidence of a cosmological polarization. The result of the subtraction is given in Table 4.1.

Now I must ask whether or not there is any significance to what is left after the DC contribution is subtracted? This poses a statistical question. To be answered, the statistics of the data must be investigated. The Q and U parameters in Table 4.1 are averages of samples drawn from normally distributed populations whose means are the true signal in each bin. Because the samples are large (on the order of several hundred members), the population variance can be replaced by the sample variance defined as[47]

TABLE 4.1

STOKES PARAMETERS AFTER SUBTRACTION OF DC POLARIZATION

$Q = T_{NS} - T_{EW}$

σ_Q = Experimental error in Q

$U = T_{NE,SW} - T_{NW,SE}$

σ_U = Experimental error in U

N_Q = Number of measurements of Q in average

N_U = Number of measurements of U in average

Bin Folded in Solar Bins	Q	σ_Q	N_Q	U	σ_U	N_U
1	0.98	0.61	1034	-0.19	0.60	1035
2	-0.40	0.61	1044	-0.31	0.61	1047
3	0.16	0.60	1051	-0.24	0.60	1054
4	-0.24	0.57	1053	0.62	0.59	1055
5	1.27	0.58	1050	0.22	0.58	1050
6	0.16	0.59	1055	-0.51	0.59	1048
7	-0.54	0.63	1010	0.52	0.62	1012
8	-0.94	0.65	936	0.54	0.65	928
9	1.32	0.72	635	-0.71	0.67	636
10	-0.33	0.87	445	0.45	0.85	447
11	-0.46	1.10	283	-1.84	1.10	279
12	-0.57	1.27	224	-1.07	1.27	217
13	-0.46	1.24	211	-0.13	1.24	214
14	-0.53	1.10	274	-0.73	1.11	274
15	-1.82	0.93	437	-0.63	0.95	436
16	-0.68	0.80	578	0.01	0.79	568
17	-0.54	0.69	830	0.89	0.70	833
18	0.82	0.71	936	0.10	0.65	933
19	-0.73	0.67	933	0.25	0.67	918
20	0.10	0.64	963	0.57	0.65	962
21	0.90	0.61	975	-1.34	0.61	975
22	0.16	0.60	1000	0.40	0.60	1003
23	0.72	0.60	1037	0.33	0.59	1034
24	-1.25	0.62	1038	0.16	0.60	1039

TABLE 4.1 (continued)

Bin	Q	σ_Q	N_Q	U	σ_U	N_U
Folded in Sidereal Bins						
1	0.0	0.67	779	0.67	0.66	776
2	-0.24	0.67	813	0.24	0.65	805
3	0.44	0.72	813	1.53	0.68	811
4	-1.62	0.66	809	1.13	0.67	813
5	0.65	0.65	810	0.47	0.67	815
6	-0.13	0.64	809	0.98	0.67	800
7	-0.15	0.66	769	0.21	0.66	773
8	-1.40	0.70	730	0.06	0.67	718
9	1.14	0.72	706	-0.17	0.74	704
10	-0.09	0.74	681	0.03	0.74	681
11	0.83	0.74	664	-0.26	0.72	663
12	0.09	0.73	648	-0.29	0.74	641
13	1.06	0.80	646	0.04	0.80	641
14	0.75	0.82	643	0.72	0.80	642
15	1.89	0.78	708	-0.64	0.77	710
16	0.19	0.68	838	-0.95	0.68	847
17	0.14	0.62	1003	-0.56	0.62	989
18	-0.23	0.62	1024	-0.08	0.62	1014
19	-0.87	0.60	1022	0.18	0.58	1021
20	0.15	0.63	1008	-0.69	0.63	1027
21	1.10	0.69	842	-0.01	0.71	839
22	-0.55	0.72	762	-1.66	0.72	773
23	-0.79	0.73	732	-1.45	0.73	734
24	-1.03	0.70	773	0.14	0.70	760

$$\sigma^2 = \frac{1}{N-1} \sum_{i=1}^{N} (X_i - \bar{X})^2$$
$$\simeq \frac{1}{N} \sum_{i=1}^{N} (X_i - \bar{X})^2 \quad . \tag{4.4}$$

It should be noted that this is not the variance of the original measurements and is therefore not a fair estimate of the experimental error. When I performed the subtraction between points 90 degrees apart in position in order to subtract out the switch offset, I formed a new data set by averaging adjacent points in the old. When each point is assigned its characteristic sign dependent upon polarimeter position, the process may be written as

$$P_i' = \frac{P_i + P_{i+1}}{2}, \tag{4.5}$$

where P is a given Stokes parameter. By the propagation of errors one can show that the variance of the new data set is related to the old by

$$\sigma_{P_i'}^2 = \frac{\sigma_{P_i}^2}{2} \quad . \tag{4.6}$$

Thus in terms of the original measurements, Equation 4.4 is an estimate of the variance divided by two; therefore, I must multiply by two to get back a true estimate of the scatter in the data.

There still remains one step left in order to determine the error in the measurements as they are binned. As the data is folded, five consecutive readings from each day's data are averaged into a given bin. Because of the method of subtraction, these five points are derived from six independent points in the original set of measurements. Because a whole day intervenes between each successive group of five measurements in a particular bin, these sets of five are independent

and averaging over all the points in a bin is just equivalent to averaging together the averages of each day's contribution. This daily average can be written as

$$P'_{Avg} = \frac{P_i + 2\,P_{i+1} + 2\,P_{i+2} + 2\,P_{i+3} + 2\,P_{i+4} + P_{i+5}}{10} \quad , \qquad (4.7)$$

and has a variance given by

$$\sigma^2_{P'_{Avg}} = \frac{\sigma^2_{P_i}}{5.56} \quad , \qquad (4.8)$$

where $\sigma^2_{P_i}$ is the variance of the original measurements. Just computing Equation 4.4 for the bin in question and dividing by the number of points would give

$$\sigma^2_{P'_{Avg}} = \frac{\sigma^2_{P_i}}{5} \quad . \qquad (4.9)$$

Therefore, in order to compute the variance of the mean for each of my bins, I must compute $\sigma^2_{P'_i}$ from Equation 4.4, multiply by 2/N to get $\sigma^2_{\bar{P}_i}$, and finally multiply by 5.0/5.56 to correct for the binning procedure.

In fitting a DC level to each set of Q and U, I used the method of least squares, which is to say, I minimized the function

$$F(\bar{P}) = \sum_{i=1}^{24} \frac{(P_i - \bar{P})^2}{\sigma^2_{\bar{P}_i}} \quad , \qquad (4.10)$$

where $\sigma^2_{\bar{P}_i}$ refers to the corrected variance of the mean described above.

If $\bar{P}$ is the true mean of the population in each bin, then $F(\bar{P})$ is distributed as χ^2 with 24 - 1 = 23 degrees of freedom. The hypothesis that $\bar{P}$ is the mean of <u>each</u> bin is just the statement that the polariza-

tion is isotropic for that particular Stokes parameter. Comparing the actual minimized value of $F(\bar{P})$ to the χ^2 distribution function for 23 degrees, tests whether the isotropic hypothesis is valid. The values of $F(P)_{min}$ for each of the fits to the Q and U Stokes parameters and the probabilities that each value or greater would be given by a set of random numbers are:

	SOLAR BINS		SIDEREAL BINS	
	χ^2	Probability	χ^2	Probability
Q:	30.60	15%	32.98	10%
U:	17.93	75%	27.07	25%

Except for the U parameter binned in solar time, the probabilities of the parameters having a completely random character is small. This means that statistically the measured polarization is not isotropic, or at least the probability of its being isotropic on the basis of this data is small. I must now determine whether this anisotropy has any real meaning for cosmology or whether it can be explained in terms of more local effects. In our model of an axially symmetric universe, in addition to the DC polarization, we are interested in the sinusoidal variations of the Q and U parameters which have 12 and 24 hour sidereal periods. Because I am dealing with a non-uniform, finite data string, I must also be concerned with contamination of the sidereal contributions by strong signals in the corresponding solar frequencies.

The last effect can arise in two ways. First, because we are dealing with finite data sets, adjacent bins in the power spectrum

will not be completely uncorrelated.[48] A strong peak in one bin will enhance an adjacent bin by as much as 15 percent of the value of the strong peak. This occurs because the elementary frequency bins are no longer rectangular in shape, but fall off as $\sin^2 x/x^2$ where x is in units of one over the length of the data string in seconds. When the data sets are not uniform in variance over their length (as when data are thrown away), the sine and cosine functions used to extract the Fourier components from which the power spectrum is derived are no longer orthogonal. This increases the correlation between adjacent bins. For this reason we must be careful that all large solar effects are screened out. This is particularly true of the 24 hour solar and sidereal components, which are adjacent elementary bins in the power spectrum after one year of data.

Another way in which solar effects can hurt is through seasonal effects modulating the daily solar cycles. The product of a 24 month seasonal variation with a solar period gives a beat frequency equal to the corresponding sidereal period. To look for these effects, the best starting point is to examine the data folded into solar bins for a signal which would be large enough to contaminate the sidereal results.

Table 4.2 gives the results of fitting the eight lowest frequency sine waves to the data in both solar and sidereal time. The procedure was to minimize the function

$$\sum_{i=1}^{24} \frac{(P_i - A_f \sin\omega t_i - B_f \cos\omega t_i)^2}{\sigma_{P_i}^2},$$

with respect to the parameters A_f and B_f. From A_f and B_f one can compute an amplitude and a phase for the best fit sine function

$$\text{Amplitude} = (A_f^2 + B_f^2)^{\frac{1}{2}},$$
$$\text{Phase} = \text{ARCTAN}\left(\frac{B_f}{A_f}\right), \tag{4.12}$$

for each frequency component. Starting with the 24 hour component, each wave was computed, subtracted from the data, and the residuals used to compute a χ^2. At each step I compared the χ^2 to a random distribution with two less degrees of freedom. The next fit then uses the residuals of the preceding step. Table 4.2 also gives the expected value for each frequency component. Because of the non-zero variance of each data point, there is an expected value of the amplitude of each frequency component given by

$$\langle \text{Amplitude} \rangle_f = \left\{ \frac{\sum_{i=1}^{24} \frac{\sin^2 \omega t_i}{\sigma_i^2} \left[\left(\sum_{i=1}^{24} \frac{\cos^2 \omega t_i}{\sigma_i^2} \right)^2 - \left(\sum_{i=1}^{24} \frac{\cos \omega t_i \sin \omega t_i}{\sigma_i^2} \right)^2 \right]}{\left[\sum_{i=1}^{24} \frac{\cos \omega t_i}{\sigma_i^2} \sum_{i=1}^{24} \frac{\sin \omega t_i}{\sigma_i^2} - \left(\sum_{i=1}^{24} \frac{\cos \omega t_i \sin \omega t_i}{\sigma_i^2} \right)^2 \right]^2} + \frac{\sum_{i=1}^{24} \frac{\cos^2 \omega t_i}{\sigma_i^2} \left[\left(\sum_{i=1}^{24} \frac{\sin \omega t_i}{\sigma_i^2} \right)^2 - \left(\sum_{i=1}^{24} \frac{\cos \omega t_i \sin \omega t_i}{\sigma_i^2} \right)^2 \right]}{\left[\sum_{i=1}^{24} \frac{\cos \omega t_i}{\sigma_i^2} \sum_{i=1}^{24} \frac{\sin \omega t_i}{\sigma_i^2} - \left(\sum_{i=1}^{24} \frac{\cos \omega t_i \sin \omega t_i}{\sigma_i^2} \right)^2 \right]^2} \right\}^{\frac{1}{2}}. \tag{4.13}$$

To test the statistical significance of an amplitude, one takes the difference between the amplitude and its expected value for random data and compares this with the error in the amplitude.

Investigation of the solar amplitudes shows only one with a significant value, the 4 hour period in the Q parameter. This frequency is well separated from its sidereal equivalent in the power spectrum, as one needs only two months of data to resolve the two.

TABLE 4.2

HARMONIC ANALYSIS OF DATA

P = Period in hours of solar or sidereal time.

T = Amplitude of harmonic component in mdeg K.

σ_T = Error in amplitude.

Φ = Phase of component in degrees from Bin 0 (Bin 24).

σ_Φ = Error in phase.

ν = Degrees of freedom in fit.

χ^2 = Chi-square for the fit.

$\langle T \rangle$ = Expected value of T based on experimental errors and random numbers.

$\frac{T-\langle T \rangle}{\sigma_T}$ = Number of sigma of amplitude above expected value

P	T	σ_T	Φ	σ_Φ	ν	χ^2	$\langle T \rangle$	$\frac{T-\langle T \rangle}{\sigma_T}$
Q in Solar Bins								
24	0.33	0.21	97.36	34.35	21	26.94	0.29	0.19
12	0.19	0.20	-123.61	62.45	19	25.59	0.29	-0.50
8	0.28	0.20	-42.31	42.08	17	24.21	0.29	-0.05
6	0.22	0.20	-100.89	53.08	15	23.25	0.29	-0.35
4.8	0.09	0.20	182.42	129.61	13	23.22	0.29	-1.00
4	0.60	0.20	73.14	19.40	11	14.95	0.29	1.55
3.4	0.23	0.20	30.88	51.09	9	14.96	0.29	-0.30
3	0.15	0.20	-89.83	78.45	7	14.64	0.29	-0.70
U in Solar Bins								
24	0.10	0.21	123.20	109.79	21	16.99	0.29	-0.90
12	0.23	0.20	-40.31	49.17	19	15.35	0.29	-0.30
8	0.14	0.20	139.94	84.06	17	14.45	0.29	-0.75
6	0.19	0.20	-163.76	60.61	15	13.92	0.29	-0.50
4.8	0.31	0.20	-102.86	37.02	13	11.79	0.29	0.10
4	0.24	0.20	-133.50	48.93	11	10.96	0.29	-0.25
3.4	0.08	0.20	-124.28	143.00	9	10.92	0.29	-1.05
3	0.47	0.20	52.36	24.81	7	5.61	0.29	0.90

TABLE 4.2 (Continued)

P	T	σ_T	Φ	σ_Φ	ν	χ^2	$\langle T \rangle$	$\frac{T-\langle T \rangle}{\sigma_T}$
Q in Sidereal Bins								
24	0.52	0.21	-80.52	21.79	21	25.65	0.29	1.10
12	0.20	0.20	89.61	58.59	19	24.35	0.29	-0.45
8	0.19	0.20	-83.75	61.66	17	23.10	0.29	-0.50
6	0.31	0.20	-16.64	37.81	15	20.89	0.29	0.10
4.8	0.41	0.20	84.80	28.58	13	17.11	0.29	0.60
4	0.36	0.20	62.64	31.95	11	13.68	0.29	0.35
3.4	0.10	0.20	-59.81	116.81	9	13.63	0.29	-0.95
3	0.39	0.20	-105.69	30.13	7	10.42	0.29	0.50
U in Sidereal Bins								
24	0.58	0.20	39.24	20.53	21	17.30	0.29	1.45
12	0.45	0.21	22.62	25.30	19	12.78	0.29	0.76
8	0.33	0.20	-1.32	35.01	17	9.63	0.29	0.20
6	0.30	0.20	79.77	38.67	15	7.14	0.29	0.05
4.8	0.17	0.20	187.52	67.42	13	6.46	0.29	-0.60
4	0.08	0.20	40.47	136.89	11	6.28	0.29	-1.05
3.4	0.29	0.20	183.51	40.62	9	3.85	0.29	0.00
3	0.25	0.20	-163.63	46.74	7	2.61	0.29	-0.20

The absence of significant solar values with frequencies lower than this indicates that contamination of sidereal frequencies with solar signal won't be a problem. The solar signal is not zero as evidenced by the high initial χ^2 but I would be a little surprised if it were, since most environmental variations which can affect the polarimeter are solar in nature. It appears that by shielding the polarimeter from ground radiation and by throwing away data when the sun was above the ground shield, I was able to avoid a large amount of contamination.

Before discussing the data further, there is one feature of a fit of this type that should be noted. Ordinarily when we fit sines and cosines to a set of numbers with uniform variance, the sines and cosines are orthogonal functions over the set. In my case the variances of the points are not equal but depend on the number of measurements per point and the actual scatter in those measurements. To insure that I wasn't adding any systematics to the data in the fitting process, I compared the results obtained above to the results one would obtain assuming a constant variance across the data set. For each set I chose as a variance the average variance per point of the corresponding Stokes parameter folded into sidereal bins. The results are given in Table 4.3. The most notable differences are in the solar frequencies. Here the points closest to noon, which were deweighted because of fewer measurements (due to solar contamination), were given equal weight. It is also these points which are most affected by the sun and therefore, it is not surprising that the solar amplitudes become somewhat larger. The effect on the sidereal data is small. In both cases the Chi-squares seem to follow the same general progression as

TABLE 4.3

HARMONIC ANALYSIS OF DATA ASSUMING UNIFORM VARIANCE

P	T	Φ	ν	χ^2
Q in Solar Bins				
24	0.43	93.32	21	27.44
12	0.31	-114.01	19	24.97
8	0.22	-13.12	17	23.68
6	0.17	-109.24	15	22.92
4.8	0.12	-117.86	13	22.58
4	0.59	75.56	11	13.73
3.4	0.14	9.71	9	13.20
3	0.12	-93.50	7	12.86
U in Solar Bins				
24	0.29	121.77	21	21.17
12	0.39	-46.24	19	17.26
8	0.24	140.08	17	15.72
6	0.08	-164.68	15	15.55
4.8	0.33	-105.00	13	12.71
4	0.12	181.05	11	12.31
3.4	0.21	-93.80	9	11.15
3	0.45	66.11	7	5.96
Q in Sidereal Bins				
24	0.56	-83.84	21	27.38
12	0.25	82.76	19	25.78
8	0.22	-83.32	17	24.58
6	0.34	-8.13	15	21.66
4.8	0.39	92.11	13	17.86
4	0.35	56.00	11	14.78
3.4	0.08	-50.59	9	14.63
3	0.38	-111.56	7	10.85
U in Sidereal Bins				
24	0.59	34.81	21	19.29
12	0.46	20.38	19	13.68
8	0.35	0.05	17	10.55
6	0.34	78.64	15	7.63
4.8	0.18	184.40	13	6.81
4	0.10	61.80	11	6.56
3.4	0.34	189.77	9	3.63
3	0.21	-157.64	7	2.46

in the weighted analysis, indicating that no systematics were introduced due to the non-uniform weighting.

Turning to the sidereal frequencies, there are three significant amplitudes, both 24 hour components and the 12 hour component for the U parameter. The largest of these is the 24 hour component of U. The positive maximum of the fitted sine wave falls at a right ascension of 2.88 ± 1.37 hours which is about two hours away from the plane of the galaxy in the anticenter region. The negative minimum falls in the region of the North Galactic spur at 14.88 ± 1.37 hours. Looking at the surveys of galactic continuum polarization at lower frequencies, these regions seem to exhibit significant amounts of polarization. Looking also at the plot of the U data in Figure 4.4, we note that in addition to the high values around bins 3 and 4 and the low values around bins 15 and 16, there is another low region extending from bin 20 to bin 23, or 19.5 to 22.5 hours in right ascension. Again looking at a galactic map, I find that the Cygnus arm of the galaxy, the hottest region to pass through my beam, falls at 20.5 hours. Because I cut the plane of the galaxy in two places roughly 12 hours apart in right ascension, it isn't too difficult to imagine a 12 or 24 hour component being generated if any polarized component existed in these regions.

From a galactic polarization survey at 21 cm[49] I found that individual measurements of 100 to 200 millidegrees were obtained in the regions I cover. Applying a spectral index of a -2.7 to this intensity, in order to extrapolate the reading to 3.2 cm, results in a possible polarization temperature of from .6 to 1.2 millidegrees Kelvin.

Although this arm waving proves little, it did convince me that I had better look into polarized galactic radiation in detail.

4.4 SUBTRACTION OF THE GALAXY CONTRIBUTION

In any type of extrapolation, one would like to use data which has parameters as close to those of the data being corrected as possible. For a radio survey of the galaxy, the two most important parameters are frequency and angular resolution. Of these, frequency has the edge in importance when discussing a polarization survey.

There are two ways in which frequency enters into extrapolating polarization measurements. Most directly it must be considered in terms of the spectrum of the radiation one is measuring. Most of the galactic polarized emission is thought to be non-thermal synchrotron radiation with a spectral index of -2.5 to -2.9.[50-52] By spectral index we mean the quantity β in the expression

$$\frac{T_2}{T_1} = \left(\frac{\nu_2}{\nu_1}\right)^{\beta} \quad , \tag{4.14}$$

for scaling the temperature of radiation at different frequencies. If the radiation follows this simple relation, knowing the spectral index determines the magnitude of the polarization at one frequency, given the magnitude at another.

The other aspect of polarized emission in the galaxy, the angle, also depends on frequency through the mechanism of Faraday rotation. The electron concentration in the galaxy together with the galactic magnetic field act to produce rotation of linear polarization in much the same way a magnetic field acting on a ferrite produces rotation

in the Faraday rotation switch. This effect is frequency dependent, satisfying a relation of the form[53]

$$\psi = \psi_o + R_m \lambda^2 , \qquad (4.15)$$

where R_m is called the rotation measure and is given in units of radians per meter squared, ψ_o and ψ are the angles of the radiation before and after rotation. In terms of the number of electrons and the longitudinal magnetic field along the line of sight, the rotation measure may be written as[53]

$$R_m = 8.1 \times 10^5 \int N B_L dL \ \text{RADIANS/m}^2 . \qquad (4.16)$$

Because N and B_L are not constant with direction but vary in a complex way, one cannot use them as fitting parameters to align two surveys at different frequencies. One needs at least two surveys at different frequencies to make a correction for a third. An even better situation is to have three surveys to fit the two parameters in Equation 4.10. This would give an extra degree of freedom with which to test independently for a good fit. There are three surveys in the literature at 408, 610 and 1407 MHz with which to attempt to determine the rotation measure in my region of interest.[49,54,55]

Although the resolution of all three surveys is approximately the same, 2^o of arc, they don't cover the same points. Because of this and because I have to wind up with a result which is averaged over my beamwidth, I decided to convolve the surveys with my antenna pattern before attempting to fit Equation 4.10. By doing so I felt that any systematics in individual readings or sparse coverage in a region for a particular survey would be averaged out in the large. Table 4.4

TABLE 4.4

BINNED SURVEYS AT LOWER FREQUENCY

BINNED 408 MHz SURVEY

Bin	Q	U	T	σ_T	Angle	ΔAngle
1	0.2551	-0.8107	0.8499	0.0206	143.7336	0.6947
2	1.2417	-0.0071	1.2417	0.0215	179.8353	0.4954
3	0.4868	0.2121	0.5310	0.0210	11.7738	1.1343
4	0.3362	-0.1617	0.3731	0.0170	167.1560	1.3049
5	-0.4497	-0.2569	0.5179	0.0145	104.8694	0.8029
6	-0.7188	-0.4034	0.8242	0.0148	104.6497	0.5137
7	-0.7658	-0.2550	0.8072	0.0173	99.2100	0.6157
8	-0.0240	-0.5514	0.5520	0.0223	133.7520	1.1585
9	0.1274	-0.6139	0.6270	0.0441	140.8636	2.0131
10	0.3056	-0.5857	0.6606	0.0330	148.7786	1.4292
11	0.5183	-0.4465	0.6841	0.0221	159.6279	0.9245
12	0.1812	-0.2787	0.3325	0.0196	151.5155	1.6904
13	-0.4166	-0.0449	0.4190	0.0312	93.0771	2.1354
14	0.0855	0.6023	0.6083	0.0159	40.9592	0.7475
15	-0.1455	0.5694	0.5877	0.0115	52.1664	0.5588
16	-0.1987	0.5723	0.6058	0.0121	54.5732	0.5702
17	0.2000	0.6266	0.6577	0.0131	36.1509	0.5706
18	0.3639	0.5715	0.6775	0.0148	28.7552	0.6268
19	0.2257	0.5482	0.5928	0.0160	33.8108	0.7746
20	-0.1929	0.3432	0.3937	0.0151	59.6691	1.0996
21	-0.2014	0.1726	0.2652	0.0176	69.6953	1.8996
22	0.1154	0.0236	0.1178	0.0230	5.7685	5.5845
23	0.0574	-0.0345	0.0670	0.0167	164.4988	7.1199
24	-0.3654	0.1052	0.3802	0.0186	81.9654	1.4010

BINNED 610 MHz SURVEY

Bin	Q	U	T	σ_T	Angle	ΔAngle
1	0.1924	-0.0906	0.2127	0.0061	167.3881	0.8248
2	0.2718	-0.0236	0.2728	0.0067	177.5216	0.7058
3	0.2162	0.0383	0.2196	0.0057	5.0284	0.7452
4	0.1281	0.1774	0.2189	0.0047	27.0834	0.6144
5	-0.0933	0.1882	0.2101	0.0039	58.1868	0.5368
6	-0.2577	-0.0665	0.2661	0.0039	97.2307	0.4185
7	-0.2955	-0.0299	0.2971	0.0043	92.8929	0.4141
8	-0.1610	-0.1064	0.1930	0.0050	106.7299	0.7448
9	-0.0889	-0.1318	0.1590	0.0057	117.9949	1.0280
10	-0.7657	-0.1950	0.7901	0.0057	97.1432	0.2085
11	-0.3553	-0.2296	0.4231	0.0043	106.4366	0.2926
12	-0.1789	-0.3978	0.4362	0.0034	122.8918	0.2224
13	-0.0441	-0.1889	0.1940	0.0032	128.4281	0.4664
14	-0.0413	0.1135	0.1208	0.0031	54.9980	0.7461
15	-0.0885	0.1691	0.1908	0.0032	58.8083	0.4837
16	-0.1267	0.1612	0.2051	0.0034	64.0847	0.4763
17	-0.5166	0.1374	0.5345	0.0037	82.5539	0.1973
18	-0.6184	0.3182	0.6954	0.0041	76.3853	0.1702

TABLE 4.4 (continued)

BINNED 610 MHz SURVEY (continued)

Bin	Q	U	T	σ_T	Angle	ΔAngle
19	-0.7566	0.6826	1.0190	0.0046	68.9721	0.1293
20	-0.4072	0.4526	0.6088	0.0043	65.9895	0.2016
21	-0.1798	0.2445	0.3035	0.0041	63.1695	0.3915
22	0.0294	0.5464	0.5472	0.0042	43.4574	0.2201
23	0.1441	0.3553	0.3835	0.0046	33.9612	0.3403
24	0.0594	0.0193	0.0625	0.0054	8.9797	2.4979

BINNED 1407 MHz SURVEY

Bin	Q	U	T	σ_T	Angle	ΔAngle
1	0.0524	-0.0280	0.0594	0.0058	165.9682	2.8037
2	0.1347	0.0405	0.1407	0.0058	8.3572	1.1818
3	0.1140	0.0902	0.1454	0.0058	19.1729	1.1340
4	0.0185	0.0619	0.0646	0.0055	36.6985	2.4473
5	-0.0260	0.1522	0.1544	0.0056	49.8548	1.0467
6	-0.0926	0.1388	0.1668	0.0055	61.8627	0.9396
7	-0.1452	0.0527	0.1544	0.0053	80.0338	0.9861
8	-0.1256	0.0104	0.1260	0.0055	87.6273	1.2446
9	-0.0540	-0.0008	0.0540	0.0054	90.4255	2.8782
10	-0.0090	0.0070	0.0114	0.0053	70.9943	13.3585
11	0.0195	-0.0063	0.0205	0.0053	170.9830	7.3773
12	0.0054	-0.0365	0.0368	0.0052	139.2055	4.0506
13	0.0113	-0.0537	0.0549	0.0049	140.9456	2.5499
14	0.0843	-0.0410	0.0937	0.0047	167.0171	1.4336
15	0.1101	-0.0382	0.1166	0.0044	170.4431	1.0888
16	0.0875	0.0158	0.0889	0.0044	5.1105	1.4255
17	-0.0199	0.0815	0.0839	0.0044	51.8526	1.5014
18	-0.0685	0.0232	0.0724	0.0044	80.6350	1.7262
19	-0.0701	0.0202	0.0729	0.0046	81.9476	1.7981
20	-0.0522	-0.0112	0.0534	0.0048	96.0603	2.5859
21	-0.0465	-0.0694	0.0835	0.0051	118.0791	1.7480
22	-0.0303	-0.0769	0.0826	0.0053	124.2484	1.8538
23	0.0190	-0.0859	0.0880	0.0050	141.2228	1.6261
24	0.0353	-0.0920	0.0986	0.0051	145.4948	1.4855

gives the results of the convolution, where the convolved data have been binned in exactly the same way as my actual data.

In attempting to fit the angles of these data to Equation 4.10, I fixed one of the three angles and tried the fit with various multiples of 180 degrees added to the other two angles. In this way I sought to account for possible rotations of greater than 180 degrees between frequencies. I then selected the best fit for each bin based on the χ^2 and have displayed the results in Table 4.5. In most cases the χ^2 is huge, though it should be less than one for a reasonable fit. An explanation is that the coverage in each individual survey is not good enough to allow accurate averaging. Coverage is an important factor in that the electron concentrations and fields change significantly on a small scale, at times even less than that of the resolution of the individual surveys. If not enough of the contributions are added, the average becomes inaccurate. Another possibility is that localized Faraday depolarization causes different areas at different frequencies to be important in the average of a particular bin.

Because of the poor quality of the fits obtained for the three lower frequencies, I decided that the angles obtained from them would be useless for the purpose of correcting my survey and that I should forget them entirely and concentrate on working with the amplitudes. I felt that if there were a reasonable correlation between the amplitudes from my survey and the survey at the next lowest frequency, I could fit the amplitudes, using the spectral index as a parameter.

Amplitudes obey Rayleigh rather than Gaussian statistics. The correlation coefficient and its associated expectation values for Rayleigh statistics are given by

TABLE 4.5

RESULTS OF FITTING A ROTATION MEASURE TO LOWER FREQUENCY SURVEYS

Bin	R_M	ΔR_M	χ^2
1	-32.82	0.003	14.16
2	63.18	0.001	1.92
3	63.22	0.003	21.44
4	-33.73	0.006	17.39
5	65.51	0.002	69.07
6	52.62	0.001	301.79
7	-31.10	0.001	8.17
8	1.62	0.003	0.53
9	-30.06	0.012	4.31
10	66.11	0.007	0.03
11	-38.94	0.003	3.47
12	-50.80	0.009	15.30
13	-33.48	0.012	3.49
14	-42.67	0.002	28.85
15	-42.34	0.001	18.28
16	-42.63	0.001	0.80
17	-13.23	0.001	0.08
18	-34.20	0.001	150.27
19	-33.56	0.002	7.48
20	62.61	0.004	34.27
21	-20.73	0.008	1.24
22	-23.19	0.022	0.02
23	70.47	0.019	0.36
24	35.83	0.005	0.02

$$C(1,2) = \frac{\sum_{i=1}^{N} (T_1^i - \langle T_1 \rangle)(T_2^i - \langle T_2 \rangle}{.4292\, N\, \sigma_1\, \sigma_2} ,$$

$$\langle C(1,2) \rangle = 0, \qquad (4.17)$$

$$\langle C(1,2)^2 = \frac{1}{N} \quad .$$

For the correlation between the 3.2 and 21 cm data, I find that C(9370,1407) = .1668. Comparing this with the expected error for 24 points shows that this is only about a .8 sigma effect and not a very convincing correlation.

In spite of the low correlation, I still carried out the fit, feeling that though I could not use it for purposes of subtraction, I could at least ask whether or not the scale difference between the two sets of measurements was reasonable. The value of the spectral index which minimizes the Chi-square is -2.49, which doesn't seem too unreasonable considering the possibility of Faraday depolarization. This confirms my back of the envelope calculation and indicates that on the basis of the 21 cm data I should be seeing an effect at 3.2 cm. To find the source of the lack of correlation, I plotted the scaled amplitudes of the two sets of data in Figure 4.5. The biggest discrepancy is the lack of a significant contribution at 21 cm between 19 and 23 hours of right ascension. In this area is the Cygnus arm of the galaxy, the hottest region that falls in the beam.

Going back to Table 4.4, there doesn't appear to be a contribution in this region at 408 MHz either, yet looking at a survey at the same frequency and an 8° beamwidth, there is an indication that an effect in fact does exist.[56] In this region especially, where the galactic

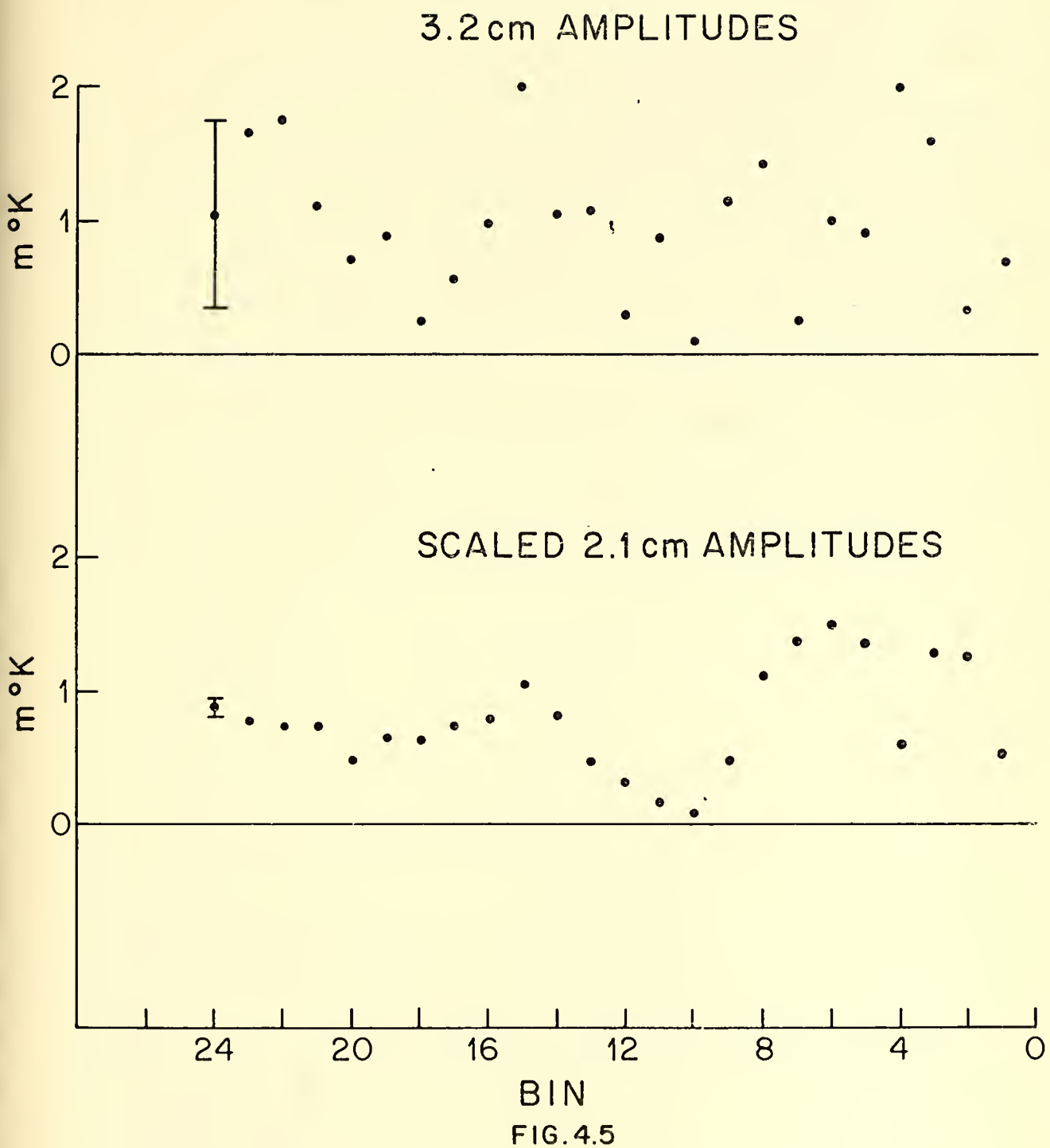

FIG. 4.5

COMPARISON OF 3.2 CM AND SCALED 21 CM AMPLITUDES

magnetic fields are complex and are directed along the line of sight, one would expect Faraday depolarization and problems of coverage to be important.

I feel that there is strong evidence for a contribution to the 3.2 cm polarization from the galaxy. Unfortunately, the data available at other frequencies does not seem capable of supplying corrections. In all fairness I can understand why they wouldn't, given the complex nature of the emission regions and magnetic fields in the galaxy, the large gap in wavelength between them and 3.2 cm , and the purpose for which these surveys was made, which was to provide high resolution coverage of the most important regions of polarized radiation at their frequencies. In their case the most important regions were close to the galactic center and therefore their coverage was concentrated in this area.

4.5 FINAL ANALYSIS

Being unable to subtract the galaxy, I have to accept the harmonic components as they are given in Table 4.2 and investigate the upper limit they infer. From here the problem lies in the complicated predictions of the model given by equation 2.16. Rewriting this equation twice, once with $\beta = 0$ and once with $\beta = 45^{o}$, I produce the predictions for the Q and U parameters, at a declination δ

$$Q = (T_w - T_a)_{max}[\sin 2\Phi \sin\delta \cos\delta \sin(t-\alpha_o - \tfrac{\pi}{2}) + \sin^2\Phi(1-\tfrac{1}{2}\cos^2\delta)\sin 2(t-\alpha_o+\tfrac{\pi}{4})],$$

$$U = (T_w - T_a)_{max}[\sin 2\Phi \cos\delta \sin(t-\alpha_o+\pi) + \sin^2\Phi \sin\delta \sin 2(t-\alpha_o)] , \qquad (4.18)$$

where everything is expressed in terms of sine functions. These may be compared directly with my data. The problem in doing this lies in the fact that the phases of the experimentally measured components don't agree well with the model. This isn't surprising, considering that most of the contribution is due to galaxy and not an asymmetrically expanding universe. For example, the measured phases of the 24 hour components for the Q and U parameters, when compared with Equation 4.13, predict values for α_o which differ by 150.24 degrees, well outside the experimental errors.

This suggests that by forcing a fit to the model, the non-agreement of phases would help toward a lower limit. I object to this course for two reasons. First the error introduced by the phases may be large enough that any lowering of the limit would probably be offset by an increase in the uncertainty. More importantly, I feel that because I do have statistically significant amplitudes, one can always argue that

even were they to be predominately from the galaxy, they might be masking a significant cosmological contribution. A fairer estimate is to compute a 90% confidence upper limit for each 12 and 24 hour harmonic of Q and U and forgetting phases, compute a result in each case for the absolute value of $(T_w - T_a)_{max}$. This procedure assumes that the phases in the data fit the model perfectly and uses the amplitudes to produce an upper limit. Another advantage of this method is that the statistics of the amplitudes are well known and setting confidence levels is relatively easy. First we form the quantity,

$$\left(\frac{T}{\langle T \rangle}\right)^2 , \tag{4.19}$$

where T is assumed to consist of a random component plus a real signal, and the expectation value is based solely on random errors. This is just the signal power divided by the noise power, a parameter which has a non-central Chi-square distribution for two degrees of freedom. Consulting the appropriate probability graph for this distribution,[64] I find the following upper limits

$$\begin{aligned} &\text{For Q} \quad 24 \text{ hr: } T < .75 \text{ mdegK} \\ &\qquad\quad 12 \text{ hr: } T < .38 \text{ mdegK,} \\ &\text{For U} \quad 24 \text{ hr: } T < .81 \text{ mdegK} \\ &\qquad\quad 12 \text{ hr: } T < .67 \text{ mdegK, with 90\% confidence.} \end{aligned} \tag{4.20}$$

Inserting these into the expressions for Q and U along with the declination of the observation, 40.35 degrees, one obtains

$$\text{For Q:}\quad |(T_w - T_a)_{max}| < 1.61 \text{ mdegK},$$
$$\text{U:}\quad |(T_w - T_a)_{max}| < 1.31 \text{ mdegK, with 90\% confidence.} \tag{4.21}$$

We must also consider the possibility of Φ being very small. In this case the cosmological contribution would be buried in the DC contribution. Assuming $\Phi = 0$ and using the upper limit on the DC level, I find from Equation 4.1

$$|(T_w - T_a)_{max}| < 1.47 \text{ mdegK, with 90\% confidence.} \tag{4.22}$$

Taking the largest of the three, I find for an upper limit on the magnitude of the polarization of the microwave background:

$$< 1.61 \text{ mdegK, with 90\% confidence.} \tag{4.23}$$

In terms of a 2.7 degree microwave background, this amounts to .06% polarization. Inserting this result into Equations 1.19 we obtain for ϵ the asymmetry parameter and $\Delta h_o/h_o$:

$$|\epsilon| \lesssim 8.15 \times 10^{-4}$$
$$\frac{\Delta h_o}{h_o} \lesssim 6.41 \times 10^{-5}, \tag{4.24}$$

where I have assumed the nominal values $n_o = 10^{-5}/cm^3$ and $h_o = 50 km/sec\ Mpc^{-1}$. It should be remembered that Equations 1.19 were derived assuming that I(t), the ionized fraction, was equal to one for all times. In general this is an unreasonable assumption, but Rees has shown that in the event of a reheating phase at a redshift of $z \gtrsim 7$ (due perhaps to galaxy formation), that the solution applies and defines the upper limit on the expansion asymmetry.[42]

In the event that there was no reheating between recombination at

$z \approx 1000$ and the present, the power anisotropy measurements imply a polarization smaller than that given in 4.18, and in this case provide the upper limit.

4.6 FUTURE DIRECTIONS

As in any enterprise, there is always room for improvement and this one is no exception. The two most glaring limits on this experiment are the galactic contribution and the effects of ground radiation. In principle,the latter could be solved by improving the ground shield and by using an antenna with somewhat better sidelobe characteristics. In the case of the galactic contribution,there doesn't seem to be any reasonably clean way of correcting for it at 3.2 cm. For this reason, I feel the best solution is to try a frequency where the expected contribution from the galaxy is less than the expected limit from receiver noise. For example, at 1.6 cm and assuming a spectral index of -2.5, the galaxy emission should be down by a factor of 5.7. If one were to use a receiver of comparable noise figure to the one used in this experiment, the galaxy would be well down in the noise, while the power from the microwave background, having a blackbody spectrum, would be roughly constant. If there were still no evidence of a cosmological polarization, the improvement in the limit would be roughly a factor of two.

Another major improvement could be made by using the second part of the dual mode transducer on the switch in a two receiver system. This would be a form of Graham's receiver which would decrease the effective system noise by the square root of two. Because the signal

in the two arms of the transducer are out of phase at the switching frequency, while the switch offset is in phase, it also offers the opportunity of balancing out the switch offset before entering the lock-in. In this way the immunity to gain drifts is enhanced.

Taken together, these changes would give an improvement of 2.5 in overall sensitivity to the background polarization.

APPENDIX A

A1. TIME DEPENDENCE OF THE SCALE FACTORS IN AN AXIALLY SYMMETRIC EUCLIDEAN UNIVERSE WITH NO MAGNETIC FIELD

In order to obtain the time dependence of the scale factors, one has to obtain the solutions to Einstein's equations for the metric in question, given an appropriate stress tensor. In this work I deal with an axially symmetric Euclidean metric given by $ds^2 = dt^2 - A(t)^2\,(dx^2 + dy^2) - W(t)^2\,dz^2$. Metrics of this type have been considered by many authors, including Thorne (1967),[43] who has given the following results and whose notation I follow.

In the absence of magnetic fields, I assume a stress energy tensor of the form,

$$T^{\mu}_{\ \nu} = \begin{bmatrix} \rho & 0 & 0 & 0 \\ 0 & -p/c^2 & 0 & 0 \\ 0 & 0 & -p/c^2 & 0 \\ 0 & 0 & 0 & -p/c^2 \end{bmatrix} , \qquad \text{(A1.1)}$$

for use in the equations. The equations for a quite general metric have been written down in detail by Dingle (1933).[57] In particular, for the above metric we obtain

$$\frac{8\pi G P}{c^4} = \frac{\ddot{A}}{A} + \frac{\ddot{W}}{W} + \frac{\ddot{A}\ddot{W}}{AW} , \quad \text{(2 equations)}$$

$$\frac{8\pi G P}{c^4} = \frac{2\ddot{A}}{A} + \frac{\dot{A}^2}{A^2} , \qquad \text{(A1.2)}$$

$$\frac{8\pi G}{c^2} = \frac{\dot{A}^2}{A^2} + \frac{2\ddot{A}W}{AW} .$$

By subtracting the first equation from the second we find the following expression,

$$\frac{\ddot{A}}{A} - \frac{\ddot{W}}{W} + \frac{\dot{A}^2}{A^2} - \frac{\ddot{AW}}{AW} = 0 \ , \qquad \text{(A1.3)}$$

for which $W = A$ is clearly a solution. In order to find others, we will make the following two assumptions. Since in the limit of $A = W$, we have an Einstein-de Sitter universe for which $A = A_0(t/t_0)^{2/3}$, and since the case we are considering is a small simple departure from the symmetric case, I will assume that A is a power law in t, i.e. $A = A_0(t/t_0)^{\alpha}$. In addition, I will assume that W is of the form $W = A + qA^N$, where q is some arbitrary constant. In effect this says that for small asymmetry, we expect a solution close to that of the Einstein-de Sitter universe and for that reason I choose to expand A in terms of the Einstein-de Sitter solution. The choice of q for a constant is unfortunate and shouldn't be confused with q_0, the deceleration parameter. I use it to provide continuity with Thorne's results. Inserting $A + qA^N$ for W into Equation A1.3 we find

$$q[(1-N)\, A^{N-1}\, \ddot{A} + (1-N^2)\, A^{N-2}\, \dot{A}^2] = 0. \qquad \text{(A1.4)}$$

Inserting the explicit form for A gives

$$\left(\frac{A_o}{t_o^{2/3}}\right)^N [\alpha(\alpha-1)t^{\alpha N-2} + (1+N)\alpha^2 t^{\alpha N-2}] = 0, \qquad \text{(A1.5)}$$

which reduces to

$$(N+2)\alpha = 1. \qquad \text{(A1.6)}$$

Next, taking the third of Equations A1.2, we note that the left side depends on the density, which is inversely proportional to the volume, meaning that A^2W is a constant. Multiplying this equation through by A^2W thus gives

$$\dot{A}^2W + 2A\dot{A}W = \text{constant}, \tag{A1.7}$$

which becomes, after substituting for W:

$$3A\dot{A}^2 + qA^N\dot{A}^2 (1+2N) = \text{constant}. \tag{A1.8}$$

Again substituting for A and using the result A1.6, we obtain the expression for α,

$$3t^{3\alpha-2} - \left(\frac{3\alpha-2}{\alpha}\right) q \left(\frac{A_o}{t^{2/3}}\right)^{\frac{1}{\alpha}-3} t^{-2} = \text{constant}, \tag{A1.9}$$

which is constant if $3\alpha-2 = 0$ or $\alpha = 2/3$. This, with equation A1.6, implies that $N = 1/2$, giving the following forms for A and W:

$$\begin{aligned} A &= A_o(t/t_o)^{2/3} \\ W &= A + qA^{-1/2} \end{aligned} \tag{A1.10}$$

From the above we can now produce an explicit form for the differential Hubble's constant:

$$\Delta h = \frac{\dot{W}}{W} - \frac{\dot{A}}{A} . \tag{A1.11}$$

By plugging in the appropriate expressions for A and W, we find

$$\Delta h = \frac{qA_o^{3/2}}{3t_oA^2W} , \tag{A1.12}$$

which gives us the result that $A^2W\Delta h = \Delta h_o$ is a constant.

A2. THE ANGULAR DISTRIBUTION OF THE TEMPERATURE OF RADIATION IN AN ANISOTROPIC EUCLIDEAN COSMOLOGICAL MODEL

This appendix will demonstrate how, in the absence of interactions, anisotropically expanding Euclidean models give rise to an anisotropy in the temperature of the microwave background. By Euclidean models we mean models with a metric of the form $ds^2 = dt^2 - A(t)^2dx^2 - B(t)^2dy^2 - W(t)^2dz^2$.

In order to effect this, it is convenient to first show that $p_i = U_i = dx_i/d\tau$ is conserved over the trajectory of each individual blackbody photon. In the standard way, I define the metric tensor as $g^{i\nu}$, in terms of which the affine connection is given by

$$\Gamma^{\alpha}_{\beta\gamma} = 1/2q^{\alpha\mu}\left[g_{\beta\mu,\ \gamma} + g_{\mu\gamma,\ \beta} - g_{\gamma\beta,\ \mu}\right], \tag{A2.1}$$

in terms of which the geodesic equations of motion of a photon may be expressed as

$$\frac{du^i}{d\tau} = -\Gamma^{i}_{\alpha\beta}\, u^{\alpha}u^{\beta}\ . \tag{A2.2}$$

From these definitions, the evolution of p_i along the trajectory of a photon may be obtained. Consider first

$$\begin{aligned}\frac{dp_i}{d\tau} &= \frac{du_i}{d\tau} \\ &= \frac{d}{dt}\left(g_{i\gamma}u^{\gamma}\right) \\ &= u^{\gamma}\frac{d}{d\tau}\left(g_{i\gamma}\right) + g_{i\gamma}\frac{du^{\gamma}}{d\tau}\ .\end{aligned} \tag{A2.3}$$

Substituting from Equations A2.2 we get

$$\frac{dP_i}{d\tau} = g_{i\gamma}{}_{,\beta} u^\gamma u^\beta + g_{i\gamma} (- \Gamma^\gamma{}_{\alpha\beta} u^\alpha u^\beta), \tag{A2.4}$$

which by the definition of the affine connection, Equation A2.1 becomes

$$\begin{aligned}\frac{dP_i}{d\tau} &= g_{i\gamma}{}_{,\beta} u^\gamma u^\beta - \tfrac{1}{2} g_{i\gamma} (g^{\gamma\delta}) [g_{\alpha\delta}{}_{,\beta} + g_{\delta\beta}{}_{,\gamma} - g_{\beta\alpha}{}_{,\delta}] u^\alpha u^\beta \\ &= g_{i\gamma}{}_{,\beta} u^\gamma u^\beta - \tfrac{1}{2} g_{\alpha i}{}_{,\beta} u^\alpha u^\beta - \tfrac{1}{2} g_{i\beta}{}_{,\alpha} u^\alpha u^\beta + \tfrac{1}{2} g_{\beta\alpha}{}_{,i} u^\alpha u^\beta. \end{aligned} \tag{A2.5}$$

In the above, γ is only a dummy index and may be replaced with α, giving

$$\begin{aligned}\frac{dP_i}{d\tau} &= (g_{i\alpha}{}_{,\beta} - \tfrac{1}{2} g_{\alpha i}{}_{,\beta}) u^\alpha u^\beta - \tfrac{1}{2} g_{i\beta}{}_{,\alpha} u^\alpha u^\beta + \tfrac{1}{2} g_{\alpha\beta}{}_{,i} u^\alpha u^\beta \\ &= \Gamma_{\alpha i\beta} u^\alpha u^\beta. \end{aligned} \tag{A2.6}$$

Because $dp_i/d\tau$ has to be symmetric in α and β, which are just dummy indices, it must be equal to the same expression as follows:

$$\begin{aligned}\frac{dP_i}{d\tau} &= \tfrac{1}{2} [\Gamma_{\alpha i\beta} + \Gamma_{\beta i\alpha}] u^\alpha u^\beta \\ &= \tfrac{1}{2} [\tfrac{1}{2} g_{i\alpha}{}_{,\beta} + g_{\beta\alpha}{}_{,i} - gi\beta,\alpha) + \tfrac{1}{2} (g_{i\beta}{}_{,\alpha} + g_{\alpha\beta}{}_{,i} - g_{i\alpha}{}_{,\beta})] u^\alpha u^\beta \\ &= \tfrac{1}{4} (g_{\beta\alpha}{}_{,i} + g_{\alpha\beta}{}_{,i}) u^\alpha u^\beta \\ &= \tfrac{1}{2} g_{\alpha\beta}{}_{,i} u^\alpha u^\beta . \end{aligned} \tag{A2.7}$$

The last line is the needed result. It states that if the metric tensor is not a function of x^i, then $p_i = U_i$ is a conserved quantity along the trajectory of a photon, in the absence of scattering. In this work I deal with metric tensors which are functions of coordinate time alone, which implies that the photon momenta p_i, $i = 1, 2, 3$, are constants of the motion. This key result allows us to compute the redshift of a photon emitted at an epoch t and observed at the present

time t_o from the direction $\hat{n}$. Starting with the original energy of the photon, as measured by an observer at rest with respect to the x, y, and z coordinates, we can write

$$\begin{aligned}(h\nu)^2 &= E^2 \\ &= p^2 \\ &= P_x\, g^{x\ell} P_\ell + P_y\, g^{y\ell}\, P_\ell + P_z g^{z\ell}\, P_\ell \\ &= -\left[\frac{1}{A^2(t)}\,(P_x)^2 + \frac{1}{B^2(t)}\,(P_y)^2 + \frac{1}{C^2(t)}\,(P_z)^2\right],\end{aligned} \tag{A2.8}$$

which by conservation of the momenta p_i is equal to

$$(h\nu)^2 = -\left[\frac{1}{A^2(t)}\,(P_{xo})^2 + \frac{1}{B^2(t)}\,(P_{yo})^2 + \frac{1}{C^2(t)}\,(P_{zo})^2\right]. \tag{A2.9}$$

For each component of the momentum we can show the following:

$$\begin{aligned}(P_{xo})^2 &= P_{xo}\, g^{x^o \ell}\, P_\ell \\ &= P_{xo}\, P^{x^o} \\ &= P_o^2\, (\hat{n} \cdot \hat{x})^2 \\ &= (h\nu_o)\, (\hat{n} \cdot \hat{x})^2,\end{aligned} \tag{A2.10}$$

which taken together with Equation A2.8 gives

$$(h\nu)^2 = -\left[\frac{A_o^2}{A^2(t)}\,(\hat{n} \cdot \hat{x})^2 + \frac{B_o^2}{B^2(t)}\,(\hat{n} \cdot \hat{y})^2 + \frac{C_o^2}{C^2(t)}\,(\hat{n} \cdot \hat{x})^2\right](h\nu_o)^2.$$

By rearranging terms and taking square roots we arrive at the following equation for the redshift z:[58]

$$\frac{1}{1+z} = \frac{\nu_o}{\nu}$$
$$= \left[\frac{A_o^2}{A^2(t)} (\hat{n} \cdot \hat{x})^2 + \frac{B_o^2}{B^2(t)} (\hat{n} \cdot \hat{y})^2 + \frac{C_o^2}{C^2(t)} (\hat{n} \cdot \hat{z})^2 \right]^{-\frac{1}{2}} . \tag{A2.12}$$

With this result, the temperature of the microwave background as a function of the direction of observation can finally be computed. The argument used is similar to that given for the isotropic case by Tolman and rests on the proof of Liouville's theorem for general relativity.[59] Liouville's theorem states that in the absence of interactions, the density of states, N, along the geodesic of a particle, is a constant. Assuming that we are considering a universe containing radiation with a blackbody distribution at recombination, or at least at the epoch of the last scattering, implies

$$N = \frac{1}{e^{h\nu/kT} - 1}$$
$$= \frac{1}{e^{h\nu_o/kT_o} - 1} \tag{A2.13}$$
$$= N_o ,$$

using the Planck distribution characteristic of a blackbody. Equality here implies equality of the arguments of the exponentials giving

$$\frac{\nu}{T} = \frac{\nu_o}{T_o} \tag{A2.14}$$

or

$$\frac{\nu_o}{\nu} = \frac{T_o}{T} = \frac{1}{1+z} . \tag{A2.15}$$

Combining this with Equation A2.11, one obtains the final expression for the angular distribution of the temperature of the microwave background in an anisotropically expanding Euclidean universe,

$$T_o = \frac{T}{1+z} = T\left[\frac{A_o^2}{A^2}\sin^2\theta\cos^2\theta + \frac{B_o^2}{B^2}\sin^2\phi\sin^2\theta + \frac{C_o^2}{C^2}\cos^2\theta\right]^{-\frac{1}{2}} . \tag{A2.16}$$

The result for an axially symmetric universe is a specialization with A = B and C = W_2

$$T_o = T\left[\frac{A_o^2}{A^2}\sin^2\theta + \frac{W_o^2}{W^2}\cos^2\theta\right]^{-\frac{1}{2}} , \tag{A2.17}$$

manipulation of which gives

$$T_o = T\frac{W}{W_o}\left[1 + \frac{A_o^2 W^2}{A^2 W_o^2} - 1\ \sin^2\theta\right]^{-\frac{1}{2}} . \tag{A2.18}$$

In the event that the anisotropy in the expansion is small or, in other words, for $A_o^2W^2/A^2W_o^2 \simeq 1$, the binomial theorem allows us to write

$$T_o = T_{av}\,(1 + \epsilon\,\sin^2\theta), \tag{A2.19}$$

where $T_{av} = TW/W_o$ and $\epsilon = \frac{1}{2}\,(1 - A_o^2W^2/A^2W_o^2)$, a small number .

From Appendix A1 we can write the explicit expressions for A and W

$$A = A_o\,(t/t_o)^{2/3}$$
$$W = A + q\,A^{-\frac{1}{2}} . \tag{A2.20}$$

Insertion of these into Equation A2.17 allows us to compare the extent of the expansion asymmetry with the asymmetry in the temperature distribution,

$$\epsilon = \frac{q}{2A_o^3} \left[\frac{q\,(1 - (t_o/t)^3) + 2A_o^{3/2}\,(1 - (t_o/t)^{3/2})}{1 + 2q/A_o^{3/2} + q^2/A_o^3} \right] \quad . \quad (A2.21)$$

From this it is clear that the requirement that ϵ be small, so that the binomial expansion in Equation A2.16 is valid, is equivalent to the parameter q being a small number and thus, the asymmetry in the expansion being small, which is exactly our above assumption.

A3. EFFECT OF A SINGLE THOMSON SCATTERING ON THE POLARIZATION OF THE MICROWAVE BACKGROUND IN AN AXIALLY SYMMETRIC UNIVERSE

When the energy of a photon is much less than the rest energy of an electron, its primary interaction with ionized matter is through the mechanism of Thomson scattering. This elastic form of scattering can be looked on as radiation by an electron which has been accelerated by an incident electromagnetic wave. Since this is electric dipole type radiation, the polarization of the outgoing wave can be derived from the solution for a simple radiating dipole. If the acceleration of the electron were considered to be in the a direction, the polarization of the outgoing wave would be perpendicular to the direction of propagation and would lie in the plane containing the direction of propagation and the direction of the acceleration of the charge (see Figure A3.1). To obtain $\hat{E}$, the unit vector in this direction, we make the following definitions:

$\hat{r} = (\sin\theta_1, 0, \cos\theta_1)$, the line of sight to the observer

$\hat{a} = (\sin\theta\cos\Phi, \sin\theta\sin\Phi, \cos\theta)$, the direction of the acceleration of the charge.

ψ = the angle between $\hat{r}$ and $\hat{a}$.

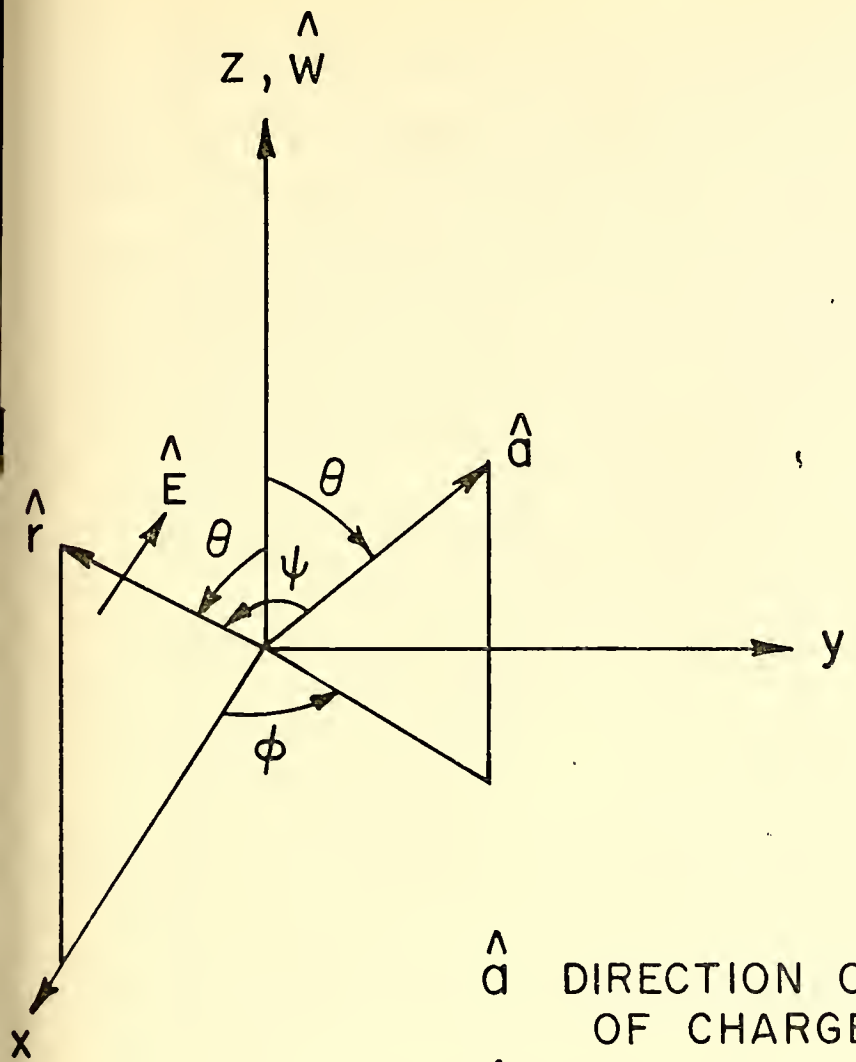

$\hat{a}$ DIRECTION OF ACCELERATION OF CHARGE

$\hat{r}$ LINE OF SIGHT TO OBSERVER

$\hat{E}$ POLARIZATION OF SCATTERED RADIATION

z $\hat{w}$ AXIS OF THE UNIVERSE

FIG. A3.1

DIRECTION OF SCATTERED RADIATION FOR THOMSON SCATTERING

From the description given above of the constraints imposed on the polarization of the scattered radiation, we can write down three equations for the three components of $\hat{E}$. Perpendicularity to the direction of propagation $\hat{r}$ requires that $\hat{E} \cdot \hat{r} = 0$, while lying in the plane containing $\hat{r}$ and $\hat{a}$ means that $\hat{E} \cdot (\hat{r} \times \hat{a}) = 0$. Finally, being of unit length implies $E_x^2 + E_y^2 + E_z^2 = 1$.

Writing these out in detail, we obtain ;

$$\hat{E} \cdot \hat{r} = E_x \sin\theta_1 + E_z \cos\theta_1 = 0,$$

$$\hat{E} \cdot (\hat{r} \times \hat{a}) = -\cos\theta_1 \sin\theta \sin\Phi\, E_x + (\sin\theta_1 \cos\theta - \cos\theta \sin\theta \cos\Phi)\, E_y + \sin\theta_1 \sin\theta \sin\Phi\, E_z,$$

$$E_x^2 + E_y^2 + E_z^2 = 1. \qquad \text{(A3.1)}$$

Another expression which will prove useful is

$$\sin^2\psi = |\hat{r} \times \hat{a}|^2 = \sin^2\theta \sin^2\Phi + (\sin\theta_1 \cos\theta - \cos\theta_1 \sin\theta \cos\Phi)^2. \qquad \text{(A3.2)}$$

Solution of the above equations yields the following for the components of E

$$E_x^2 = \frac{\cos^2\theta_1 (\sin\theta_1 \cos\theta - \cos\theta_1 \sin\theta \cos\Phi)}{\sin^2\psi},$$

$$E_y^2 = \sin^2\theta \sin^2\Phi / \sin^2\psi,$$

$$E_z^2 = \frac{\sin^2\theta_1 (\sin\theta_1 \cos\theta - \cos\theta_1 \sin\theta \cos\Phi)}{\sin^2\psi}, \qquad \text{(A3.3)}$$

which can now be used to describe the polarization of the scattered wave. In order to put this information in a more useful form, I shall follow Rees' notation and define the polarization of the outgoing wave in terms

of the plane containing the direction of propagation, $\hat{r}$ and the symmetry axis of the universe, $\hat{W}$. The direction perpendicular to this plane will be called the 'a' direction, while vectors lying in this plane and perpendicular to $\hat{r}$ will be said to be in the 'w' or coplanar direction. Applying these definitions to Equations A3.3, we find

$$\begin{aligned} E_a^2 &= E_y^2 \\ &= \sin^2\theta \sin^2\Phi/\sin^2\psi \ , \\ E_w^2 &= E_x^2 + E_z^2 \\ &= (\sin\theta_1 \cos\theta - \cos\theta_1 \sin\theta \cos\Phi)^2/\sin^2\psi \ . \end{aligned} \tag{A3.4}$$

If the incident radiation is polarized in the 'a' direction and has direction of incidence θ_2, Φ_2, the acceleration of the charge will lie in the x, y plane and be perpendicular to the direction of incidence. Thus $\theta = \pi/2$ and $\Phi = \theta_2 \pm \pi/2$. If it is in the 'w' direction $\theta = \theta_2 \pm \pi/2$ and $\Phi = \Phi_2 + \pi$. Taking these cases separately, the two components of scattered radiation (as seen by an observer whose line of sight $\hat{r}$, makes an angle θ, with respect to the axis of the universe $\hat{W}$) will be computed.

In Appendix A2 it was shown that in an anisotropically expanding axial universe with a small anisotropy, the temperature of the radiation can be characterized as having a distribution of the form $T = T_{av}\ (1 + \epsilon \sin^2\theta)$, where ϵ is an asymmetry parameter and θ is the angle between the direction of observation and the axis W. In this case, in order to deal with the polarization, define two asymmetry parameters ϵ_a and ϵ_w and specify the temperature of the

radiation in a given polarization in terms of them by writing $T_a = T(1 + \epsilon_a \sin^2\theta_1)$ and $T_w = T(1 + \epsilon_w \sin^2\theta_1)$. Any change in the polarization due to scattering or other effects can now be characterized by its effect on these parameters.

The amount of radiation scattered in any given direction is given by the product of the incident flux and $\frac{d\sigma}{d\Omega} = \frac{3}{8\pi}\sigma_T \sin^2\psi$, the differential Thomson scattering cross section, where σ_T is the total scattering cross section and ψ is the angle between the direction of acceleration of the charge and the direction of scattering. A fraction, E_a^2, of this is scattered with polarization in the 'a' direction and a fraction, E_w^2, with polarization in the 'w' direction. Taking the 'a' direction first, the amount scattered into this polarization from incident radiation, initially polarized in the same direction is given by

$$
\begin{aligned}
T_{a_1}' &= \int T_a \frac{d\sigma}{d\Omega} E_a^2 \, d\Omega_2 \\
&= \frac{3T\sigma_T}{8\pi} \int (1 + \epsilon_a \sin^2\theta_2) \sin^2\psi \, \frac{\sin^2\theta \sin^2\Phi}{\sin^2\psi} \, d\cos\theta_2 \, d\Phi_2 \\
&= \frac{3T\sigma_T}{8\pi} \int (1 + \epsilon_a \sin^2\theta_2) \cos^2\Phi_2 \, 2d\cos\theta_2 \, d\Phi_2 \qquad \text{(A3.5)} \\
&= \frac{T\sigma_T}{2} \left(\frac{3}{2} + \epsilon_a\right).
\end{aligned}
$$

In a similar way, radiation scattered into the 'w' polarization is given by

$$T_{w_1}' = \int T_a \frac{d\sigma}{d\Omega} E_w^2 \, d\Omega_2$$

$$= \frac{3T\,\sigma_T}{8\pi} \int (1 + \epsilon_a \sin^2\theta_2) \sin^2\psi \frac{(\sin\theta_1\cos\theta - \cos\theta_1\sin\theta\cos\Phi)^2}{\sin^2\psi} \, d\cos\theta_2 d\Phi_2$$

$$= \frac{3T\,\sigma_T}{8\pi} \int (1 + \epsilon_a \sin^2\theta_2) \cos^2\theta_1 \sin^2\theta_2 \, d\cos\theta_2 d\Phi_2$$

$$= \frac{T\,\sigma_T}{2} \cos^2\theta_1 \left(\frac{3}{2} + \epsilon_a\right). \qquad \text{(A3.6)}$$

Starting with incident radiation polarized in the 'w' direction, the corresponding results are

$$T_{a_2}' = \int T_w \frac{d\sigma}{d\Omega} E_a^2 \, d\Omega_2$$

$$= \frac{3T\,\sigma_T}{8\pi} \int (1 + \epsilon_w \sin^2\theta_2) \sin^2\psi \frac{\sin^2\theta \sin^2\Phi}{\sin^2\psi} \, d\cos\theta_2 \, d\Phi_2$$

$$= \frac{3T\,\sigma_T}{8\pi} \int (1 + \epsilon_w \sin^2\theta_2) \cos^2\theta_2 \sin^2\Phi_2 \, d\cos\theta \, 2d\Phi_2$$

$$= \frac{T\,\sigma_T}{2} \left(\frac{1}{2} + \frac{1}{5} \epsilon_w\right), \qquad \text{(A3.7)}$$

for radiation scattered into the 'a' polarization. For the 'w' polarization,

$$T_{w_2}' = \int T_w \frac{d\sigma}{d\Omega} E_w^2 \, d\Omega_2$$

$$= \frac{3T\,\sigma_T}{8\pi} \int (1 + \epsilon_w \sin^2\theta_2) \sin^2\psi \frac{(\sin\theta_1\cos\theta - \cos\theta_1\sin\theta\cos\Phi)^2}{\sin^2\psi} d\cos\theta_2 d\Phi_2$$

$$= \frac{3T\,\sigma_T}{8\pi} \int (1 + \epsilon_w \sin^2\theta_2)(\sin\theta_1\sin\theta_2 - \cos\theta_1\cos\theta_2\cos\Phi_2)^2 d\cos\theta_2 d\Phi_2$$

$$= \frac{T\,\sigma_T}{2} \left(\frac{1}{2} + \frac{1}{5} \epsilon_w\right) + \frac{T\,\sigma_T}{2} \sin^2\theta_1 \left(\frac{3}{2} + \frac{7}{15} \epsilon_w\right). \qquad \text{(A3.8)}$$

Adding these results gives the total contribution to each polarization

$$T_a' = T_{a_1}' + T_{a_2}' = T\sigma_T \left(1 + \tfrac{1}{2}\epsilon_a + \frac{1}{10}\epsilon_w\right)$$

$$T_w' = T_{w_1}' + T_{w_2}' = T\sigma_T \left[\left(1 + \tfrac{1}{2}\epsilon_a + \frac{1}{10}\epsilon_w\right) + \left(\frac{7}{30}\epsilon_w - \tfrac{1}{2}\epsilon_a\right)\sin^2\theta_1\right]. \tag{A3.9}$$

If we now re-express equations A3.9 in terms of new asymmetry parameters ϵ_a' and ϵ_w' we obtain to first order in ϵ_a and ϵ_w, the following solutions for the new parameters:

$$\epsilon_a' = 0$$

$$\epsilon_w' = \frac{7}{30}\epsilon_w - \frac{1}{2}\epsilon_a, \tag{A3.10}$$

where the new average temperature is $T' = T\sigma_T\left(1 + \tfrac{1}{2}\epsilon_a + \frac{1}{10}\epsilon_w\right)$.
In matrix form this can be written

$$\begin{pmatrix} \epsilon_a' \\ \epsilon_w' \end{pmatrix} = \begin{pmatrix} 0 & 0 \\ -\frac{1}{2} & 7/30 \end{pmatrix} \begin{pmatrix} \epsilon_a \\ \epsilon_w \end{pmatrix} . \tag{A3.11}$$

This last expression is the final result for the effect of a single Thomson scattering.

A4. TERRESTRIAL OBSERVATION OF A COSMOLOGICAL LINEAR POLARIZATION

In previous sections I have shown how cosmological causes can give rise to a linear polarization of the microwave background of the form

$$(T_w - T_a) = (T_w - T_a)_{max} \sin^2\theta, \qquad (A4.1)$$

where θ is the angle between the line of sight of the observer and the direction defined by the symmetry axis of the universe. Now, the question is what form does this polarization take for a ground observer trying to measure its effect? In my case I will assume the following measurement scheme. A microwave polarimeter will be aimed at the zenith and, as the earth rotates, will be allowed to sweep out a circle of constant declination in the sky. Given this situation, we need to find the variations in the signal produced by the rotation of the earth. We can diagram the experimental setup as in Figure A4.1, where $\hat{E}_a$ and $\hat{E}_w$, the unit vectors in the perpendicular and coplanar directions as defined in Appendix A3, have been drawn in.

By stating their relationships to the directions R and W and to the normal to the $\hat{R}$, $\hat{W}$ plane $\hat{R} \times \hat{W}$, we can develop equations for the determination of $\hat{E}_a$ and $\hat{E}_w$. First, because both of them are parallel to the polarization of incident radiation, they must be perpendicular to the line of sight, $\hat{R}$. Next, $\hat{E}_w$ lies in the $\hat{R}$, $\hat{W}$ plane and must be perpendicular to its normal while $\hat{E}_a$ is perpendicular to this plane and thus must be perpendicular to $\hat{W}$. Finally each of them must be a unit vector. In vector notation these conditions become

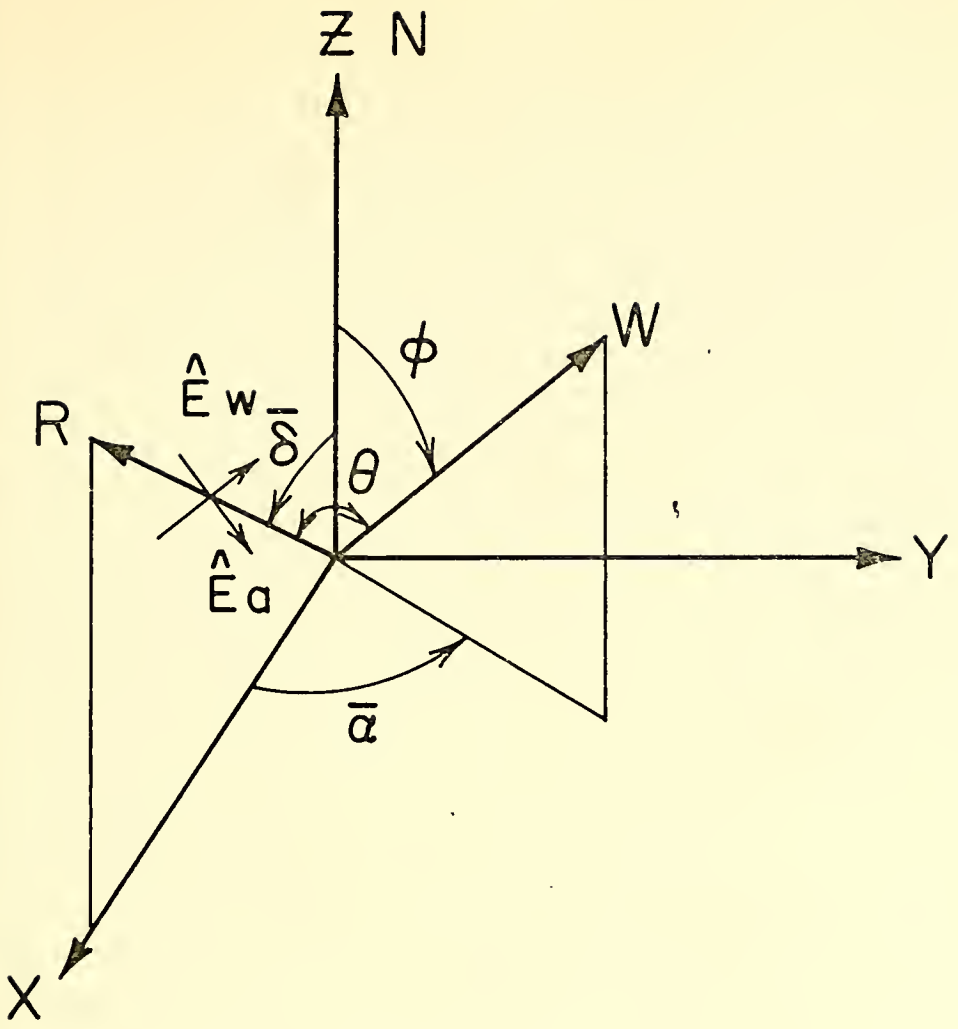

N - NORTH CELESTIAL POLE

W - AXIS OF THE UNIVERSE

R - LINE OF SIGHT OF THE OBSERVER

$\bar{\delta} = \pi/2 - \delta$

$\alpha = \alpha_0 - \tau$ (where τ is local sidereal time in angular units)

FIG. A 4.1

RELATION BETWEEN THE AXIS OF THE UNIVERSE, THE ROTATION AXIS OF THE EARTH AND THE LINE OF SIGHT TO THE OBSERVER

$$\hat{E}_w \cdot \hat{R} = 0 \qquad \hat{E}_a \cdot \hat{R} = 0$$

$$\hat{E}_w \cdot (\hat{W} \times \hat{R}) = 0 \qquad \hat{E}_a \cdot \hat{W} = 0$$

$$E_{wx}^2 + E_{wy}^2 + E_{wz}^2 = 1 \qquad E_{ax}^2 + E_{ay}^2 + E_{az}^2 = 1, \qquad \text{(A4.2)}$$

while written out in detail, they are

$$E_{wx} \sin\bar{\delta} + E_{wz} \cos\bar{\delta} = 0 \qquad E_{ax} \sin\bar{\delta} + E_{az}\cos\bar{\delta} = 0$$

$$E_{wx} \sin\Phi \sin\bar{\alpha} \cos\bar{\delta} + \bar{E}_{wy}(\cos\theta\sin\bar{\delta} \qquad E_{ax}\sin\Phi \cos\bar{\alpha} + E_{ay}\sin\theta \sin\bar{\alpha}$$

$$-\sin\Phi\cos\bar{\alpha}\cos\bar{\delta}) + E_{wz}\sin\Phi \sin\bar{\alpha} \sin\bar{\delta} = 0 \qquad + E_{az}\cos\Phi = 0$$

$$E_{wx}^2 + E_{wy}^2 + E_{wz}^2 = 1 \qquad E_{ax}^2 + E_{ay}^2 + E_{az}^2 = 1.$$

(A4.3)

Taking these with the expression

$$|W \times R| = \sin^2\theta = \sin\Phi \sin^2\bar{\alpha} + (\cos\Phi \sin\delta - \sin\Phi \cos\bar{\alpha} \cos\bar{\delta})^2, \qquad \text{(A4.4)}$$

leads to the following solutions for the unit vectors:

$$E_{wx} = -\frac{\cos\bar{\delta}\,(\cos\Phi \sin\bar{\delta} - \sin\Phi \cos\bar{\alpha} \cos\bar{\delta})}{\sin\theta} \qquad E_{ax} = -\frac{\cos\bar{\delta} \sin\Phi \sin\bar{\alpha}}{\sin\theta}$$

$$E_{wy} = +\frac{\sin\Phi \sin\bar{\alpha}}{\sin\theta} \qquad E_{ay} = -\frac{\sin\bar{\delta} \cos\Phi - \sin\Phi \cos\bar{\alpha} \cos\bar{\delta}}{\sin\theta}$$

$$E_{wz} = +\frac{\sin\bar{\delta}\,(\cos\Phi \sin\bar{\delta} - \sin\Phi \cos\bar{\alpha} \cos\delta)}{\sin\theta} \qquad E_{az} = \frac{\sin\bar{\delta} \sin\theta \sin\bar{\alpha}}{\sin\theta}$$

(A4.5)

this allows us to express the resultant field seen by the observer as

$$\vec{E} = E_a \hat{E}_a + E_w \hat{E}_w , \qquad \text{(A4.6)}$$

with the amplitudes E_a and E_w complex numbers and functions of t. In order to resolve these into components relative to directions with

respect to the north celestial pole, we notice from Figure A4.1 that our choice of coordinates implies that the East-West component of $\vec{E}$ is the E_y component while the North-South component is given by the projections in the plane of the other two or

$$E_{ns} = E_z \sin\bar{\delta} - E_x \cos\bar{\delta}$$
$$E_{ew} = E_y. \tag{A4.7}$$

By applying a rotation to these two components, the field can be expressed relative to any direction we choose. For an axis at an angle β with respect to North, we can give the components with respect to the new axis as

$$\begin{pmatrix} E_1 \\ E_2 \end{pmatrix} = \begin{pmatrix} \cos\beta & \sin\beta \\ -\sin\beta & \cos\beta \end{pmatrix} \begin{pmatrix} E_{ns} \\ E_{ew} \end{pmatrix} . \tag{A4.8}$$

For a polarimeter of the type I am using, the important quantity is $T_1 - T_2$, which is equal to $C(|E_1|^2 - |E_2|^2)$. The quantity in brackets can be written in terms of E_{ns} and E_{ew} as

$$|E_1|^2 - |E_2|^2 = (|E_{ns}|^2 - |E_{ew}|^2)\cos 2\beta + 2|E_{ns} \cdot E_{ew}^*| \sin 2\beta, \tag{A4.9}$$

or in terms of E_a and E_w as

$$\begin{aligned} |E_1|^2 - |E_2|^2 = {} & \left\{ \frac{(|E_w|^2 - |E_a|^2)}{\sin^2\theta} [(\cos\Phi \sin\bar{\delta} - \sin\Phi \cos\bar{\alpha} \cos\bar{\delta})^2 - \sin^2\Phi \sin^2\bar{\alpha}] \right. \\ & \left. + \frac{2|E_w \cdot E_a^*|}{\sin^2\theta} (\cos\Phi \sin\bar{\delta} - \sin\Phi \cos\bar{\alpha} \cos\bar{\delta}) \sin\Phi \sin\bar{\alpha} \right\} \cos 2\beta \\ & + 2 \left\{ \frac{(|E_w|^2 - |E_a|^2)}{\sin^2\theta} (\cos\Phi \sin\bar{\delta} - \sin\Phi \cos\bar{\alpha} \cos\bar{\delta}) \sin\Phi \sin\bar{\alpha} \right. \\ & \left. + \frac{|E_w \cdot E_a^*|}{\sin^2\theta} [\sin^2\Phi \sin^2\alpha - (\cos\Phi \sin\bar{\delta} - \sin\Phi \cos\bar{\alpha} \cos\bar{\delta})^2] \right\} \sin 2\beta. \end{aligned} \tag{A4.10}$$

In a practical situation where the signal is integrated for times much greater than the reciprocal of the receiver bandwidth, we are taking a time average of the above expression. Because the signals in the two polarizations, E_a and E_w, are independent, the time average of their product is zero and we obtain

$$T_1 - T_2 = (T_w - T_a)_{max} \left\{ [(\cos\Phi \sin\bar{\delta} - \sin\Phi \cos\bar{\alpha} \cos\bar{\delta})^2 - \sin^2\Phi \sin^2\bar{\alpha}] \cos 2\beta \right. \qquad (A4.11)$$
$$\left. + 2(\cos\Phi \sin\bar{\delta} - \sin\Phi \cos\bar{\alpha} \cos\bar{\delta}) \sin\Phi \sin\bar{\alpha} \sin 2\beta \right\} ,$$

where we have multiplied through by the constant C and made the substitution $(T_a - T_w)/\sin^2\theta = (T_a - T_w)_{max}$. This result is the signal desired. Replacing $\bar{\alpha}$ and $\bar{\delta}$ with their equivalents in terms of the local sidereal time t (this is equal to the right ascension of the zenith), the right ascension of the axis of the universe, α_o, and the declination, δ, and doing some manipulation we arrive at the following: which is the polarization signal received by a switched polarimeter pointed at the zenith which has its positive axis making an angle β with respect to North. Here, positive is defined as the T_1 direction:

$$T_1 - T_2 = (T_w - T_a)_{max} \left\{ [\cos^2\delta \left(1 - \tfrac{3}{2} \sin^2\Phi\right) + \sin^2\Phi \left(1 - \tfrac{1}{2} \cos^2\delta\right) \cos 2(\alpha_o - t) \right.$$
$$- \tfrac{1}{2} \sin 2\Phi \sin 2\delta \cos(\alpha_o - t)] \cos 2\beta - [\sin^2\Phi \sin\delta \sin 2(\alpha_o - t)$$
$$\left. - \sin 2\Phi \cos\delta \sin(\alpha_o - t)] \sin 2\beta \right\} . \qquad (A4.12)$$

APPENDIX B

B1. THE ANTENNA

As I had nothing to do with design of the antenna, I will not go into detail on the techniques of design but will only present a description of its operating characteristics. Interested readers can refer to the references, in particular the paper by Roll and Wilkinson,[60] for further information.

The antenna used was a conical, optimum gain horn with an aperture choke for suppression of the backlobes. Provision was made as shown in Figure B1.1 for the insertion of a calibration probe in the side of the horn, and this feature was in place during about two months of observations. The full width between half power points is about 15 degrees which gives the polarimeter a resolution of one hour in right ascension. Figure B1.2 is a plot of antenna gain as a function of angle from the horn axis for illumination by orthogonal polarizations. As the procedure varies slightly from that used for a power radiometer, a little explanation is in order. In making the measurement, the polarimeter was mounted horizontally on a rotating table with the apex of the horn at the center of rotation. One polarization sensitive axis of the polarimeter was aligned horizontally and the other vertically. Incident radiation was provied by a klystron radiating through rectangular waveguide and a standard gain horn, which gave a linearly polarized source. Horn to horn distance was a little over twenty meters, giving a good approximation to a plane wave at 3.2 centimeters. Two scans were made, one with the incident polarization horizontal, which corresponded to the E-plane measurement of a single

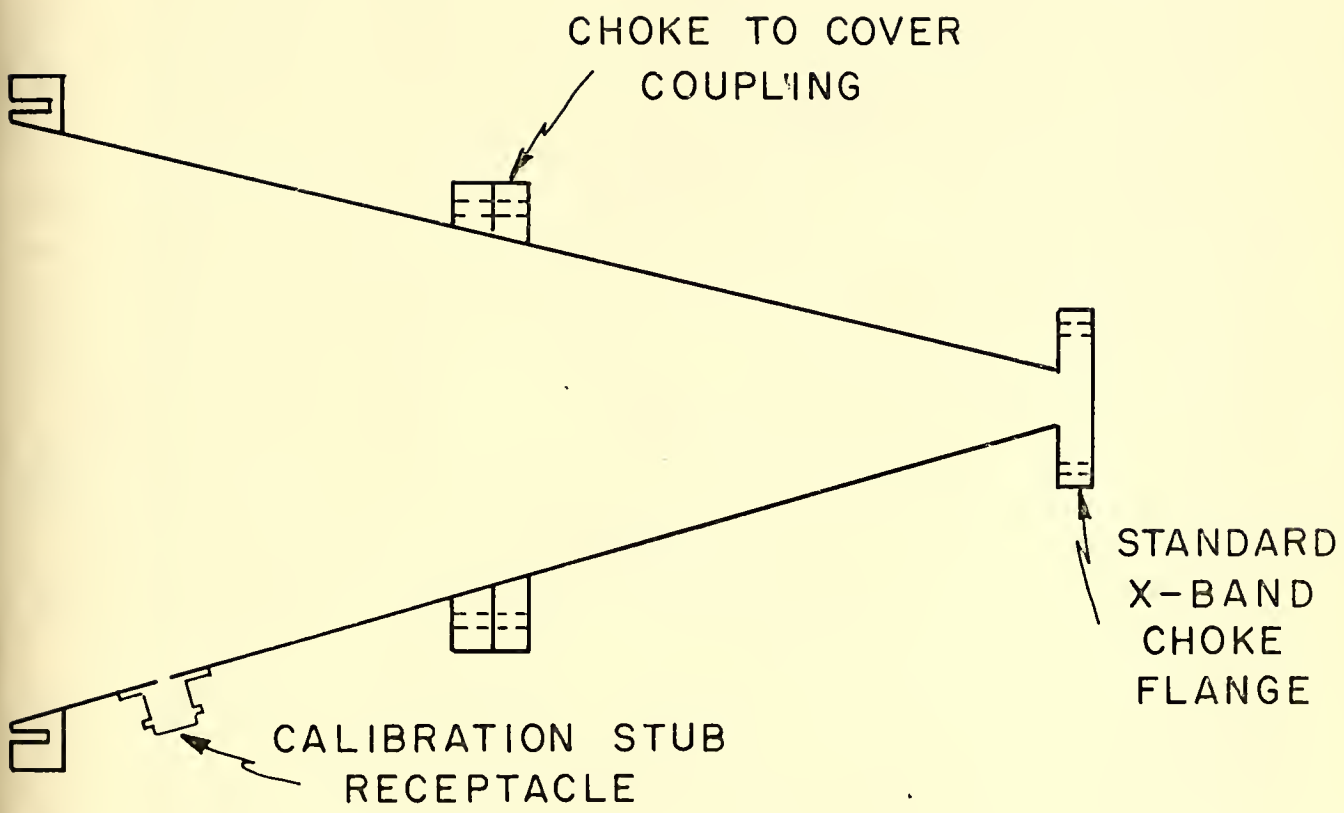

THE ANTENNA

FIG. B1.1

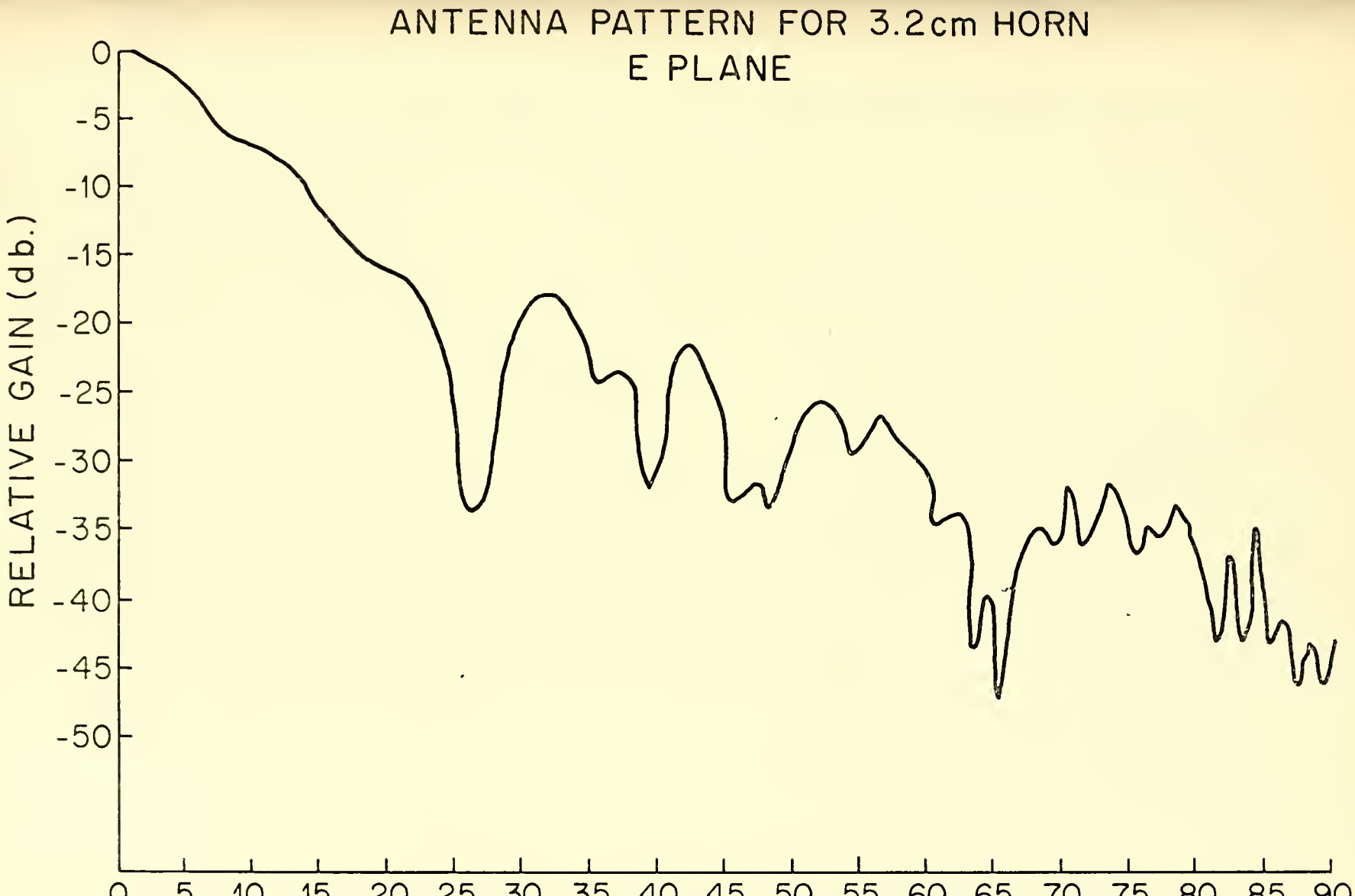
ANTENNA PATTERN FOR 3.2cm HORN
E PLANE
RELATIVE GAIN (db.)
0
-5
-10
-15
-20
-25
-30
-35
-40
-45
-50
0 5 10 15 20 25 30 35 40 45 50 55 60 65 70 75 80 85 90
ANGLE FROM HORN AXIS

FIG. B 1.2(a)

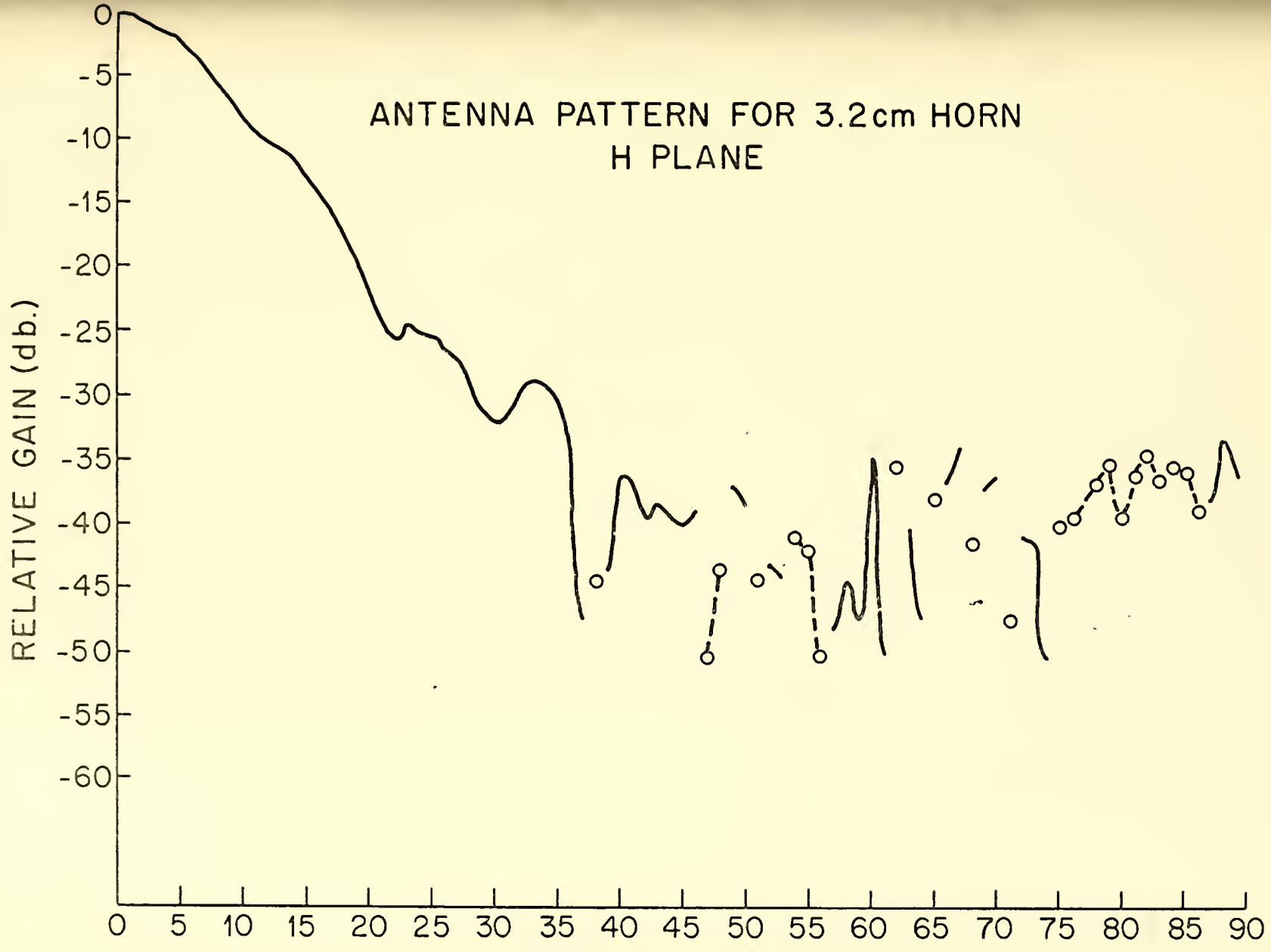
ANTENNA PATTERN FOR 3.2cm HORN
H PLANE
RELATIVE GAIN (db.)
0
-5
-10
-15
-20
-25
-30
-35
-40
-45
-50
-55
-60
0 5 10 15 20 25 30 35 40 45 50 55 60 65 70 75 80 85 90
ANGLE FROM HORN AXIS

FIG. B 1.2(b)

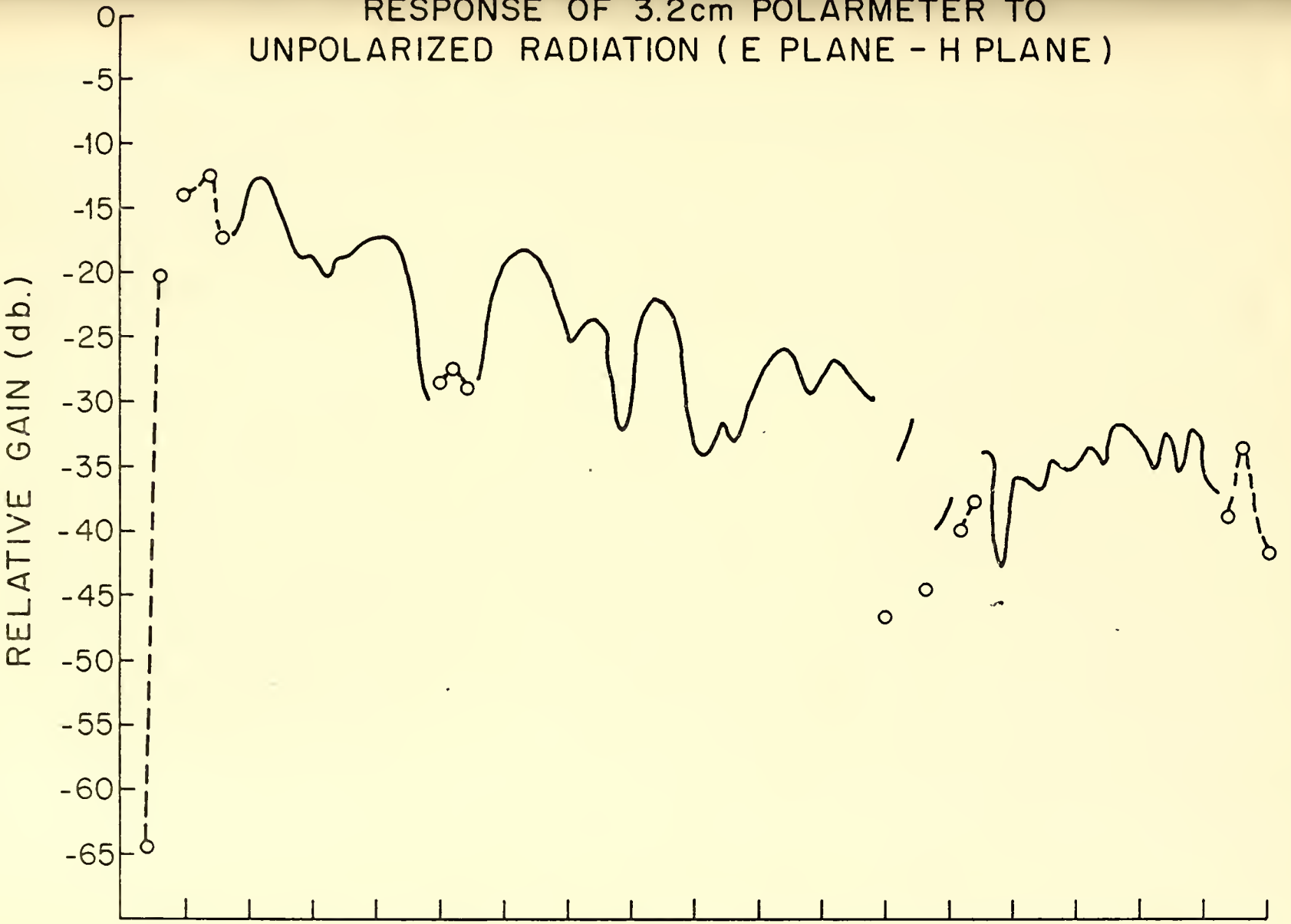
RESPONSE OF 3.2cm POLARMETER TO
UNPOLARIZED RADIATION (E PLANE - H PLANE)
RELATIVE GAIN (db.)
0
-5
-10
-15
-20
-25
-30
-35
-40
-45
-50
-55
-60
-65
0 5 10 15 20 25 30 35 40 45 50 55 60 65 70 75 80 85 90
DEGREES FROM HORN AXIS

FIG. B1.3

polarization microwave horn, and the other with polarization vertical, corresponding to the H plane measurement. Because of these analogies I have used the terms E and H plane in labeling the resultant plots. The appearance of the E plane measurement is very similar to what one would find for a power radiometer, while the H plane measurement has a striking difference. For some angles the sign of the signal changes, indicating a coupling between the polarizations. It is not known whether the observed effect is due to external reflections or to coupling within the polarimeter itself. Because the effect occurs at levels of -35db and below, it has little effect on the experiment and was thus not pursued further.

The primary purpose of the measurements was to produce Figure B1.3, which is the difference between the E and H gain patterns. This difference gives directly the response to unpolarized radiation, which can then be used to compute the expected contribution from ground radiation. The antenna temperature due to any source falling within the beam pattern is[61]

$$T_a = \int TP(\Omega)d\Omega / \int P(\Omega)d\Omega, \qquad \text{(B1.1)}$$

where T is the equivalent blackbody temperature of the source at 3.2 centimeters and $P(\Omega)$ is the gain of the antenna. The denominator can be evaluated by noting that calibration is performed by covering the entire antenna pattern with a source at temperature T and calling the resultant antenna temperature T. For a rough approximation of ground radiation we can use the form

$$T_a = TP_{AV}(\Omega)\Delta\Omega / \int P(\Omega)d\Omega. \qquad (B1.2)$$

At the observation site on the roof of Jadwin Physics building, the most prominent terrain feature and the expected source of most of the ground radiation is a structure on the roof adjacent to the polarimeter. This structure houses the elevator motors and is approximately two stories high or an angle of about a half radian above the horizontal. Its width is about a third radian, giving it a size of about one sixth steradian located between an angle of sixty and ninety degrees from the horn axis. In this position the antenna gain from Figure B1.3 is about -37db for unpolarized radiation. If we take 290°K as an average temperature for the structure we obtain

$$T_G \simeq \frac{TP_{POL}(\Omega)\Delta\Omega}{\int P(\Omega)d\Omega} = \frac{1}{6}\ (10^{-3.7})\frac{(290)}{.07206} = 0.1338\ ^{\circ}K\ , \qquad (B1.3)$$

as an appropriate contribution to the signal from ground radiation for an unshielded antenna.

During the experiment the antenna was shielded from ground radiation by a shield which extended from below a zenith angle of ninety degrees to a zenith angle of thirty degrees. Measurements of its effectiveness using the klystron source were done for zenith angles of between eighty and ninety degrees. The average reduction in sensitivity produced by the shield in this range was 12.3db. If we take this figure and apply it to the above calculation, we find, assuming that the shielding factor is valid over this range, that a reasonable figure for the expected contamination from ground radiation is 7.9 mdeg. K. In the first two months of the experiment I noticed a DC level of polarization of 6.66 mdeg. K., which agrees with the rough estimate above. I felt that this

was probably not unreasonable. An order of magnitude measurement, using the shielding factor and a piece of eccosorb as a source inside the shield, showed rough agreement. In fact, this measurement was correct at that time. It wasn't until I later decided that I would not need the calibration probe and therefore removed it from the horn that I discovered that the high degree of sensitivity to ground radiation was due to the perturbing influence of the probe. In the months that followed the level of DC polarization dropped to less than 1.5 mdeg K. By scrutinizing the level as a function of time I was able to localize the effect to the approximate time of the probe removal. Subtraction of this effect is covered under data analysis.

From the above discussion one can see that effects from ground radiation are no trivial matter and, in fact, form part of the limit on the sensitivity of this whole experiment. This was one of the key reasons for observing only the zenith where these effects would be minimized.

B2. THE SWITCH

In order to study the effect of the switch in detail, I'll first consider it as an ideal Faraday rotator. This is done in order to determine precisely the signal as a function of the direction of the incident polarized radiation and of the magnetic field used to drive the switch. A convenient reference system for specifying the direction of polarization of incoming radiation is the symmetry plane, which contains the axis of the ferrite and bisects the right angle formed by the orthogonal directions defined by the dual mode transducer (See Figure B2.1). Incoming radiation will be specified in terms of the magnitude of its electric vector and angle between this vector and the symmetry plane θ_o.

After propagating along the ferrite the E vector has been rotated by an amount determined by the longitudinal magnetic field applied to the ferrite. In our case we are driving the switch with a sinusoidally varying current and thus the angle will be equal to $A\cos\omega t + B$ where A is the maximum rotation angle and B is the rotation caused by any DC magnetic fields present. Combining these we get an expression for the angle between the direction of the $\vec{E}$ vector and symmetry plane of the switch just before the radiation enters the dual mode transducer

$$\theta = \theta_o + A\cos\omega t + B. \qquad \text{(B2.1)}$$

Looking at the signal from one arm of the dual mode transducer, we obtain the following for the electric field in the waveguide entering the receiver

$$E_{arm_2} = E\cos\left(\frac{\pi}{4} - \theta\right). \qquad \text{(B2.2)}$$

In the detection process the receiver produces a signal proportional to the square of the electric field, which, in turn, is proportional to the temperature of the received radiation. In this way the signal leaving the receiver can be expressed in terms of the temperature of the incident radiation as

$$S \propto T \cos^2 \left(\frac{\pi}{4} - \theta\right). \tag{B2.3}$$

Substituting for θ and expanding, we obtain

$$S = \frac{CT}{2} \Big\{ 1 + \cos 2B \left[\sin 2\theta_o \cos(2A \cos(\omega t)) + \cos 2\theta_o \sin(2A \cos(\omega t))\right] + \sin 2B \left[\cos 2\theta_o \cos(2A \cos(\omega t)) - \sin 2\theta_o \sin(2A \cos(\omega t))\right] \Big\} \tag{B2.4}$$

for the signal present at the input to the lock-in amplifier, where C is a proportionality constant depending on the gain of the receiver.

The action of the lock-in is to extract the Fourier component of the fundamental at the switching frequency. The labor can be eased considerably by noting that most of the terms in the above expression do not have this period. The first term is DC and, of course, gives no contribution. The terms in $\cos(2A\cos(\omega t))$ are symmetric about $\omega t = 0$ and have a frequency twice that of the driving current. For $A = \pi/4$ the waveform is similar to Figure 2.6b, which also does not have a Fourier component at the switching frequency. All that remains are terms in $\sin(2A\cos(\omega t))$, which give signals like Figure 2.6a and are the only terms that contribute. By adjusting the phase of the lock-in for maximum signal, we account for phase shifts in the apparatus and find for the Fourier component and thus the output of the lock-in

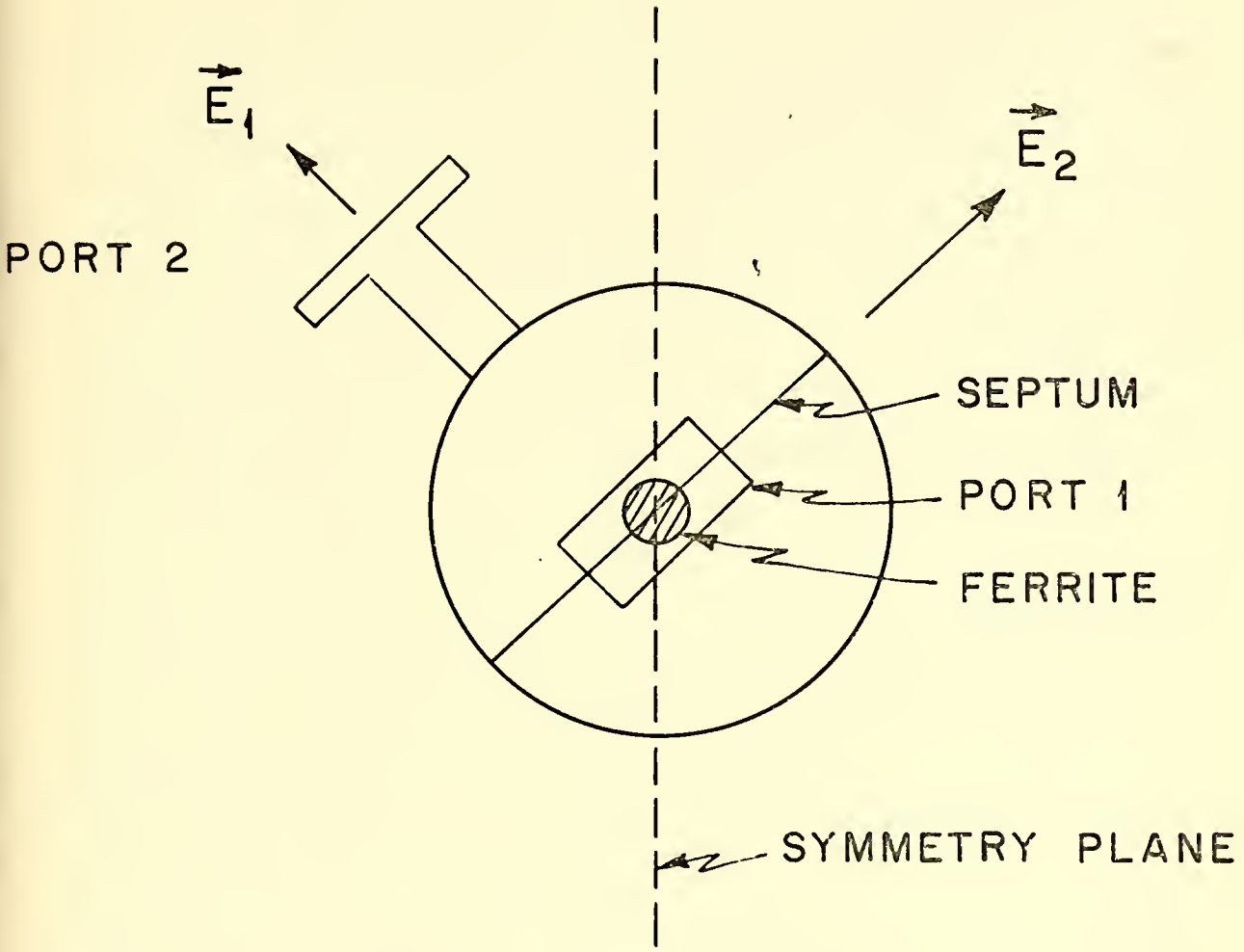

THE SYMMETRY PLANE
OF THE SWITCH

FIG. B2.1

$$V_{\text{lock-in}} = \frac{CDT}{2} [\cos 2B \cos 2\theta_o - \sin 2B \sin 2\theta_o] \left(\frac{2}{\pi}\right) \int_{oo}^{\pi} \sin(2A \cos\omega t) \cos\omega t dt, \tag{B2.5}$$

where D is a constant depending on the gain of the lock-in.

The solution to this integral is the Bessel function $J_1(2A)$ which gives[62]

$$V_{\text{lock-in}} = \frac{CDT}{2} \cos 2(\theta_o + B)\, 2J_1(2A). \tag{B2.6}$$

In order to maximize the output, $J_1(2A)$ has to be maximized. Setting $dJ_1(2A)/dA = 0$, we note that the first zero of $J_1'(x)$ occurs at $x = 1.841$ and corresponds to a maximum. This implies that for the greatest signal, the maximum rotation A is 52.7 degrees. The value for $J_1(2A)$ is .58187, or in terms of the output voltage,

$$V_{\text{lock-in}} = \frac{CDT}{2} \; (1.164) \cos 2(\theta_o + B), \tag{B2.7}$$

which differs from that obtained for a purely sinusoidal signal by the factor 1.164. This has to be included when interpreting the results. The minimum detectable signal for the polarimeter is also altered to account for the change in effective amplitude of the modulating signal

$$\Delta T_{\text{min}} = 2\sqrt{2} \; \frac{T_{\text{sys}}}{(1.164)\sqrt{\Delta\nu \Delta t}} \; . \tag{B2.8}$$

Returning now to equation B2.6, we note that if the residual fields represented by the rotation B are DC in nature, the only effect is a change in the effective position of the symmetry plane of the switch, an effect which can easily be calibrated out. If there is an AC component due to rotation or other movement of the device, we can, given that it is small, give the following expression for the lock-in output to first order in B,

$$V_{\text{lock-in}} = \frac{CDT}{2} (1.164) [\cos 2\theta'_o - 2B' \sin 2\theta'_o], \qquad (B2.9)$$

where $\theta'_o = \theta_o + B_{dc}$ and B' is the AC component of B.

In my case, where the radiometer is mounted vertically and rotated about the vertical axis, the maximum possible variation in the longitudinal magnetic field is that due to changes in the projection of the horizontal component of the earth's field on the axis of the ferrite, caused by deviation in the alignment of this axis with the vertical. The horizontal component of the earth's field in Princeton is about .2 Gauss. Because a misalignment would have a small projection in the horizontal direction, .2 Gauss is clearly an upper limit on this effect for any orientation. Therefore, an upper limit on the change is twice this number. My best estimate of the driving field of the switch was 5.3 Gauss and came from wrapping a coil around the switch throat and measuring the induced voltage. This number should be less than the maximum driving field because the coil was about five centimeters above the center of the ferrite, thus it should provide a conservative estimate. If one makes the assumption that the Faraday rotation in the ferrite is a linear function of field strength, then the earth's field can amount to no more than a 7.5% effect. In actual practice, magnetic shielding of the switch reduced this effect by another factor of 150 and, hence, to insignificance.

Another and more important effect and the one which actually made the shielding necessary was the change in the absorption coefficient of the ferrite with longitudinal magnetization. Figure B2.2a is an abosrption curve for a typical ferrite used in microwave work.[63] In order to demonstrate the effect we are considering, it is only necessary to

note that, in general, the curve is non-linear and in any particular ferrite one is somewhere on the curve in a non-linear region. In a device like the switch, where an alternating field is applied, the absorption varies sinusoidally with the applied field around the zero field value (Figure B2.2b). If we change the zero field absorption by biasing the switch with an external magnetic field, such as the earth's field, the magnitude of the sinusoidal component of the absorption changes due to the change in slope of the curve.

Because I am detecting the signal with a lock-in amplifier, I am only sensitive to changes in the absorption at the switching frequency. In order to display this explicitly, I will write the absorption, α, in the following form:

$$\alpha = \alpha_{DC}(M) + \alpha_{AC}(M)\cos\omega t, \qquad \text{(B2.10)}$$

where the departure from exact sinusoidal dependence to non-linearity of the absorption curve has been neglected, as it is only the first harmonic I am sensitive to.

In passing through the switch, unpolarized radiation undergoes absorption, which is proportional to the product of the absorption coefficient and the temperature of the radiation:

$$\frac{dt}{dx} = -\alpha T_{in}. \qquad \text{(B2.11)}$$

In addition, there is a gain in power due to emission in the ferrite, giving rise to a signal proportional to the emission coefficient β times the temperature of the ferrite T_o:

$$\frac{dt}{dx} = \beta T_o. \qquad \text{(B2.12)}$$

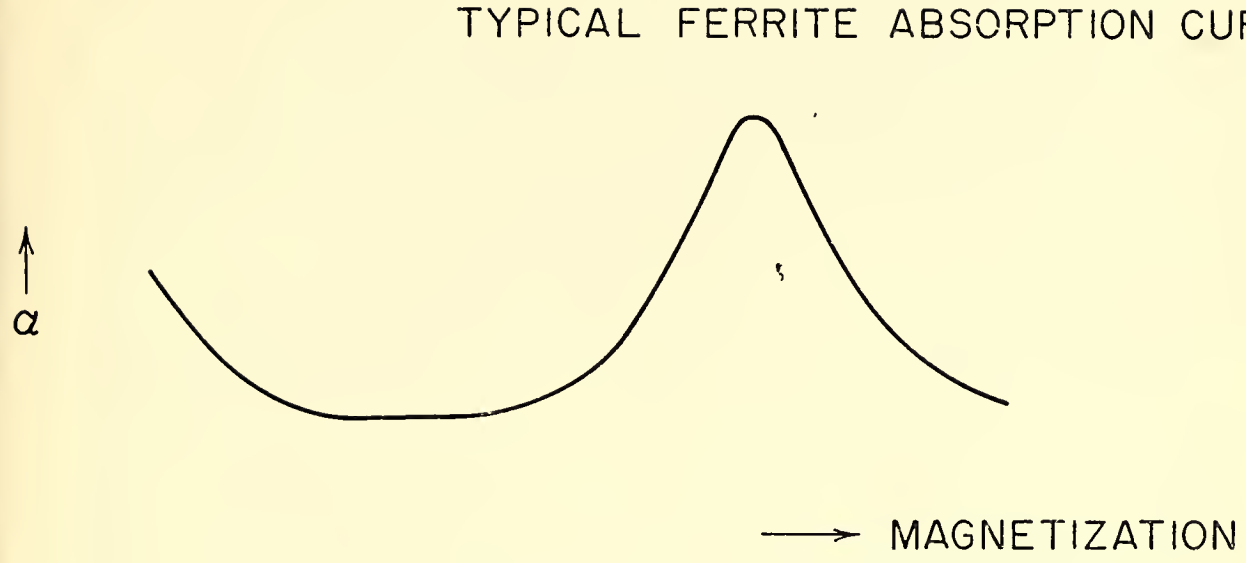

FIG. B2.2 (a)

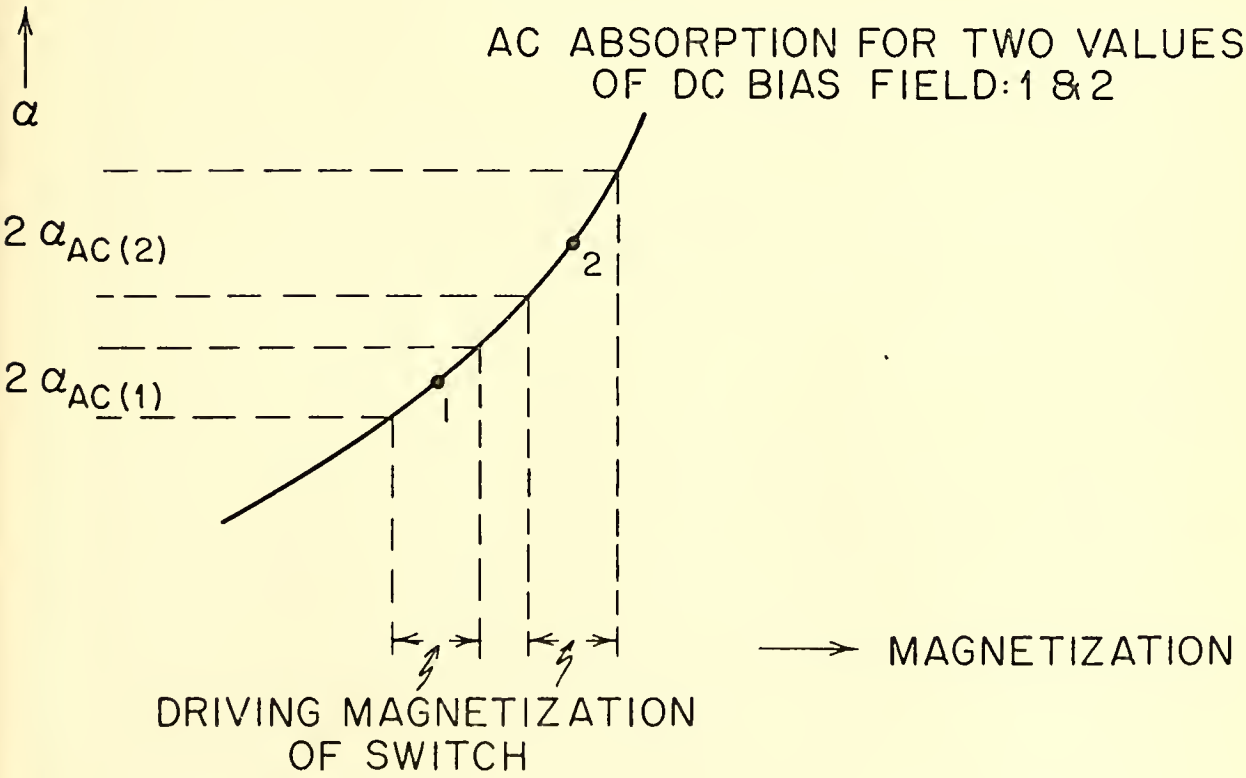

FIG. B2.2 (b)

TYPICAL FERRITE ABSORPTION CURVES

The relation between α and β can be established from consideration of detailed balance. If the input radiation were made to be equal in temperature to the switch, the expressions in B2.11 and 12 would have to be equal in order that thermal equilibrium be maintained, which would imply that $\alpha = \beta$. We can write for the change in temperature of the radiation in passing through the switch,

$$\frac{dT}{dx} = (T_o - T_{in})\,\alpha, \tag{B2.13}$$

which has as its solution,

$$T_{out} = T_{in}\, e^{-\tau} + T_o\,(1 - e^{-\tau}), \tag{B2.14}$$

where τ is α times the length of the ferrite and is, in effect, the 'optical depth' of the switch. For τ small this result can be given to first order in τ by

$$T_{out} = (T_o - T_{in})\,\tau. \tag{B2.15}$$

Under normal operating conditions $T_o - T_{in}$ is about $300^{o}K$. With the AC portion of the absorption this gives an offset signal at the switching frequency of

$$T_{out} = 300\,\tau_{ac}\,(M)\,\cos\omega t\,^{o}K. \tag{B2.16}$$

Actual measurement of this quantity gave a value of 20 to 100 mdeg. K depending on the temperature of the ferrite. This evidence gives two pieces of important information. First, it says that $\tau_{ac}(M)$ for the switch is of the order of 3.0×10^{-4} and thus, direct modulation of the input polarized signal by the absorption in the ferrite can be neglected. Secondly and more important, it demands that one look carefully at the variation of magnetization with radiometer orientation due to the

earth's magnetic field.

Direct measurement of the sensitivity of the switch to perturbing longitudinal magnetic fields showed a change in switch effect of 156 ± 3 mdeg. K/Gauss for a change of 2.4 Gauss; and a change in offset of 130 ± 5.5 mdeg. K/Gauss for a change of 1.1 Gauss. Application of up to 11 Gauss differences perpendicular to the ferrite axis failed to show any effect to the same order of accuracy as the longitudinal results. In order to gauge the effect of these offsets, assume that the ferrite axis was ten degrees from the vertical. The projection of the horizontal component of the earth's field on the ferrite would result in a maximum change in the longitudinal field of .4 sin (10^{o}) or about .07 Gauss. From the above data this would result in a variation in the signal of up to 9.3 mdeg. K, a whopping signal! In the early days of debugging the apparatus, signals of this order were actually observed and on the basis of this, it was decided to shield the switch with high permeability material. Tests run on the actual shield used showed that the shield reduced the variation in the horizontal component of field by a factor of 150 and all fields by better than a factor of 100. In this way the problem of stray magnetic fields was also eliminated.

The final item to be considered is the change in switch offset with temperature of the ferrite. Good numbers on this were available from the actual data taken in the experiment itself. In addition to measuring polarization of the microwave background, I measured the switch temperature as a function of time. By averaging together all the data at a given temperature, I can obtain the DC offset as a function of temperature (see Figure B2.3). It may seem odd that I was able to observe

a significant change in temperature in spite of controlling the environment inside the experiment shed. As it turned out, heating of the horn antenna by the sun during the day and conduction of this heat to the switch by the metal waveguide caused an uncontrollable variation in the switch temperature. Compensating for extreme changes in temperature during a single day was also hard. My controlling apparatus had a limited capacity and had to be biased into a proper range by controlling the ventilation to compensate for the season of the year. Abnormal fluctuation caused the temperature to depart from the controlling range.

Luckily, the increase of offset with temperature variation is not serious as long as the variations occur on the time scale of a few integration times. The analysis process subtracts out offsets and under these conditions the temperature induced ones would be eliminated. The worst conditions are heating by the sun on a hot day where the temperature can go up by as much as 3 degrees C/hr during the heating phase and drop by about 2 degrees C/hr in the cooling phase. I ignore the heating because data taken during this time is contaminated by the sun and not used anyway. The variation during the cooling phase and Figure B2.3 can be used to estimate an offset change of approximately 15 mdeg K/hr during the first couple of hours after the sun goes down behind the ground shield. This effect did not contribute enough solar signal in the analysis to warrant discarding additional data.

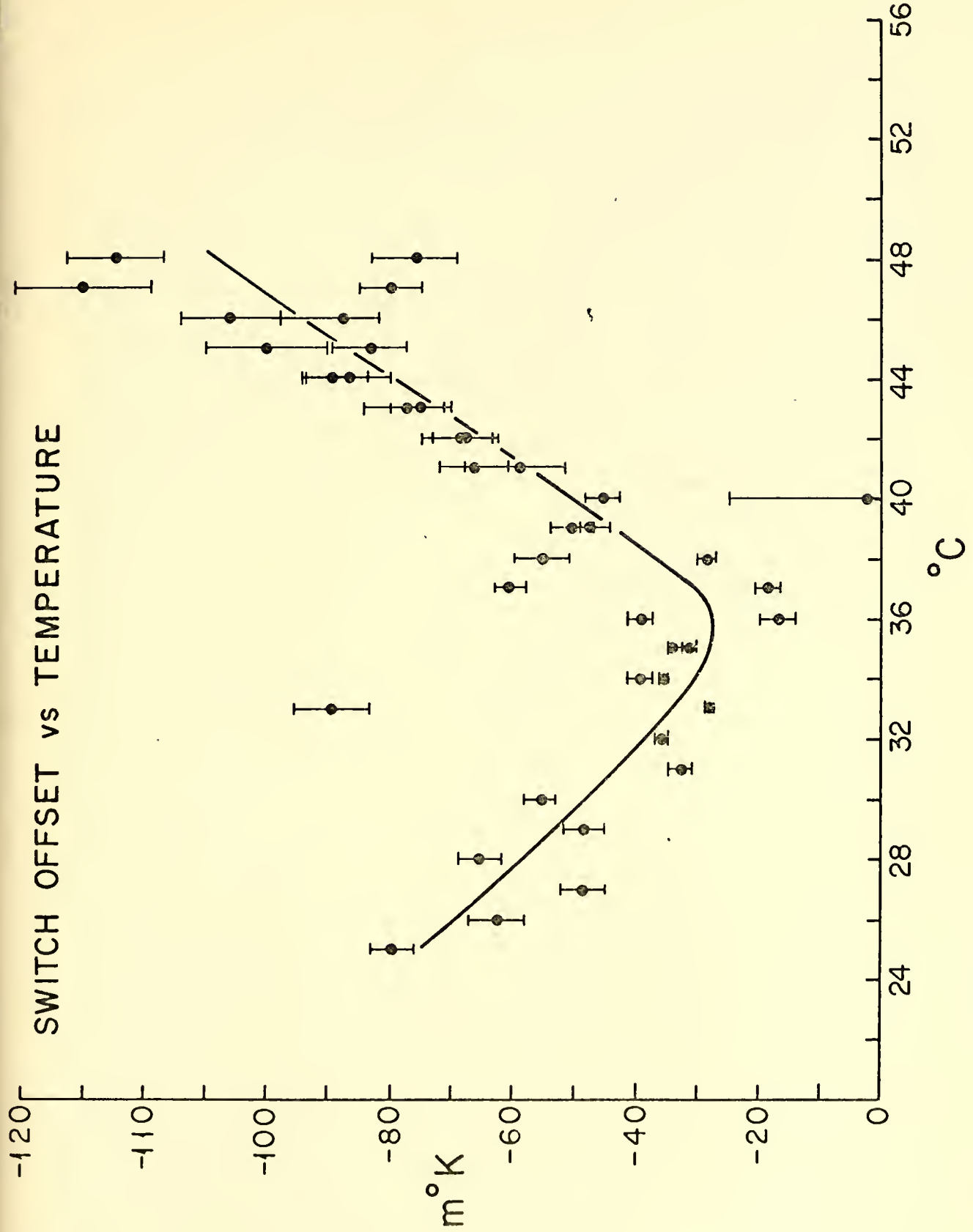
SWITCH OFFSET vs TEMPERATURE
m°K
°C
-120
-110
-100
-80
-60
-40
-20
0
24
28
32
36
40
44
48
52
56

FIG. B2.3

SPECIFICATIONS OF THE SWITCH

Ferrotec Rotational Circulator Switch (with 1 dual mode transducer removed)

Model	R-165LS
Serial Number	11
Insertion Loss	.1 db
Frequency	8.2-10.0 GHz
Current for optimum switch rotation	64 ma
Optimum switch rotation	52.7°
Sensitivity to $B_{Long.}$	130 ± 5.5 mdeg/Gauss
Sensitivity to $B_{\perp}$	0 ± 10.0 mdeg/Gauss
Offset vs. temp.	+6.7 mdeg/$^{\circ}$C temp. > 36°C
	-4.7 mdeg/$^{\circ}$C temp. < 36°C

B3. THE RECEIVER

The receiver consisted of the following components:

MIXER

BHG Electronics Laboratory Model MP8/4AARFI

Serial Number	5-163-1
Frequency	8.5-9.6 GHz
IF Frequency	60 MHz
IF Bandwidth	70 MHz
Power Gain	29 db
Noise Figure	7.2-7.3 db

IF AMPLIFIER

RHG Electronics Laboratory Model EBT101MGC

Serial Number	5-163-2
Center Frequency	60 MHz
3 db Bandwidth	48 MHz
Maximum Power Gain	75 db

LOCAL OSCILLATOR

Microwave Associates Gunn Oscillator Model MA86101

Serial Number	1190
Frequency	9.37 GHz
Power Output	10 mw

A useful comparison can be made between the quoted noise figure of the mixer given above and the actual system noise. A total temperature of $1445^{\circ}K$ was observed by covering the polarimeter with a $294^{\circ}K$ absorber and measuring the variance of the data. This gives a system temperature of $1445-294 = 1151^{\circ}K$. It must be noted that this number is referenced to the $290^{\circ}K$

temperature difference between the sky and the piece of eccosorb used for calibration. Because of inscrtion loss in the front end of the polarimeter, the size of the calibration load is reduced in magnitude by the time it reaches the mixer. A rough insertion loss can be obtained from summing the following contributions:

The Switch	.1 db
The Circulator	.2 db
The Isolator	.8 db
Waveguide joints	.2 - .3 db
Total	1.4 db

Reducing the input reference load by this amount, we find that the noise figure is based on a standard of 210°K rather than 290°K, when referenced to the input of the mixer. In these units the system noise becomes

$$T_{sys} = 1151 \quad \frac{210}{290} \quad = \quad 833^{\circ}K. \tag{B3.1}$$

In addition to absorbing radiation, the components before the mixer emit radiation with emission coefficient equal to their absorption coefficient. A 1.4 db insertion loss and 290°K device temperatures gives rise to 81°K worth of emission which must be subtracted from the system noise to isolate the mixer contribution:

$$T_{mix} = 833 - 81 = 753^{\circ}K. \tag{B3.2}$$

Multiplication by two gives the standard form for a single sideband,

$$\begin{aligned} T_{mix} &= 1506^{\circ}K \\ &= 7.92 \text{ db.} \end{aligned} \tag{B3.3}$$

This result, when compared with the manufacturer's quoted noise figure for the mixer, indicated that there is about a half db worth of extra

insertion loss or receiver noise in the system.

To find the sky noise, a comparison can be made between the receiver noise figure and the effective noise figure derived from Equation 44, using the actual data from the experiment. The system temperature from the entire years data is about 1400°K, which is about 250 degrees higher than the 1151 degree system temperature observed with the apparatus terminated in a 300 degree load. This additional noise is due to the sum of the environmental effects operating on the polarimeter and is probably "sky noise" from weather and other atmospheric fluctuations.

B4. THE CIRCULATOR AND ISOLATOR

The factory specifications of the circulator and isolator are:

THE CIRCULATOR

Ferrotec Model T-384L

Serial Number	2
Isolation	30.3 db
Insertion Loss	.2 db
VSWR	1.06
Frequency	8.5-10.1 GHz.

THE ISOLATOR

E & M Laboratories Model X112 LIA

Serial Number	171
Isolation	40 db
Insertion Loss	.8 db
VSWR	1.05
Frequency	9.2-9.55 GHz.

B5. THE MAGNETIC SHIELDING

The magnetic shielding was constructed from .050" thick Moly-Permalloy, high permeability shielding material by Allegheny Ludlum Steel Corporation. It consisted of two 11 inch diameter cylinders each 20 inches long and so constructed that one would slide within the other. Each end was covered with a spun cap of the same material, having holes for either the antenna and sky horns or the electronics cables. When assembled for use, the shield formed a covered cylinder 11 inches in diameter and 30 inches long. Moly-Permalloy, when properly annealed has the following magnetic properties:

Operating Permeability	85,000-135,000
Maximum Permeability	300,000-600,000
Induction at Maximum Perm.	3000 Gauss
Saturation Induction	8000 Gauss
Specific Gravity	8.74

REFERENCES

1. Hubble, E., Proc. Nat. Acad. Sci. 15, 168, 1929.

2. Friedman, A., Z. f. Physik, 10, 377, 1922.

3. Lemaitre, G., M.N.R.A.S., 91, 483, 1931.

4. Tolman, R. C., Relativity, Thermodynamics, and Cosmology, Sec. 171, Oxford (1934).

5. Alpher, R. A., Bethe, H. A., and Gamow, G., Phys. Rev., 73, 803, 1948.

6. Dicke, R. H., Peebles, P. J. E., Roll, P. G., and Wilkinson, D. T., Ap. J., 142, 414, 1965.

7. Penzias, A. A., and Wilson, R. W., Ap. J., 142, 419, 1965.

8. Roll, P. G., and Wilkinson, D. T., Phys. Rev. Letters, 16, 405, 1966.

9. Howell, T. F., and Shakeshaft, J. R., Nature, 210, 1318, 1966.

10. Howell, T. F., and Shakeshaft, J. R., Nature, 216, 753, 1967.

11. Field, G. B., and Hitchcock, J. L. Phys. Rev. Letters, 16, 817, 1966.

12. Thaddeus, P. and Clauser, J. F., Phys. Rev. Letters, 16, 819, 1966.

13. Wilkinson, D. T., Phys. Rev. Letters, 19, 1195, 1967.

14. Stokes, R. A., Partridge, R. B., and Wilkinson, D. T., Phys. Rev. Letters, 19, 1199, 1967.

15. Penzias, A. A., and Wilson, R. W., Astron. J., 72, 315, 1967.

16. Welch, W. J., Keachie, S., Thornton, D. D., and Wrixon, G., Phys. Rev. Letters, 18, 1068, 1967.

17. Ewing, M. S., Burke, B. F., and Staelin, D. H., Phys. Rev. Letters, 19, 1251, 1967.

18. Puzanov, V. I., Salmonovich, A. E., and Stankevich, K. S., Soviet Astronomy-A.J., 11, 905, 1968.

19. Kislyakov, A. G., Chernyshev, V. I., Lebskii, Yu.V., Mal'tsev, V. A., and Serov, N. V., Soviet Astronomy-A.J., 15, 29, 1971.

20. Pelyushenko, S. A., and Stankevich, K. S., Soviet Astronomy-A.J., 13, 223, 1969.

21. Boynton, P. E., Stokes, R. A., and Wilkinson, D. T., Phys. Rev. Letters, 21, 462, 1968.

22. Milles, M. F., McColl, R. J., Pederson, R. J. and Vernon, F. L. Jr., Phys. Rev. Letters, 26, 919, 1971.

23. McKellar, Publs. Dominion Astrophys. Observatory (Victoria, B. C.) 7, 251, 1941.

24. Bortolot, V. J., Clauser, J. F., and Thaddeus, Phys. Rev. Letters, 22, 307, 1969.

25. Shivanandan, K., Houck, J. R., and Harwit, M. O., Phys. Rev. Letters, 21, 1460, 1968.

26. Houck, J. R., and Harwit, M. O., Ap. J., 157, L45, 1969.

27. Muehlner, D., and Weiss, R., Phys. Rev. Letters, 24, 742, 1970.

28. Blair, A. G., Beery, J. G., Edeskuty, F., Hiebert, R. D., Shipley, J. P., and Williamson, K. D. Jr., Phys. Rev. Letters, 27, 1154, 1971.

29. Peebles, P. J. E., Physical Cosmology, p. 139, Princeton, 1971.

30. Wilson, R. W., and Penzias, A. A., Science, 156, 1100, 1967.

31. Conklin, E. K., Nature, 222, 971, 1969.

32. Conklin, E. K., and Bracewell, R. N., Phys. Rev. Letters, 18, 614, 1967.

33. Conklin, E. K., and Bracewell, R. N., Nature, 216, 777, 1967.

34. Penzias, A. A., Schraml, J., and Wilson, R. W., Ap. J., 157, L49, 1969.

35. Partridge, R. B., and Wilkinson, D. T., Phys. Rev. Letters, 18, 557, 1967.

36. Boughn, S. P., Fram, D. M., and Partridge, R. B., Ap. J., 165, 439, 1971.

37. Epstein, E. E., Ap. J., 148, L157, 1967.

38. Pariskii, Yu. N., and Pyatunina, T. B., Soviet Astronomy-A.J., 14, 1067, 1971.

39. Sciama, D. W., Phys. Rev. Letters, 18, 1065, 1967.

40. Stewart, J. M., and Sciama, D. W., Nature, 216, 748, 1967.

41. Peebles, P. J. E., and Wilkinson, D. T., Phys. Rev., 174, 2168, 1968.

42. Rees, M. J., Ap. J., 153, L1, 1968.

43. Thorne, K. S., Ap. J., 148, 51, 1967.

44. Jacobs, K. S., Ap. J., 153, 661, 1968.

45. Dicke, R. H., Rev. of Sci. Inst., 17, 268, 1946.

46. Kraus, J. D., Radio Astronomy, p. 101, McGraw-Hill (1966).

47. Martin, R. B., Statistics for Physicists, p. 42, Academic Press (1971).

48. Blackman, R. B., and Tookey, J. W., The Measurement of Power Spectra, p. 11, Dover (1959).

49. Bingham, R. G., M. N. R. A. S., 134, 327, 1966.

50. Howell, T. F., Astrophys. Letters, 6, 45, 1970.

51. Hirabayashi, H., Ojima, T., and Morimoto, M., Nature, 223, 49, 1969.

52. Penzias, A. A., and Wilson, R. W., Ap. J., 146, 666, 1966.

53. Gardner, F. F., and Whiteoak, J. B., Ann. Rev. of Astron. and Astrophys., 4, 245, 1966.

54. Berkhuijsen, E. M., and Brouw, W. N., B.A.N., 17, 185, 1963.

55. Berkhuijsen, E. M., Brouw, W. N., and Tinbergen, J., B.A.N., 17, 465, 1964.

56. Wielebinski, R., and Shakeshaft, F. R., M.N.R.A.S., 128, 19, 1964.

57. Dingle, H., Proc. Nat. Acad. Sci., 19, 559, 1933.

58. Thorne, K. S., in High Energy Astrophysics, Vol. 3, ed. C. Dewitt, E. Schatyman, and P. Veron, Gorden and Breach, 1966.

59. Tauber, G. E., and Weinberg, J. W., Phys. Rev. 122, 1342, 1961.

60. Roll, P. G., and Wilkinson, D. T., Annals of Physics, 44, 289, 1967.

61. Kraus, J. D., Radio Astronomy, p. 62, McGraw-Hill, 1966.

62. Watson, G. N., A Treatise on the Theory of Bessel Functions, p. 20, Cambridge, 1966.

63. Lax, B., and Button, K., Microwave Ferrites and Ferrimagnetics, McGraw-Hill, 1962.

64. Groth, E. J., Notes on the Statistics of Power Spectra, unpublished.

Thesis
N242 Nanos
Polarization of the
blackbody radiation at
3.2 cm.
146599
10 JAN 74 DISPLAY

Thesis
N242 Nanos
Polarization of the
blackbody radiation at
3.2 cm.
146599

thesN242
Polarization of the blackbody radiation
3 2768 002 01756 8
DUDLEY KNOX LIBRARY